LBNE Conceptual Design Report

Volume 5: A Liquid Argon Detector for LBNE

August 13, 2010

Contents

List of Figures

List of Tables

1 LBNE Liquid Argon Detector Volume Introduction

1.1 DRAFT – Introduction to the Long Baseline Neutrino Experiment

1.1.1 The LBNE Project

The Long-Baseline Neutrino Experiment (LBNE) Project team has prepared this Conceptual Design Report (CDR) for a world-class facility that will enable the scientific community to carry out a compelling research program in neutrino physics. The ultimate goal in the operation of the facility and experimental program is to measure fundamental physical parameters, explore physics beyond the Standard Model and better elucidate the nature of matter and antimatter.

Although the Standard Model of particle physics presents a remarkably accurate description of the elementary particles and their interactions, scientists know that the current model is incomplete and that a more fundamental underlying theory must exist. Results from the last decade revealing that the three known types of neutrinos have nonzero mass, mix with one another and oscillate between generations point to physics beyond the Standard Model. Measuring the mass and other properties of neutrinos is fundamental to understanding the deeper underlying theory and will profoundly shape our understanding of the evolution of the universe.

In its 2008 report, the Particle Physics Project Prioritization Panel (P5) recommended a world-class neutrino physics program as a core component of the U.S. particle physics program. Included in the report is the long-term vision of a large detector in the proposed Deep Underground Science and Engineering Laboratory (DUSEL) and a high-intensity neutrino source at Fermi National Accelerator Laboratory (Fermilab). On January 8, 2010, the Department of Energy approved the Mission Need for a new long-baseline neutrino experiment that would enable this world-class program and firmly establish the U.S. as the leader in neutrino science. The LBNE Project is being designed to meet this Mission Need.

With the facilities provided by the LBNE Project, the LBNE Science Collaboration proposes to make unprecedentedly precise measurements of neutrino oscillation parameters, including the value of the third mixing angle and the sign of the neutrino mass hierarchy. The ultimate goal of the program will be to search for CP-violation in the neutrino sector. The preferred configuration of the LBNE facility, in which a large neutrino detector is located deep underground, could also provide opportunities for research in other areas of physics, such as nucleon decay and neutrino astrophysics.

This CDR is organized into seven stand-alone volumes: **FIXME:** *Check that titles match*

1. The LBNE Project
2. The LBNE Neutrino Beamline
3. The LBNE Near Detectors
4. A Water Cherenkov Detector for LBNE
5. A Liquid Argon Detector for LBNE
6. Conventional Facilities at FNAL
7. Conventional Facilities at DUSEL

A detailed description of the science with LBNE can be found in Volume 1 Chapter 4.

1.1.2 Mission

The primary mission of the LBNE Project is to construct facilities that will enable a search for $\nu_\mu \rightarrow \nu_e$ appearance over a distance (baseline) of greater than 1,000 km. The magnitude of this signal is governed by the yet-to-be measured mixing angle, θ_{13}. Precise measurement of this phenomenon would allow for determination of the relative masses and mass ordering of the three known neutrinos. Measurement of this neutrino oscillation channel would also allow for research into CP violation in the neutrino sector, which is possibly connected to the dominance of matter over antimatter in the universe.

To achieve precise neutrino oscillation measurements of this type requires an intense neutrino beam and detectors of unprecedented size. Such detectors, if located underground and thus shielded from the products of cosmic ray interactions, could also provide an opportunity for increased science, including the search for proton decay and observation of neutrinos generated by supernovae. In short, the LBNE Project mission is to build an experimental facility in order to further our knowledge of neutrinos and work toward the discovery of new physics.

1.1.3 Scope

The DOE Mission Need for the LBNE Project proposes four major elements:

- A primary proton beam aimed at a production target to create a neutrino beam,
- A neutrino beam aimed at the far detector site,
- A near detector complex located near the neutrino source, and
- Massive neutrino detectors located at the far detector site.

The LBNE Project scope includes construction of facilities at two separate geographical locations. The favored alternative for achieving the Project's mission is to aim neutrinos, produced by protons from the Fermilab Main Injector, toward the NSF proposed DUSEL site at the Homestake Mine in Lead, South Dakota, located 1,300 km from Fermilab. This configuration is the basis for the design presented in this CDR.

Specifically, the main scope elements on the Fermilab site include:

- Conventional facilities at Fermilab to support the technical components of the primary proton beam, the neutrino beam and the near detectors,
- Magnets and support equipment to transport the primary protons to the neutrino Target Hall,
- Target and magnetic focusing horns to direct pions and kaons into a decay tunnel,
- A decay tunnel where the pions and kaons will decay into neutrinos,
- A beam absorber at the end of the decay tunnel, and
- Near detectors.

The main scope elements at the DUSEL site will depend on the configuration of far detectors that is chosen, but at a minimum will include the cavern and infrastructure required for each detector module, as well as the detectors themselves.

1.1.4 Capabilities

Elements of the LBNE Project are being designed to optimize the measurement of neutrino oscillations, in particular electron neutrino appearance at the far detectors. The main performance characteristics of the major Project elements are given in Detailed performance characteristics are presented in the respective volumes of the subprojects.

Project Element	Performance Parameter
thing1	thing2

Table 1.1. The main performance characteristics of the major Project elements **Subproject contributors should submit candidate elements to include here**

1.1.5 Cost and Schedule

The Total Estimated Cost (TEC) of the LBNE Project is $XXX.X M. The Total Project Cost (TPC) is $YYY.Y M, which includes an NSF contribution of $ZZZ.Z M. The schedule for construction will lead to a start of operations in FY20??.

1.1.6 Acquisition Strategy

The acquisition strategy relies on Fermi Research Alliance (FRA), the Department of Energy Managing and Operating (M&O) contractor for Fermilab, to directly manage the elements of the LBNE Project. This will include design, construction, fabrication, assembly, installation and pre-commissioning of project elements that will be located on the Fermilab site, as well as those at the far detector site, for which the Department of Energy is the steward.

1.1.7 Organization

The LBNE Project consists of five sub-projects, coordinated by a central Project office located at Fermilab:

1. The LBNE Neutrino Beamline
2. The LBNE Near Detectors
3. A Water Cherenkov Detector for LBNE
4. A Liquid Argon Detector for LBNE
5. Conventional Facilities

The Fermilab Project office is headed by the Project manager and assisted by the Project engineer and Project scientist. Project office support staff include a chief financial officer, a lead project controls specialist, a documentation team and administrative support. The Neutrino Beamline, Liquid Argon and Conventional Facilities subprojects are managed out of the Fermilab Project office, while the Near Detectors and Water Cherenkov subprojects are managed

out of Project offices at Los Alamos National Laboratory and Brookhaven National Laboratory, respectively.

The LBNE Project office has developed overriding plans for project management, risk management, configuration control and quality assurance [PM]. The subprojects have developed individually tailored plans as appropriate, and these are integrated into the overriding plans by reference and appendices.

A Project organization chart will be shown in Figure 2.1.**FIXME:** *add fig* [This figure should be the same as generated for the PMP and other Project Documents.]

1.1.8 Detector Technologies

The diverse suite of measurements that can potentially be carried out in an LBNE facility require that the detectors be able to measure interaction and particle properties over a broad range of energies and topologies. Measurements with the accelerator neutrino beam will involve neutrino interactions in the several-GeV regime, while neutrinos from a supernova are tens of MeV, and atmospheric neutrinos range from 1 to hundreds of GeV. The efficiency for selecting events of interest and rejecting backgrounds depends on the complexity and rate of the interactions and the backgrounds that can mimic the signal. The ability to reconstruct the interactions of interest will depend on quantities such as the detector's energy threshold and position, as well as its energy and momentum resolution.

Measuring the properties of neutrino interactions in the GeV region can range from identifying the simple signature of a quasi-elastic (QE) interaction to distinguishing the gammas from neutral current (NC) π^0 decays from electrons. Low energy neutrino interactions in the MeV region may involve detecting the products of the inverse beta decay process, the positron and neutron. A signature of proton decay, $p \rightarrow e\pi^0$, involves detecting a back-to-back electron with two photons, whereas $p \rightarrow K_\nu$ requires a way of detecting a kaon.

Two different detector technologies are being pursued for the design of the LBNE far detectors — water Cherenkov and liquid argon.

While originally conceived for proton decay searches, large water Cherenkov detectors (WCD) have been constructed and demonstrated to be a cost-effective detector for neutrinos as well. The Super-Kamiokande II detector in Japan is a 50-kT total volume detector that has provided definitive measurements of solar and atmospheric neutrino parameters. It is currently the far detector for the JPARC [JPARC] neutrino beam program in pursuit of the measurement of the θ_{13} mixing angle [T2K]. Scaling the total mass of a water detector by a factor of two or three, though challenging, is deemed technically feasible.

The largest liquid argon detector to operate to date is the 300-T module of the ICARUS

detector, which had a brief commissioning run in a surface laboratory in 200? [ICARUS]. Currently, the two 300-T ICARUS modules in the Gran Sasso Laboratory are filled and detecting neutrinos from the CNGS neutrino beam from CERN [CNGS]. An integrated plan for LAr has been underway at Fermilab for several years, and the design of a 20-kT module for an LBNE detector is a key component of this plan [LArPlan].

This CDR presents the design for one 100-kT WCD module and one 20-kT LAr module. The ultimate far detector configuration will be determined once the designs are more mature. Full descriptions of the detector performance for each can be found in their respective volumes of this CDR (Volumes 4 and 5).

1.1.9 Depth Requirements

In 2008, the LBNE Science Collaboration undertook a detailed study of the depth requirements for the main physics topics of interest with large detectors. This work is referred to as *The Depth Document* [depth]**FIXME:** *ref*. The topics considered were accelerator-generated neutrinos; supernova, solar and atmospheric neutrinos; and nucleon decay. The requirement on the depth of the detector is guided by the rate of the desired signals and the rate of backgrounds from cosmic rays over a very wide range of energies (from solar neutrino energies of 5 MeV to high energies in the range of hundreds of GeV.) Since this study was carried out, placement of an LAr detector at a relatively shallow depth, such as 800 ft, has become a serious option, and inclusion of a veto around the detector can be used to enhance the background rejection at the shallower depth.

Table summarizes the results of these studies for both a water Cherenkov and liquid argon detector [*]. It should be noted that none of these signatures requires a depth greater than the 4,850-ft (4,300 mwe) level at Homestake.

Given the configuration of the underground spaces at the Homestake Mine, it is an obvious conclusion that a WCD should be located on the main DUSEL campus at 4,850 ft. However, conceptual designs for a LAr detector have been developed at several depth options, as this detector technology is less susceptible to cosmic-ray backgrounds.

1.1.10 Science with LBNE

Particle physics has been very successful in creating a major synthesis of its findings, the Standard Model. At successive generations of particle accelerators in the U.S., Europe and Asia, physicists have used high-energy collisions to discover many new particles and make precision measurements of fundamental parameters. Simultaneously, scientists have carried out experiments

[*]In the depth report it was assumed that there was no veto in the detector system. Inclusion of a veto may allow for operation at a shallower depth.

Physics	Water	Argon
Long-baseline accelerator	1,000	0—1,000
$p \rightarrow K^{+}\nu$	$>$ 3,000	$>$ 3,000
Day/Night ^{8}B Solar ν	$\sim$ 4,300	$\sim$ 4,300
Supernova burst	3,500	3,500
Relic supernova	4,300	$>$2,500
Atmospheric ν	2,400	2,400

Table 1.2. **Depth requirements for the two technologies for various physics measurements** This table lists the depth requirements in meters-water-equivalent (mwe) for different physics measurements and the two technologies being considered. This table is reproduced from **FIXME:** Reference [depth].

to study naturally produced particles, such as the particles resulting from ultra-high-energy cosmic ray interactions and low-energy neutrinos emerging from the core of the sun. These efforts have uncovered both new principles and many unsuspected features of nature, resulting in an ever-increasing understanding of the workings of the universe.

In the past two decades, scientists have observed muon neutrinos produced in cosmic ray reactions in the Earth's atmosphere and electron neutrinos produced in nuclear reactions in the sun's core change from one flavor to another between source and detection. Further experimentation with both natural neutrino sources and neutrinos from reactors and accelerators has confirmed that the neutrino flavor states do not remain constant in time, but rather oscillate with a frequency governed by the magnitude of the differences between the three mass states of neutrinos.

As the name implies, the primary science motivation for the LBNE Project is to study the phenomena of accelerator-generated long-baseline neutrino oscillations. To carry out this experiment, LBNE requires construction of very large detectors, with masses of tens to hundreds of kilotons, depending on the specific technology of the detector. Locating these massive detectors deep underground, where they are shielded from backgrounds created by cosmic ray interactions, provides the opportunity to extend LBNE's science reach to include searches for proton decay as well as neutrinos from supernovae, the sun, the atmosphere and other rare phenomena. More detailed information about science with LBNE can be found in Volume 1 Chapter 4 of this CDR.

1.1.10.1 Accelerator Neutrino Oscillations

Neutrino oscillations occur due to the quantum-mechanical mixing between the flavor states of the neutrinos (e, μ, τ) and the mass states. The mixing of the three flavors of neutrinos can be described by three mixing angles (θ_{12}, θ_{23} and θ_{13}) and one CP-violating phase (δ_{CP}). The probability for neutrino oscillation also depends on the difference in the squares of the masses,

Δm^2_{12}	$7.59 \pm 0.02 \times 10^{-5} eV^2$
Δm^2_{23}	$2.43 \pm 0.13 \times 10^{-3} eV^2$
$\sin^2 2\theta_{12}$	0.87 ± 0.03
$\sin^2 2\theta_{23}$	> 0.92
$\sin^2 2\theta_{13}$	> 0.19 (90% CL)

Table 1.3. Current knowledge of the three mixing angles and the two $\Delta\ m^2$ [Ref = PDG live]

$\Delta m^2_{ij} = m^2_i - m^2_j$. Three neutrinos yield two independent mass-squared differences (m^2_{21} and m^2_{32}). Oscillations of a muon-neutrino beam over a long baseline can be studied to measure θ_{23}, θ_{13}, δ_{CP} and Δm^2_{32} .

Neutrino masses are known to be very small, as must be the differences between the masses (unlike in the case of charged leptons). However, the absolute value of the neutrino mass scale is unknown, as is the hierarchical ordering of the mass states — though it has been determined from the solar neutrino data that $m_1 < m_2$ **FIXME:** *[*ref]. There are two possibilities for the mass hierarchy: $m_1 < m_2 < m_3$ or $m_3 < m_2 < m_1$ **FIXME:** *check order – the Word version had 3,1,2 on bottom line*

The first situation is called, by convention, the *normal* mass hierarchy (NH), and the second is called the *inverted* hierarchy (IH). Distinguishing these has important implications in distinguishing models of neutrino mass.

FIXME: *Add figure 'fractional flavor content'*

Neutrinos do not propagate in a vacuum, but rather traverse matter, where the oscillation probability for $\nu_\mu \rightarrow \nu_e$ is modified by the presence of the electron density in the Earth. This results in what is called the "matter effect," which enhances the oscillation probability for neutrinos and suppresses the probability for antineutrinos if the mass hierarchy is normal. The effect is opposite in the inverted hierarchy, where neutrinos are suppressed and antineutrinos are enhanced. The magnitude of this matter effect is governed by the distance the neutrinos travel and by their energy. If L is sufficiently long and E sufficiently high, it is possible to distinguish the NH from the IH by measuring the oscillation probabilities for neutrinos and antineutrinos.

To date, only an upper limit on the value of the third mixing angle exists. It should be noted that if θ_{13} were identical to 0, there would be no ν_e content in the ν_3 mass state and CP violation would not be possible in the neutrino sector. Given that the current experimental bounds indicate that θ_{13} is already known to be small relative to the other angles, it presents an a priori experimental challenge.

One of the main goals of LBNE will be the identification of $\nu_\mu \rightarrow \nu_e$ and $\overline{\nu}_\mu \rightarrow \overline{\nu}_e$ oscillations. Measurement of the appearance rate will require identification of ν_e and $\overline{\nu}_e$ interactions as a

function of neutrino energy in the far detectors. The values of θ_{23} and the absolute value of Δm^2_{32} can be probed through the study of the disappearance of ν_μ. Precise measurements of Δm^2_{32} and θ_{23} will be performed in the LBNE far detectors by measuring distortions in the ν_μ and $\overline{\nu}_\mu$ spectra due to oscillations in both neutrino and antineutrino running. Observation of $\nu_\mu \rightarrow \nu_e$ oscillations is the key to measuring θ_{13} and determining the mass hierarchy (the sign of Δm^2_{32}, which can't be determined by ν_μ disappearance). The signature of CP violation (and a measurement of δ_{CP}) is a difference in the probability for $\nu_\mu \rightarrow \nu_e$ and $\overline{\nu}_\mu \rightarrow \overline{\nu}_e$ transitions. The signal for $\nu_\mu \rightarrow \nu_e$ oscillations is a small number of ν_e interactions among a large number of ν_μ interactions.

1.1.10.2 Search for Proton Decay

The search for proton decay tests the apparent but unexplained conservation of baryon number. In the Standard Model, baryon and lepton number conservation is a consequence of the quarks and leptons being organized in separate multiplets. Grand unified theories (GUTs) organize the quarks and leptons into combined multiplets and allow for the conversion of quarks into leptons by the exchange of a force-carrying particle. There is indirect evidence for such unification at scales of 10^{14} to 10^{16} GeV, based on the evolution of the Standard Model coupling constants. However, these energy scales are forever inaccessible at accelerators. Assuming the mass of the force-carrying particle is at these scales, the proton or bound neutron is predicted to decay to leptons and mesons, but at very slow rates, commensurate with observed stability of matter. Establishing this picture of the violation of baryon number conservation would have profound implications for our understanding of cosmology and particle physics.

Experimental searches now need to be prepared to search for very long proton lifetimes, indicating the need for very massive detectors and very long exposure times. GUT theories based on a minimal supersymmetric model predict a unification energy on the order of 10^{16} GeV and push the partial lifetime in the $e\pi^0$ channel to on the order 10^{36} years — more than two orders of magnitude beyond present experimental limits. However, some of these models do predict a partial lifetime on the order 10^{34} years in the mode $\overline{\nu}K^+$, which has important implications for a next-generation search.

The primary requirements for a proton decay search are (large — **FIXME:** *quantify*) mass and (near 100%?) live-time. In addition, a low background rate and significant detection efficiency are desirable. There are two primary physics channels of study: $p \rightarrow e\pi^0$ and $p \rightarrow K^+$.

FIXME: *add table of efficiency and bkgrd for 2 decay modes WCD and LAr*

1.1.10.3 Other Topics

Locating LBNE's massive detectors deep underground where they are shielded from backgrounds created by cosmic rays provides the opportunity to extend LBNE's science reach to include searches for neutrinos from supernovae, the sun, the atmosphere and other rare phenomena.

Galactic Supernova Bursts

A core-collapse supernova provides a wealth of information via its neutrino signal. About 99% of the supernova's energy is released in an initial neutrino burst that lasts a few tens of seconds, expelling about half the neutrinos in the first second. Due to the small neutrino cross section, only massive neutrino bursts from supernovae in our own galaxy or nearby galaxies can be detected. From 10 kpc (a bit beyond the center of our galaxy), a core-collapse supernova would produce a few hundred neutrino interactions per kiloton of either a water Cherenkov or liquid argon detector. The expected number of events scales with supernova distance as $1/D^2$.

Supernova Relic Neutrinos

Core-collapse supernova explosions throughout the history of the universe left behind a diffuse background of neutrinos, which should be detectable on Earth. While these supernova relic neutrinos (SRN) undoubtedly permeate the universe, they have thus far evaded detection. The flux and spectrum of these neutrinos contain information about the rate of supernova explosions (and consequently the star formation rate) in the past. Because the existence of such a flux is a robust prediction of most models of stellar formation, observation of this flux would provide a key indication that our general idea of how and in what epoch stars formed is correct. Though valuable information can be obtained from a nearby supernova burst, it is a very rare event and one may not be detected within the next few decades. Thus detection of the relic neutrinos is especially important. Though SRN models vary, according to one widely accepted modern analysis [ref], a 300-kT water Cherenkov detector located deep underground and doped with gadolinium should record about 50 of these supernova events every year. This data would undoubtedly stimulate new theoretical (and perhaps even experimental) developments in the neutrino and cosmology communities.

1.2 Introduction to the Liquid Argon Far Detector Concept

1.2.1 Liquid Argon Technology

The extraction of future physics results from neutrino experiments requires detectors that are both extremely massive and able to make detailed measurements of the patterns of energy deposition. Because neutrinos interact only weakly with ordinary matter, large detector mass (at least a few times 10^4 metric tons) is necessary to obtain a measureable interaction rate for pro-

cesses of current and future interest, such as ν_μ to ν_e oscillation. Conclusive identification of specific neutrino-induced events, for example, ν_e appearance, also requires detailed energy-deposition measurements to reject similarly-appearing background interactions from other processes.

The ability of current detectors, such as MINOS, to search for ν_μ to ν_e oscillation and potentially measure leptonic CP violation is limited by both interaction rate and background rejection capability. Improvements in both these detector capabilities will facilitate finding answers to important questions, such as the mechanisms for the matter-antimatter asymmetry in the universe. The next generation detector following MINOS is NOvA, with a mass of ≈ 15 kton, a spatial resolution of a few centimeters and an energy resolution of a few percent. A new, large-scale detector with at least the mass and energy resolution of NOvA, but with a few millimeters spatial resolution will represent a significant advance beyond NOvA in capabilities for the study of weak interactions and neutrinos, and their implications for the evolution of the universe.

Current and under-construction neutrino detectors use a range of technologies. Super–Kamiokande is a water Cherenkov detector (WCD); MINOS is a segmented, plastic-scintillator and iron detector; MiniBooNE is a mineral oil Cherenkov detector; ICARUS uses liquid argon and NOvA is constructed from PVC extruded channels filled with liquid scintillator. Each of these technologies has advantages and disadvantages.

The design of an LBNE detector involves a trade-off between mass, background-rejection and localization capabilities, depth —and ultimately — cost. Background rejection and localization include both the ability to withstand and reject cosmic ray-induced backgrounds and the ability to uniquely identify the various types of neutrino-induced events. The better the ability to withstand and reject cosmic rays, the shallower the depth required for siting the detector. The better the ability to uniquely identify neutrino-induced events, the more efficient the detector will be, thus requiring less mass to achieve the same physics goals.

The very large Water Cherenkov Detector included in the conceptual design for LBNE is an extension of current technology, particularly of Super–Kamiokande. Here, in contrast, we describe a newer technology: Liquid Argon Time Projection Chamber (LArTPC). While at least one large LArTPC exists (ICARUS), it does not have the same level of operational experience as Super–Kamiokande. An LArTPC features a couple of notable strengths, however. First, it enables detailed, reconstructed images of neutrino scattering events, which leads to a high level of background rejection. Secondly, it allows for comparatively localized event topologies, which lets the detector simultaneously measure multiple events from, for example, cosmic rays, and distinguish nicely between them.

More specifically, LAr technology provides:

- Highly accurate differentiation of electrons vs. photons by high-resolution measurements of electromagnetic shower development in the vicinity of the interaction vertex,
- High-resolution reconstruction of the recoil hadronic shower, including nuclear debris, and

- Excellent sensitivity to low-energy hadrons, that are below Cherenkov threshold in water.

Detector simulations indicate that an LArTPC detector can be located at a moderate depth ($\approx$ 800 ft) and still achieve sufficient rejection of cosmic ray-induced background, even for non-beam-event related studies, such as the searches for proton decay and supernova neutrinos. In addition, LAr pattern-recognition capabilities make this technology more efficient. The physics observational capabilities of an LAr Detector are comparable to those of a much larger Cherenkov detector, which provides less detailed information about events. Although the exact equivalence factor between LAr and Cherenkov technologies depends on specific event topologies, simulation studies suggest that an LAr detector has equivalent physics reach to a water Cherenkov detector approximately six times larger in mass.

While LArTPC technology is very promising because of its likely high spatial and excellent energy resolutions, it clearly requires development and operational experience. It is also important to assess the scalability of LArTPC technology to masses of as much as 10^5 tons that may be required for future neutrino experiments.

Advisory committees, such as NuSAG and P5 have strongly endorsed the development of LArTPC technology as a significant step forward for both the neutrino and the wider particle physics communities [x].

1.2.2 Historical Precedents

FIXME: *need text – added 8/5 because WCD has this section*

1.2.3 An LArTPC Implementation for LBNE

1.2.3.1 Scientific Requirements

See figure 1.2 for a table of requirements.

FIXME: *I propose moving the following to Vol 1 sec 3.4 Depth Req; and making sure the numbers are in the table – I don't know, still thinking about this*

The depth for the LAr20 Detector location represents a trade-off between physics background and detector size and cost. For a fixed-dollar budget, we must choose between a larger detector at shallower depth (due to lower cost per ton), or a smaller one placed deeper underground. The former option offers higher potential measurement capability due to size, whereas the latter offers minimization of cosmic-ray-induced backgrounds due to depth. For detector op-

timization, the layout of the Homestake Mine suggests strong consideration of three possible depths:

300 feet At this shallow depth, approximately horizontal access is possible by constructing tunnels from the canyon east of the Yates Shaft. However, cosmic ray background, including from both the east and west sides, is likely to complicate non-neutrino beam measurements.

800 feet At this moderate depth, cosmic ray background is reduced from that at the 300-ft level by about a factor of 10, by both increased vertical overburden and a depth profile that in percentage terms is more flat and less like a mountain. Adding an active shield to the LAr20 Detector at this depth would likely enable achieving physics goals for a range of beam and non-beam experiments, competitive with the same detector at 4850 ft. Primary access to the LAr20 Detector Laboratory would be through a decline-road tunnel, thus mostly isolating LAr20 from shaft contention with other DUSEL activities.

4850 feet This location at DUSEL's most active level would significantly limit the rate of background events and remove the necessity for an active shield. It would likely be necessary to raise-bore one new, dedicated LAr20 shaft, combined with use of the Yates and Ross Shafts for secondary access. This location would require more careful coordination with other DUSEL activities.

The conceptual design process concludes that the most favorable depth for LAr20 is 800 feet. With the active shield described later in this report, this depth should provide sensitivity to most, if not all, of the possible physics range of such a detector. Compared to the 4850-ft level, the preferred 800-ft level simplifies both access and the cryogenics system design, and reduces the possibility of shaft-access contention with DUSEL and its other experiments.

1.2.3.2 Reference Design

In the LBNE Conceptual Design Report, we describe a particular LArTPC implementation, called the LAr20 Detector, as a step towards achieving the scientific goals of the Long- Baseline Neutrino Experiment (LBNE). The LAr20 conceptualization has a total active mass of 20.5 kton and a fiducial mass of 16.7 kton. High-purity LAr serves as both the neutrino target and the tracking medium for the particles produced in the interaction. The overall dimensions of the active volume are 15.0 m wide (in x) by 14.0 m high (in y) by 71.1 m long (in z).

The LAr20 Detector will identify neutrino events through the observation of the outgoing charged particles resulting from neutrino interactions in the LAr. A uniform electric field in the LAr volume will cause ionization electrons produced by the passage of these charged particles to drift to three wire planes. The electric potentials of the three wire planes will be arranged such that the electrons will pass through the first two planes, to be collected on the third.

The passage of electrons through the first two planes will produce induced, bipolar signals on those wires. The deposition of electrons on the third plane will produce negative unipolar pulses. ÃćâĆňÅŞColdÃćâĆňÂİ electronics within the LAr20 vessel will amplify the signals on each wire and continuously digitize the amplified waveforms at 2 MHz. The proposed LAr20 wire pitch in all planes is 3 mm; therefore, LAr20 position resolutions will be at the millimeter scale. The trajectory of particles in the detector will be reconstructed from the known wire positions and the arrival times of electron signals on the wires, combined with the time the interaction took place in the detector. The amplitude of the ionization electron signals measures the energy loss of the particles, which enables an estimate of their momentum and their particle type.

The main features of the LAr20 Detector are shown in **FIXME:** *Fig. [XXX]*. LAr20's single cryogenic volume will be divided into 168 Time Projection Modules (TPMs), three modules wide in x, two modules high in y and 28 modules long in z. The TPM dimensions are 5.0 m in x (the drift direction), 7.0 m in y and 2.5 m in z.

Each TPM will consist of two cathode planes (each plane 2.5 m wide and 7.0 m high in the y-z plane) and a central Anode Plane Assembly (APA) of the same size. The maximum drift distance will be 2.5 m. The TPMs will be arranged to share cathode planes, so that in the x direction, there will be four cathode planes interleaved by three APAs to form three TPMs. Thus, in all, the LAr20 Detector will have 168 APAs and 224 cathode planes.

The LAr20 cathode planes will be held at an electric potential of -123 kV to create an electric field of 500 V/cm between the cathode and anode planes. This field will produce an electron drift velocity in the LAr of 1.6 mm/μs. Each APA will contain four planes of wires in a wrapped configuration, as shown in Fig. 2.**FIXME:** *add ref* The wire planes are labeled *grid plane*, *induction plane 1*, *induction plane 2* and *collection plane*. The purpose of the grid plane is solely to improve the effectiveness of induction plane 1. It will not be instrumented with readout electronics. In total, LAr20 will have 645,065 readout wires and 282,240 grid wires.

Each row of cathode planes and APAs will be surrounded by a "field cage" constructed of copper-plated, circuit-board material. The purpose of the "field cage" is to shape the electric field in the LAr to ensure uniform electron-drift trajectories near the detector edges. A resistor chain between the cathodes and anodes will establish the electric potential of the field.

A major feature of LAr20 will be the use of cryogenic, or "cold," electronics. Signals from each wire channel will be amplified, shaped and digitized by the analog section of integrated electronics, mounted directly on the APA and within the cryogenic volume. The digital section of these same electronics will provide zero-suppression and 128-fold multiplexing. Multiplexed signals will be routed by optical fibers through cryogenic feedthroughs, located at the top of the cryostat. A local computer cluster will provide triggering and event selection. Data will be stored at the detector location and also transported to Fermilab and other collaborating institutions for archival storage and offline analysis.

A single cryostat will house all the TPMs, containing the LAr at a temperature of 87 K

and insulating it from external heat. Conceptual design studies resulting in this report suggest that the optimal choice for cryostat design is a single "membrane cryostat." The most notable feature of a membrane cryostat is the use of a thin metallic liner to contain the liquid argon. A cross-sectional view of the membrane cryostat is shown in Fig. **FIXME:** *3*. The metallic liner will be constructed of 1.2-mm-thick stainless steel, corrugated in both directions to enable thermal expansion and contraction. The liner will attach to insulation units constructed of plywood boxes filled with polyurethane foam. The plywood will be of "marine grade," typically used for the construction of boats. The hydrostatic load of the liquid argon will transfer through the liner and insulation to the walls of the cavern, resulting in a highly efficient use of the excavated cavern volume. A secondary liner will provide an annular space for argon gas purges. A tertiary liner will prevent ground water infiltration. Membrane cryostats have been used for ocean transport and on-shore storage of liquefied natural gas for several decades.

The LAr in the membrane cryostat will be cooled by a cryogenics system that will primarily be located on the surface. Insulated cryogenic piping will connect the surface refrigeration plant with the underground cryostat and the LAr purification system that must be located adjacent to the cryostat. A surface location simplifies installation and maintenance and minimizes Oxygen Deficiency Hazard (ODH) because of the enhanced possibilities for air circulation and venting. Redundant LAr pumps, located inside the cryostat, will be used to recirculate the LAr through the purification system.

Drifting electrons over several meters requires minimizing electronegative contaminants in the liquid argon. Water vapor and oxygen are the major sources of electronegative contamination. The maximum design electron-drift time is 1.54 ms. The design electron lifetime is 1.4 ms. The design equivalent-O_2-contamination is 214 ppt. Contaminants will be removed by recirculating LAr through molecular sieves and copper filters. Purity monitors at the filter outlets will monitor their effectiveness. Argon flow will be diverted to a second set of filters when the first set is saturated. Saturated filters will be regenerated by circulating a 95% argon – 5% hydrogen gas mixture through them at elevated temperature. Argon gas boil-off from the top of the detector will be reliquified by a condenser and purified before it is returned to the cryostat.

The detector electronics will be configured to enable both continuous and triggered data acquisition. A trigger may be initiated by either a beam-spill signal from Fermilab or by a signal from a scintillation light-detection system. A beam spill will trigger data acquisition from the entire detector. Upon initiation of a photon detector trigger, only wires in the vicinity of the source of the scintillation light will be read out. Signals from some processes of physics interest (e.g., relic supernovae) may be below threshold for the light-detection system. Continuous readout of the detector will enable the study of such processes, given sufficient computing resources to store and offline-analyze the large amount of data that will be generated in a continuous readout mode.

1.2.3.3 Alternatives

1.2.4 Detector Performance

1.2.4.1 Reference Design

1.2.4.2 With Alternatives

1.3 Civil Construction Requirements

The civil construction requirements for LAr20 are mostly conventional — a major strength of its design. LAr20 will be installed in a "rural mailbox-style" cavern, a rectangular solid with a slightly domed roof. The LAr20 Detector will completely fill the cryostat pit excavated in the cavern floor, so that the cavern walls provide both secondary containment for the argon and support for the hydrostatic pressures produced by the contained liquid volume. Access tunnels will be located near the top of the cavern. Conventional steel truss-work will support the insulated cover comprising the top of the cryostat. Mechanical, electrical, telecommunications and other support systems will be located above the cryostat or in smaller caverns, adjacent to the top of the main detector cavern.

The LAr20 cavern will be excavated by conventional means (drill, blast, muck). The ceiling and walls will be stabilized by rock-bolting as necessary. The ceiling will be lined with shotcrete to prevent oxidation and exfoliation of the excavated rock. The walls and floor will be lined with poured concrete in direct contact with the surrounding rock to achieve the strength and smoothness required to support the LAr20 Detector.

The LAr20 cavern will be excavated on the 800-ft level near the existing Yates Shaft. A short tunnel will connect the cavern to the existing 800 ft-level tunnels. Primary access to the cavern will be made through a 1.4 km decline-access tunnel that will reach the surface near the existing Kirk portal. The tunnel will be 4 m wide x 6 m tall and will be excavated at a 12% grade.

Fresh air will be supplied to the LAr20 cavern via the decline access tunnel and will return to the surface through a 1 m-diameter ventilation shaft, thus completely isolating the LAr20 cavern from the DUSEL facility ventilation system. Multiple emergency egress routes will be provided. The primary route will be through two isolation bulkhead doors in the tunnel between the LAr20 cavern and the existing 800-ft-level access tunnel to the Yates Shaft. The space between the two isolation bulkhead doors will be outfitted as a refuge area. The secondary route will be through the decline access tunnel.

Cryogenic piping to the surface will be made through a second 1 m-diameter shaft.

1.4 Risk Overview

Risks associated with the LAr20 Detector can be categorized as either technology risks or project risks. The major risks associated with liquid argon TPC's have been highlighted in various reports and presentations over the past several years. While LAr20 will be the largest liquid argon TPC ever to be constructed, smaller LAr detectors, such as ICARUS and ArgoNeut, have worked well. Thus, the underlying design principles are already proven; the technology risks are associated with scaling up by significant factors. With regard to project risk, much can be learned from considerable experience at the 10^5 ton level with Liquified Natural Gas (LNG). Outside engineering firms with considerable LNG experience have contributed significantly to the development of this Conceptual Design Report.

A brief summary of risks associated with the LAr20 Detector is given here.Chapter 12 of this volume discusses risks and risk mitigation strategies in more detail. It is important to note that none of the risks associated with LAr20 are considered major despite their identification for discussion in this Conceptual Design Report.

The "Integrated Plan for LArTPC Neutrino Detectors in the U.S." was developed in 2009 to identify LAr technology risks using a bottoms-up approach. Some risks originally designated as technology risks were re-categorized as project risks during the analysis. The likelihood and consequence of each risk was classified using a semi-quantitative method adopted from the NSLS II project. The conclusion of the study is that the R&D activities (ArgoNeut, LAPD & MicroBooNE) mitigate LAr20 technology risks to an acceptable level. This study also identified project risks for a large LAr TPC and recommended new R&D activities. These R&D activities are being addressed by the LAr20 project, following plan was reviewed by the Fermilab Directorate and submitted to the DOE in December 2009.

The principal technology risks are associated with the efforts to:

- Achieve adequate purity in the liquid argon
- Develop effective LAr pattern-recognition and physics-analysis software tools
- Develop large-scale, low-noise cryogenic electronics
- Scale up from MicroBooNE to LAr20

Major LAr20 project risks are associated with:

- Underground safety
- DUSEL itself:

- funding and political risks
- possible impacts of other experiments

1.5 Summary

The conclusion of this Conceptual Design Report is that LAr20 represents a bold, but achievable step towards implementing detecror technology that can address fundamental questions in elementary particle physics, astrophysics and cosmology. There is no other technology visible on the horizon that might produce the type of detailed images of neutrino and other particle physics interactions that can be achieved with liquid argon. At least for the next several decades, liquid argon is the best we can do. A stepwise program with LAr20 as the next step after MicroBooNE will provide valuable experience in operating successively detectors that will have increasingly better ability to answer fundamental physics questions such as the nature of matter interactions and the detailed history of the formation of the Universe in the "Big Bang" about 14 billion years ago.

Version 4.4 - 6/28/2010

Parameter	Value	Units	Quality	Notes
Anode Plane Assembly (APA)				
Wire spacing - X plane	3	mm	***	
Wire spacing - U,V plane	3.3	mm	**	Should be ~3mm. Size chosen to have an integral num of readout cards
Wire angle	45	deg	***	
APA length	2.52	m	**	Should be ~2.5m. Size chosen to have integral number of readout cards
Num grid wires	1680			Assume grid wires have same orientation as the X plane
Num U wires	1080			
Num V wires	1080			
Num X wires	1680			
APA num readout wires	3840			
Num readout channels	30			
APA total num wires	5520			
Drift distance	2.47	m	***	Any value near 2.5m is OK. Set to give 2.5m cell incl APA thickness
Wire wrap length	2.52	m		
Num wire wraps	2.78			
APA height	7.0	m	***	Any value near 7m is OK
APA thickness	7	cm	***	2" thick SS frame + 3 wire planes on both sides
APA weight	250	kg	**	
Cathode plane weight	100	kg	**	
U,V Wire length	9.9	m		
Wire capacitance (in air)	15	pF/m		H. Jostlein measurement of prototype
U,V wire capacitance (in LAr)	238	pF		Apply dielectric constant for LAr
APA Cell Volume	87	m^3		Each cell has one APA in the middle
APA Cell Active Mass	0.122	kton		
APA Transverse Fiducial cut	0.3	m	*	Approx value for neutrino oscillation physics
APA Fiducial Volume	73	m^3		Transverse fid cut on both sides of APA + one cut at the top/bottom)
APA Fiducial Fraction	84%			
APA Fiducial Mass	0.102	kton		
Detector				
Num Vertical APA's	2		***	
Detector Vertical APA gap	2	cm	*	Reasonable guess. No detailed design yet
Detector Height	14.0	m		
Num Transverse APA's	3		***	
Detector Width	15.0	m		
Num Longitudinal APA's	28		***	
Detector Longitudinal APA gap	2	cm	*	No detailed design yet. Allow space for cell stiffeners
Detector Length	71.1	m		
Total number of APAs	168			
Total number of cathode planes	224			
Detector Longitudinal Fid cut	1.5	m	*	Approx value for neutrino oscillation physics. 10cm US, 140cm DS
Longitudinal Fid fraction	98%			
Detector Fiducial Mass	16.8	kton		
Number of readout wires	645,065			
Number of readout channels	5040			
Number of grid wires	282,240			
Cryostat				
Distance btw cathode plane & wall	0.5	m	**	No design yet. Space for purity monitors, instrumentation, etc
Cryostat Width	16.0	m		
APA height above floor	0.5	m	*	No design yet. Space for LAr piping, APA suppt rail, electronics
LAr depth above APA	0.5	m	*	No design yet. Space for electronics
LAr Depth	15.0	m		
Ullage %	5.0%		***	
Ullage depth	0.8	m		
Cryostat Depth	16.0	m		Should be integral # of meters for membrane panels
Distance btw detector & far end wall	0.5	m	*	No design yet. Space for purity monitors, instrumentation, etc
Hatch & pump clearance at near end	2.0	m	*	No design yet. Space for access hatch, LAr recirc pumps
Cryostat Length	74.0	m		Should be integral # of meters for membrane panels
Cryostat Volume	18944	m^3		
Total LAr Mass	25	kton		

Fig. 1.1. Design parameters - part 1

Version 4.4 - 6/28/2010

Parameter	Value	Units	Quality	Notes
Cryostat Pit				
Insulation thickness	1	m	**	No detailed design yet. Set by the heat loss coefficient
Insulation heat loss coefficient	5.0	W/m^2	**	The insulation design goal
Concrete pit thickness	0.5	m	***	
Pit Width	19.0	m		
Pit Depth	18.5	m		
Pit Length	77.0	m		
Pit Volume	27066	m^3		
Pit Surface Area	6478	m^2		
Insulation heat loss	32	kW		
Electronics				
Mux level	128		***	
Analog front end power	10		**	Design goal
Digital front end power	5		*	Needs to be defined
Power conversion efficiency	100%		*	Needs to be defined
Electronics power dissipation	15	mW/chan	**	
Electronics power total	9.7	kW		
ENC	743	electrons		Paul Rubinov parameterization. Ref BNL docdb 626
Ionization (1 MIP after recombination)	3	fC		
Electron drift velocity	1.6	mm/micro-sec	***	
Electron drift time	1.54	ms		
Electron lifetime assumption	1.4	ms	**	Set to achieve minimum S/N = 8
Equivalent O2 contamination	214	ppt		
Signal to noise ratio max	25			
Signal to noise ratio min	8			
Sampling rate	2	MHz		
High Voltage				
Drift field	500	V/cm	***	
Cathode high voltage	123	kV		
Grid bias voltage	-480	V	**	Adjust to achieve transparency
U plane bias voltage	-280	V	**	Adjust to achieve transparency
V plane bias voltage	0	V	**	Adjust to achieve transparency
Collection plane bias voltage	700	V	**	Adjust to collect electrons
Cryogenics				
Num recirculation pumps	4		*	Provides redundancy during operation. None during initial purification
Recirculation pump flowrate	47,000	kg/hr	**	Set to achieve LAr volume turnover similar to ICARUS
	34	m^3/hr		
	150	gpm		
Recirculation pump flowrate - max	188,000	kg/hr		
	136	m^3/hr		
	598	gpm		
LAr volume turnover @ max flowrate	5	days		
Pump power	6	kW	**	Assumes 30m (60 psi) head pressure
Pump power - max	24	kW	**	Assumes 30m (60 psi) head pressure
Refrigeration load	48	kW		
Refrigeration load - max	66	kW		
Refrigeration plant capacity	50	kW	**	From Arup concept report
Refrigeration plant margin	4%			
Refrigeration power	560	kW	**	From Arup concept report
Refrigerator output	140	kW	**	From Arup concept report
LN2 storage dewar	100	m^3	**	From Arup concept report
LN2 storage dewar backup capacity	3	days	**	From Arup concept report
Detector Depth				
Detector Depth	800	ft	*	
	240	m		
Cosmic ray rate	0.06	Hz/m^2		
Cosmic ray rate - detector top	64	Hz		
Cosmic ray rate - APA top	0.7	Hz		

Fig. 1.2. Design parameters - part 2

Bibliography

[1] "Title", Month, year.

2 Cryogenics System And Cryostat (WBS 1.5.2)

2.1 Cryostat and Cryogenics Overview

Two key elements comprise the LAr20 Detector: the cryostat to contain the liquid argon (LAr) and the cryogenics system to acquire, maintain and purify the LAr. Because these two subsystems are highly related, we discuss them together in this chapter.

The reference conceptual design for the LAr20 Detector cryostat specifies a single, rectangular vessel measuring 16.0 m in width, 16.0 m in height and 74.0 m in length, and containing a total active mass of 20 kton of LAr. The reference design is of the "membrane" type, commonly used for liquified natural gas (LNG) storage and transport tanks. A membrane tank uses a thin, stainless-steel liner to contain the liquid cryogen. The pressure loading of the liquid cryogen is transmitted through rigid foam insulation to the surrounding rock. Thus the surrounding rock provides external support for the liner. The membrane liner is corrugated to provide strain relief resulting from temperature-related expansion and contraction.

The reference design was selected on the recommendation of the highly-experienced, engineering consultants from Arup after consideration of an alternative design (see Chapter **FIXME: ??**) using segmented, modular cryostats, which are internally self-supporting. The major advantage of the membrane cryostat is a significantly reduced cost compared to the modular cryostat alternative. The membrane cryostat is itself cheaper, because of the relative simplicity of a single cryogenic volume. The membrane cryostat also uses the underground cavern volume more efficiently, which reduces the civil construction costs for the project. Finally, the single volume of the membrane cryostat results in fewer "dead spots" in the detector and thus improves the ratio of usable (fiducial) mass to total mass.

Conceptual design studies indicate that the implementation strategy for the cryogenics system is independent of the cryostat design. The major design decision for the cryogenics system is its location. Siting the majority of the system on the surface would simplify access for maintenance and would reduce the oxygen deficiency hazard. This configuration requires long insulated pipe runs and high pumping power for the deeper options. At the 4850 level, the vertical cryogenic piping would require pressure-reducing devices for downward flow and multiple pumps at

Fig. 2.1. Sample membrane tank interior

intermediate vertical levels for upward flow. These effects are mitigated by siting the detector at the 800 level.

The scope of the cryostat and cryogenics system for both the reference design membrane cryostat and the alternative design modular cryostat encompasses:

- The 20-kton LAr20 Detector cryostat
- Liquid argon (LAr) offloading and receipt facilities
- Transfer system to deliver LAr to the underground detector cryostat
- Boil-off gas reliquefaction equipment
- LAr purification apparatus
- Cryostat purge facilities

2.2 The LAr20 Membrane Cryostat

2.2.1 Cavern Layout for Cryostat

The membrane tank is a sealed container that relies on external support from the surrounding rock to resist the hydrostatic load of the contents. The tank is comprised of a formed, concrete liner poured against the sides and bottom of the excavated rock pit. Anchor bolts are then embedded into the concrete at ≈ 3-meter intervals. Factory-made 1-meter × 3-meter insulation boxes are bolted onto anchor bolts. The insulation contains a secondary membrane. The secondary membrane portions between boxes are joined to form a continuous liner that can hold the liquid cryogen if the inner primary membrane leaks. Foam bridge panels are applied over the secondary membrane to form a planar surface to which 1-meter × 3-meter primary membrane panels are attached. A steel-truss structure spans the top of the concrete wall forming the roof of the cryogen container. The roof truss has a solid-plate underside that forms a moisture-tight vapor barrier similar in function to the concrete lining of the walls and floor slab. The details of these various layers are shown in Figure 2.2 and specified in Table 2.1.

The stainless steel membrane and the intermediate layers of insulation and vapor barrier continue across the top of the detector, providing a vapor-tight seal. These layers across the top are supported by a steel plate, tied to a steel truss structure that bridges across the detector. The truss structure is itself tied to the cavern walls and ceiling with rock bolts. The hydrostatic load of the LAr in the cryostat is carried by the bottom and the side walls. However, everything else within the cryostat (TPC planes, electronics, sensors, cryogenic and gas plumbing connections)

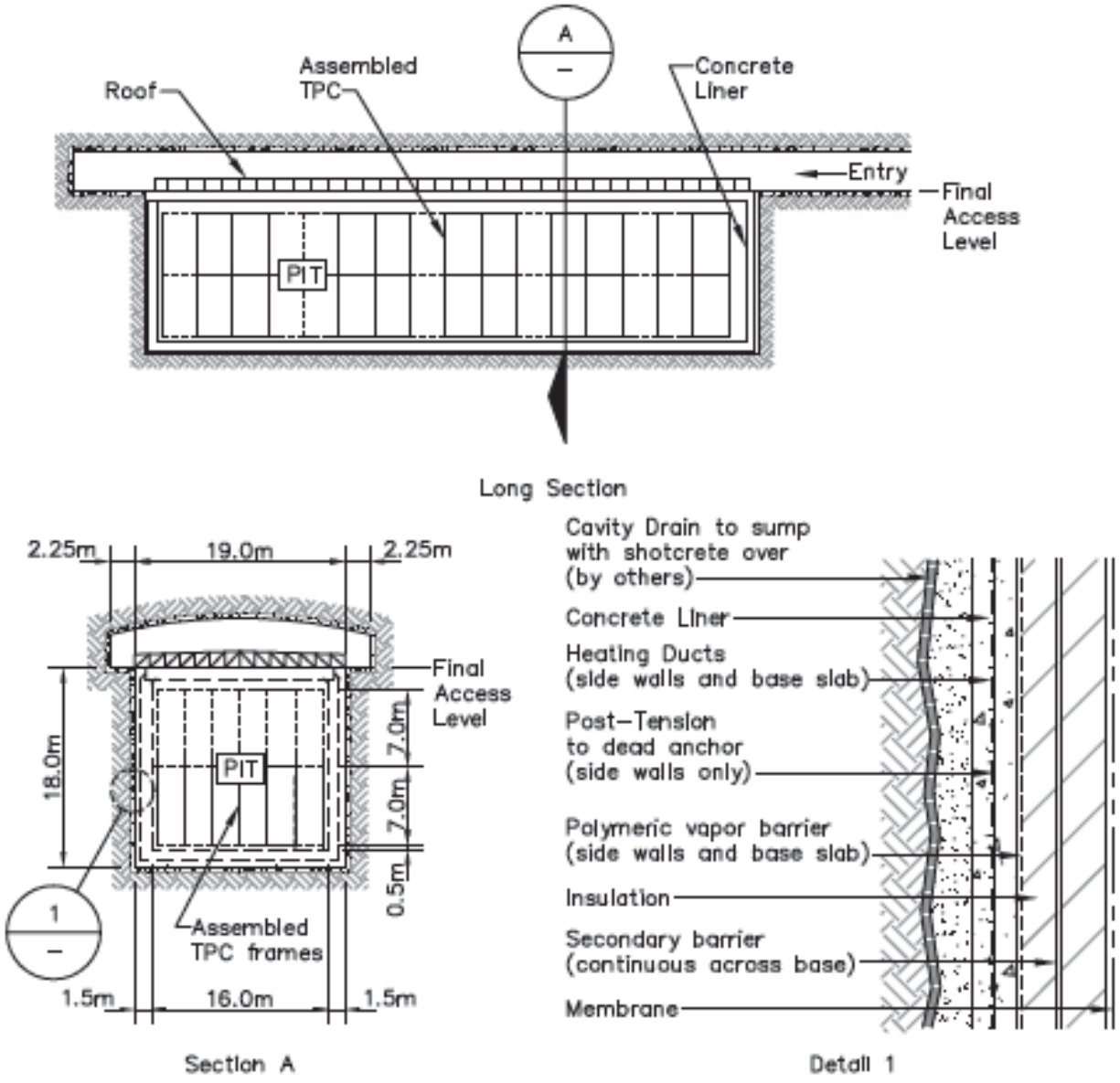

Fig. 2.2. Membrane tank key components

Table 2.1. Summary of parameters for the LAr20 Cryostat

Total Volume:	
LAr Total Mass:	
Inner/Outer Height of the Tank:	16 m/19 m
Inner/Outer Width of the Tank:	16 m/19 m
Inner/Outer Length of the Tank:	74 m/77 m
Insulation:	Reinforced Polyurethane; inner layer is 30 cm thick, outer layer is 70 cm thick
Secondary Containment:	$\approx$ 0.5 mm thick aluminum, located between insulation layers
Outer Concrete Layer:	0.5 m thick, inner surface treated with a vapor barrier
LAr Temperature:	89 $\pm$ 1 K
Depth of the Liquid (Liquid Head):	15.0 m
Design Operating Pressure (Above Liquid):	0.113 MPa
Design Operating Pressure (Bottom of Liquid):	0.316 MPa
Rated Pressure Capacity of Tank:	0.52 MPa (calculated according to BS EN 14620) (British-Adopted European Standard / 29-Dec-2006 / 60 pages ISBN: 0580497763)

are supported by the top plate. All piping and electrical penetrations into the interior of the cryostat are also made through the top plate, in order to minimize the possibility of leaks.

FIXME: *I need orig jpg – this is too fuzzy*

2.2.2 Cryostat Parameters

FIXME: *Why is table 2.1 (below in source file) above this heading in PDF?*

Side walls of the membrane tank will be completely surrounded by (in order) insulation, a secondary thin aluminum membrane, more insulation, concrete, and rock. This "in-ground" tank arrangement (i.e., offering access only from the top) gives fundamental protection against possible cryogen leaking out of the tank — there is no place for the cryogen to go because it is surrounded on all sides by rock. The membrane cryostat is considered a "full containment" system in the LNG industry lexicon. The basic components of the membrane tank are illustrated in Figure 2.2.

2.3 Cavern Layout

The LAr20 Detector cavern will be excavated with a "mushroom" cross section. The "mushroom stem," which fits tightly around the cryostat, will have the same inner dimensions as the outer dimensions of the cryostat, including its insulation, namely 19 m wide by 19 m high by 77 m long. The "mushroom top," located above the cryostat pit, will be 25 m wide by 91 m long. The cavern roof will have a domed cross section, providing a clearance of 8 m in the center and $\approx$ 5 m on the sides. The "mushroom top" will extend 7 m beyond each end of the detector, in order to provide additional space (25 m wide by 7 m long) for ancillary equipment and installation and maintenance operations. The long axis of the cavern will point towards Fermilab. Walkways will run the entire length of the cavern on each side of the detector to provide personnel access. A separately ventilated emergency egress passageway will be located on one side of the cavern. The cryostat cover will be designed to allow easy access to the the emergency passageway from the other side of the cavern. One walkway is 3 m wide which provides sufficient clearance to remove the largest component of the refrigeration system.

2.3.1 Concrete liner

If left unheated, eventually the concrete and rock surrounding the tank would cool and possibly introduce problems associated with freezing water and heaving. Some underground LNG storage caverns rely on the insulating properties of frozen rock to minimize construction cost. The GEOSTOCK pilot plant in South Korea is an example of such a cavern that also uses a membrane cryostat. The reference design includes conduits and heating tape embedded in the concrete to maintain rock temperatures above freezing to alleviate potential concerns about rock heaving. See figure 2.3.

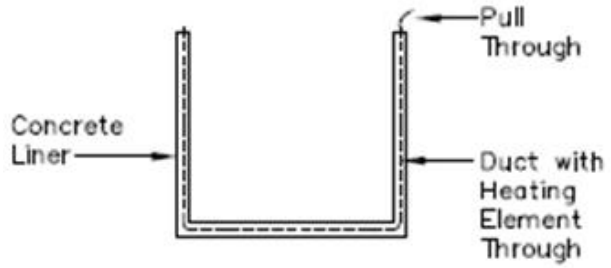

Section A

FIXME: *This is fuzzy even at .5 width; need original, plus it needs to illustrate all the components discussed*

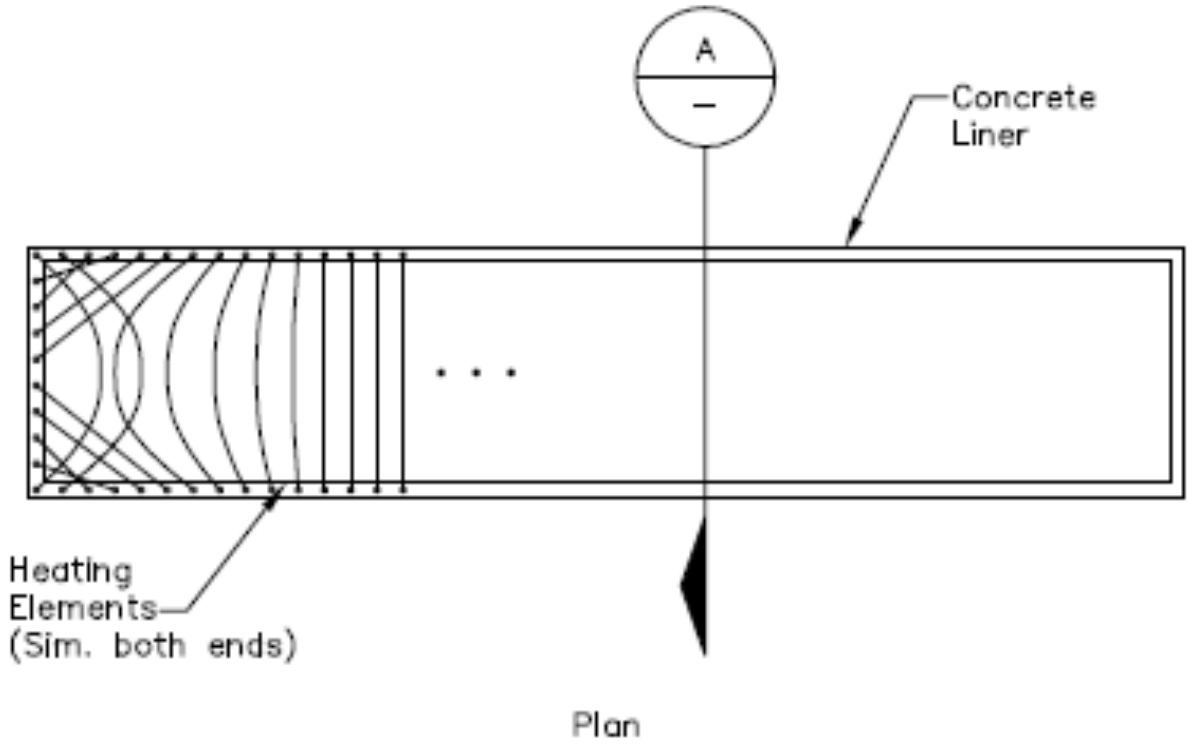

Fig. 2.3. Membrane cryostat heating system

A secondary, aluminum barrier placed within the insulation space surrounds the internal tank on the bottom and sides, and separates the insulation space into two distinct, leak-tight, inner and outer volumes. The barrier is placed 30 cm into the insulation from the primary membrane. A thickness of 70 cm of insulation is placed between the secondary barrier and the concrete. This barrier is connected to embedded metal plates in the vertical concrete wall at the upper edge of the tank. In the unlikely event of an internal leak from the cryostat's primary membrane into the inner insulation space, it will prevent liquid cryogen from migrating all the way through the insulation to the concrete liner.

2.3.2 Roof structure

The cryostat roof is made of a truss structure. Stiffened steel plates are hermetically welded to the underside of the truss. The plates form a flat surface onto which the roof insulation and membrane may be directly attached. Insulation boxes **FIXME:** *Needs an illustration* are attached to the roof plates and inner primary membrane panels attached to that. The lightweight, steel roof truss will be post-tensioned to the top of the poured-concrete-liner walls to resist the uplift caused by internal tank overpressure (refer to figure 2.5). The roof truss will be pre-fabricated off-site in ∼2 m wide, fully welded modules and transported to the cavern as required by the installation schedule.

The steel modules are relatively lightweight (∼ 8,000 kg each) and require only moderate crane capacity. If the steel trusses need to be separated into smaller pre-fabricated units for transport to the shallow or deeper site, assembly within the cavern space prior to installation is relatively straightforward. The steel roof truss was selected during the screening process since it is an efficient, gas-tight solution that can be readily constructed within the cavern space.

2.3.3 Vapor barrier

A vapor barrier is required on all internal surfaces of the concrete liner (base slab, side walls, end walls) and roof to prevent the ingress of any water vapor into the insulation space. Water in this space could freeze and impede the thermal performance of the insulation. The barrier must also reliably absorb the stresses and strains from all normal loading conditions.

We discussed the vapor barrier for the roof in the previous section. For the other surfaces, we have selected a polymeric liner that has been used successfully in onshore LNG tank applications.

2.3.4 Insulation system

The membrane cryostat requires insulation applied to all internal surfaces of the concrete liner (base slab, side walls, end walls) and roof in order to control the heat ingress and required

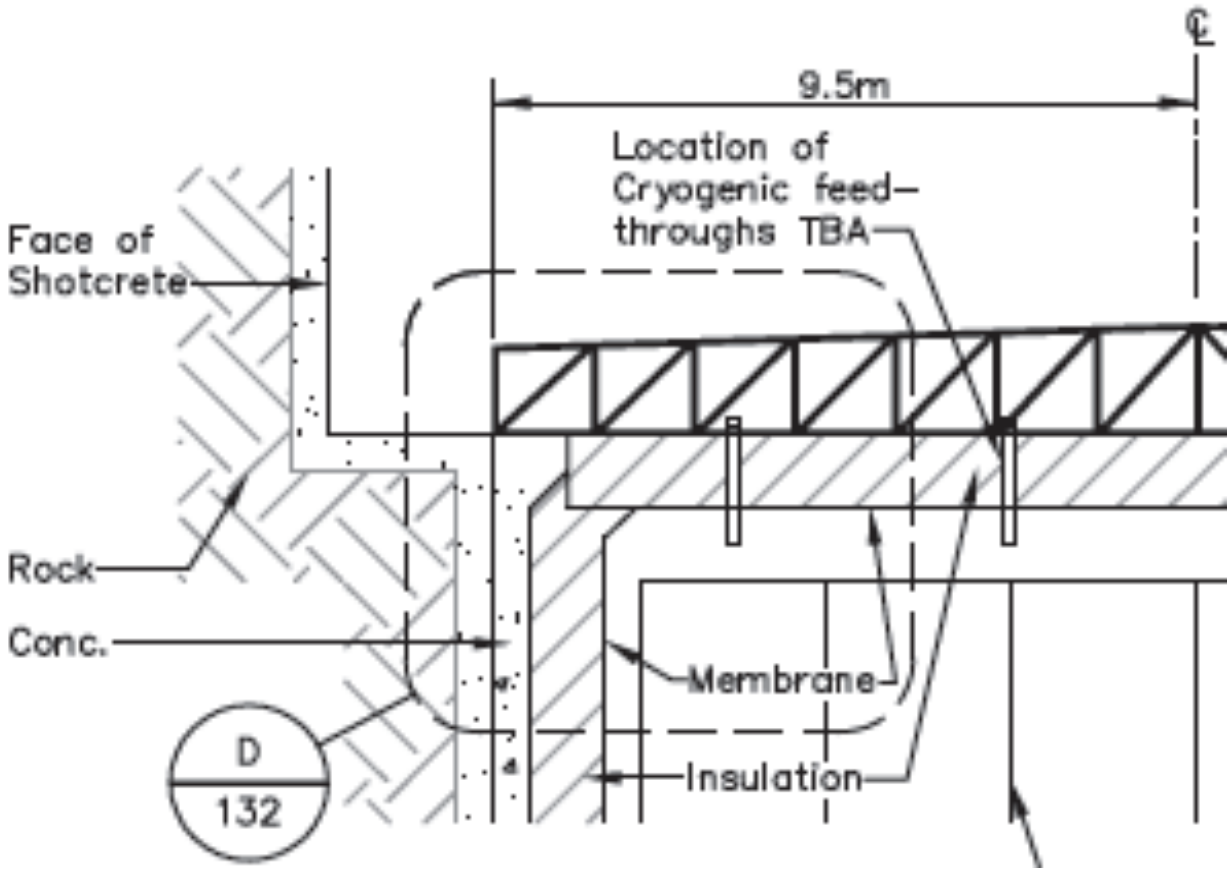

Fig. 2.4. THIS NEEDS A CAPTION. And a pointer to the truss area. Otherwise

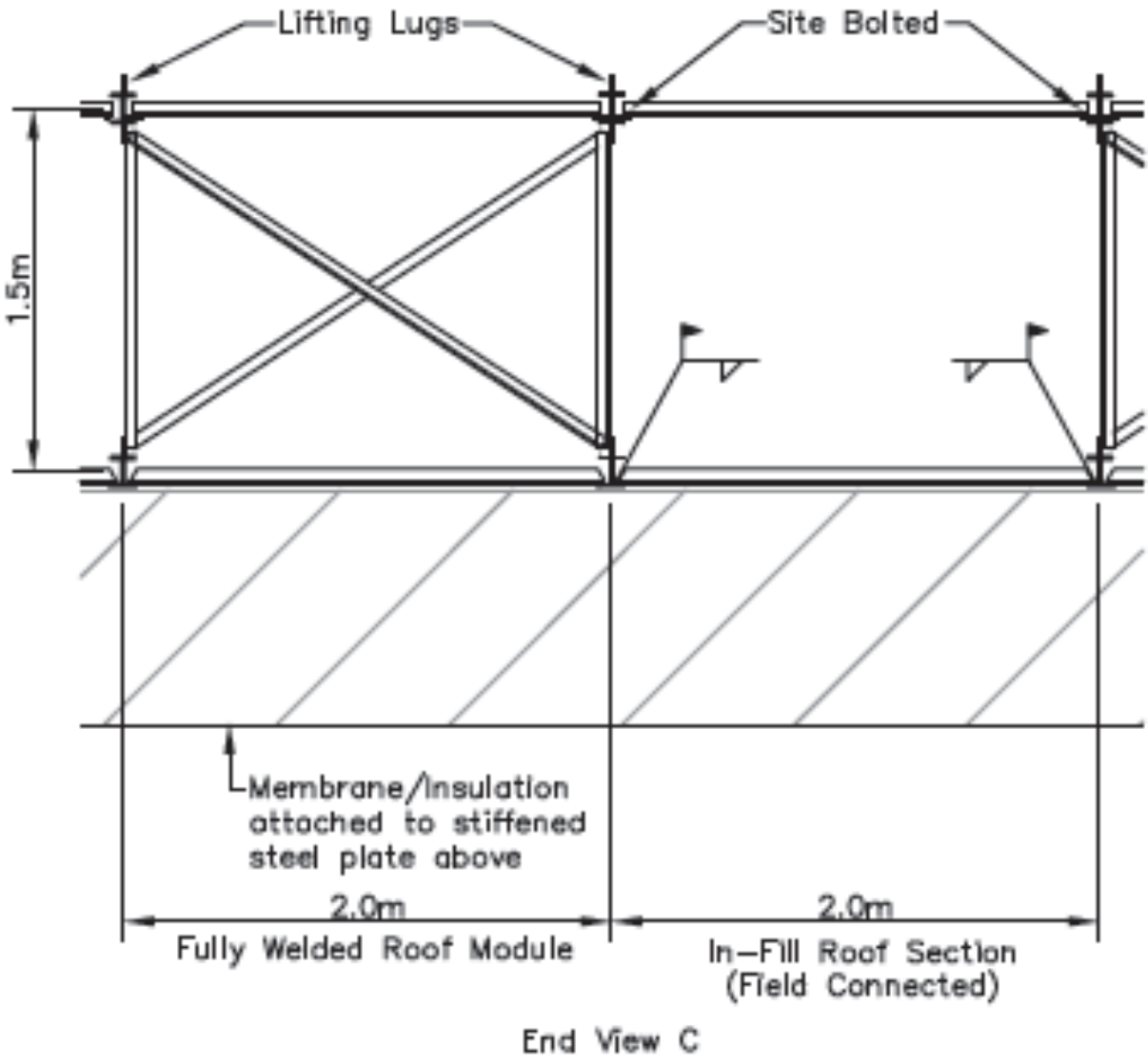

Fig. 2.5. Steel roof truss with lower steel plate **FIXME:** *need arrow to steel plate*

Table 2.2. Heat load calculation (Thickness = 1 m for all) **FIXME:** *fix bottom line of table*

Element	Area (m^2)	C (W/mK)	ΔT (K)	Heat input (kW)
Base	1150	0.031	191	6.8
End walls	570	0.031	191	3.4
Side walls	2230	0.031	191	13.2
Roof	1150	0.031	207	7.6
			Total	31.0

refrigeration load. Membrane tank vendors have a "cryostat in a kit" design that incorporates insulation and secondary barriers into packaged units. See figure 2.6. Choosing a reasonable, maximum insulation thickness of 1 m, and given an average conductivity coefficient for the foam insulation of C≈0.031 W/mK, the heat input from the surrounding rock is expected to be ∼33 kW.

This is shown in table 2.2. See figure 2.7 for an illustration of the membrane technology system applied to our chosen reference design.

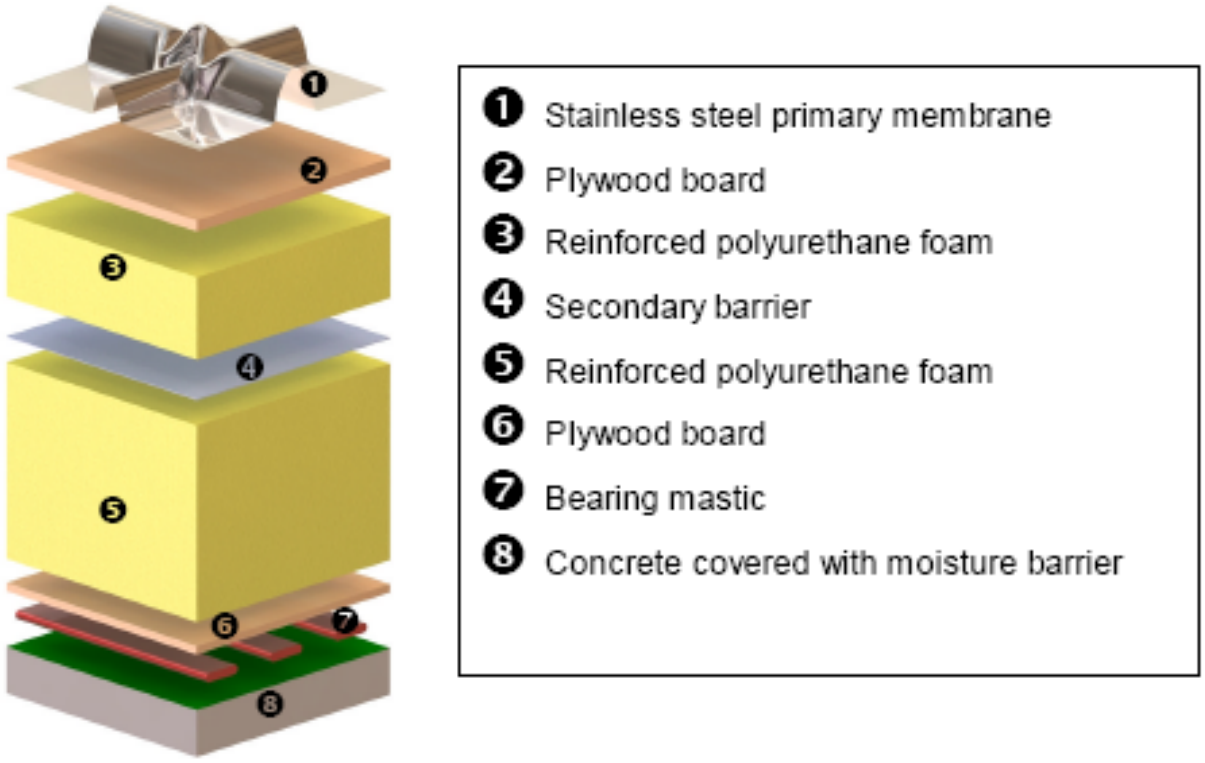

Fig. 2.6. GST composite system build-up

The primary membrane will be subjected to several leak tests and weld remediation. A dye penetrant test will be performed on 100% of the welds by two different welders. After cleaning

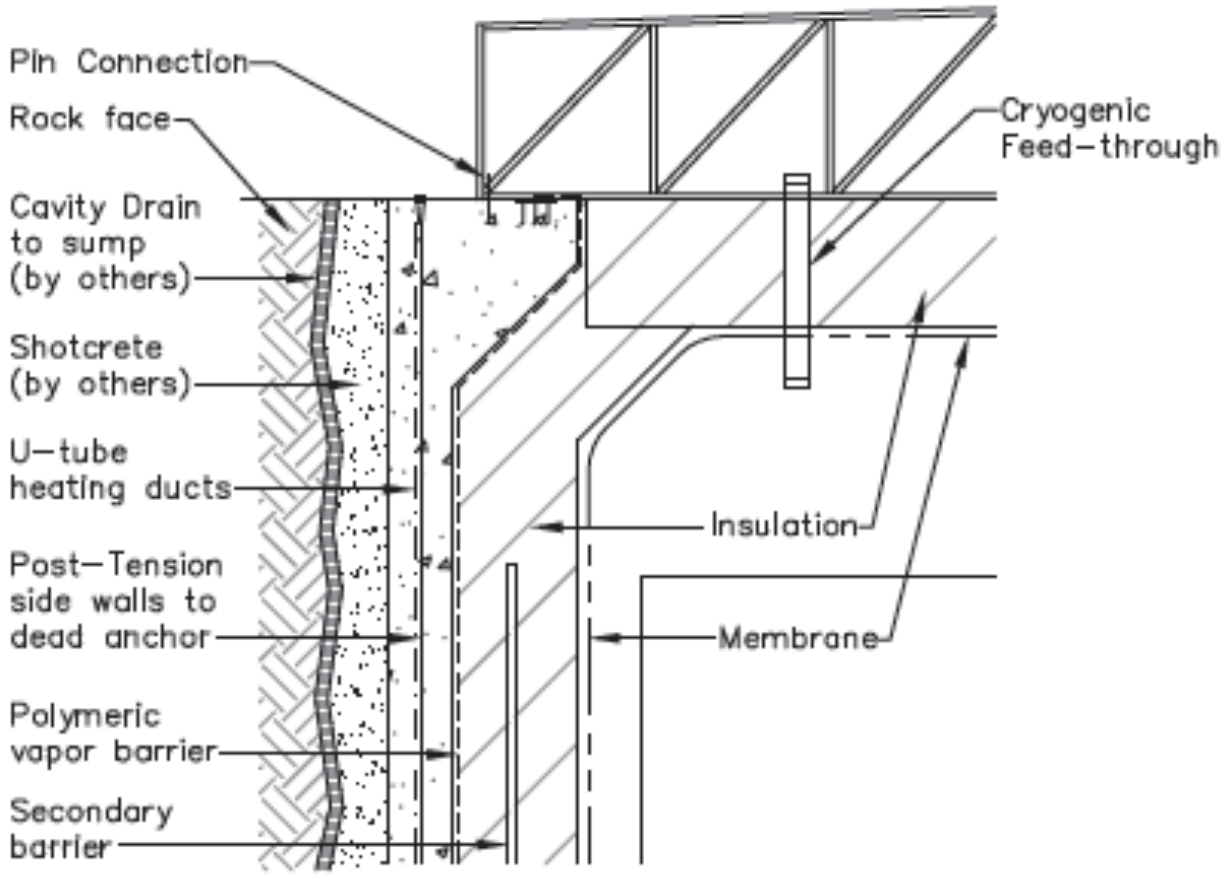
Pin Connection
Rock face
Cavity Drain to sump (by others)
Shotcrete (by others)
U–tube heating ducts
Post–Tension side walls to dead anchor
Polymeric vapor barrier
Secondary barrier
Cryogenic Feed–through
Insulation
Membrane

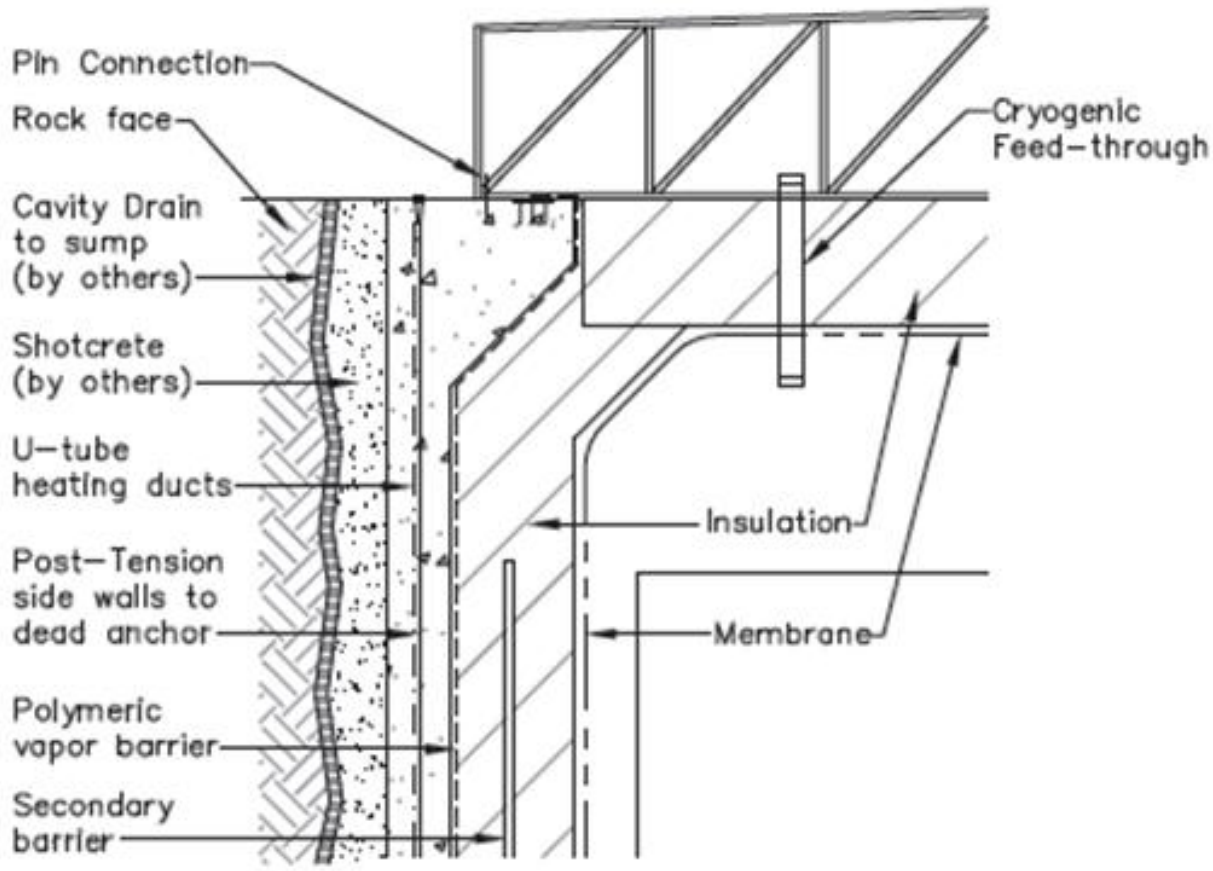

Fig. 2.7. Composite system installed

of the vessel, a “global" test will be performed by evacuating the space between the primary stainless steel membrane and the secondary barrier and measuring the rate-of-rise of the pressure in this space over a 24 hour period when the space is isolated. Microscopic leaks will be localized by injecting a mixture of helium and nitrogen in the insulation space and “sniffing" the welds.

It is conceivable that a microscopic leak would only develop at cryogenic temperatures and that it would be undetectable by the global test that will be performed after cool-down. The existence of the microscopic leak would only become known after the cryostat is filled and the argon purity did not reach the expected level due to infiltration of water vapor through the leak. The insulation purge system described in the next section will eliminate the effects of this occurrence.

2.3.5 Insulation Purge system

To prevent infiltration of water vapor and oxygen in the event of a microscopic leak, we will continuously harness approximately 10% of the boil-off argon gas and use it, at a flow rate of 20 m^3/hr, to continuously purge the insulation space around the cryostat. We have conservatively estimated that the gaseous spaces in the insulation should not exceed 60 m^3. This leads to approximately one volume change every three hours.

The insulation space between the primary and secondary barrier will be maintained at 0.103 MPa pressure, slightly above atmospheric pressure. The pressure and exhaust flow rates in the insulation space between these two barriers will be monitored for changes that might indicate a leak from the inner membrane. The outer insulation space will also be purged with argon at a slightly different pressure. The pressure gradient across the membrane walls will be maintained in the outward direction. Pressure-control devices and relief valves will be installed on both insulation spaces to ensure that the pressures in those spaces will not exceed the operating pressure inside the tank.

The purge gas discharged from the insulation space will be either vented or will co-mingle with the boil-off gas stream prior to the mix being recondensed, purified and returned as LAr to the cryostat.

A delivery pump will drive the purge gas through the insulation. We will not provide a spare blower. The purge system is not safety-critical, and an outage of the blower would have only a minimal, short-term impact on operations.

2.4 Cryogenic Systems Layout

The choice of the cryogenic system's layout and location is intended to optimize safety and efficiency. It will:

- Minimize the exposure of personnel to any Oxygen Deficiency Hazard (ODH)
- Minimize heat ingress to the cryogenic system (by minimizing piping length and pump power)
- Minimize the volume of the argon system external to the cryostat and hence minimize the potential for argon escape or contamination.
- Provide safe access to refrigeration equipment that requires periodic third-party maintenance.

The three figures below, 2.8, 2.9 and 2.10, show current thinking regarding the layout of the detector cavern at the 800-ft level on the DUSEL site. The layout includes drive-in access via the Kirk road portal and a tie-in to the DUSEL facility for alternate egress or access.

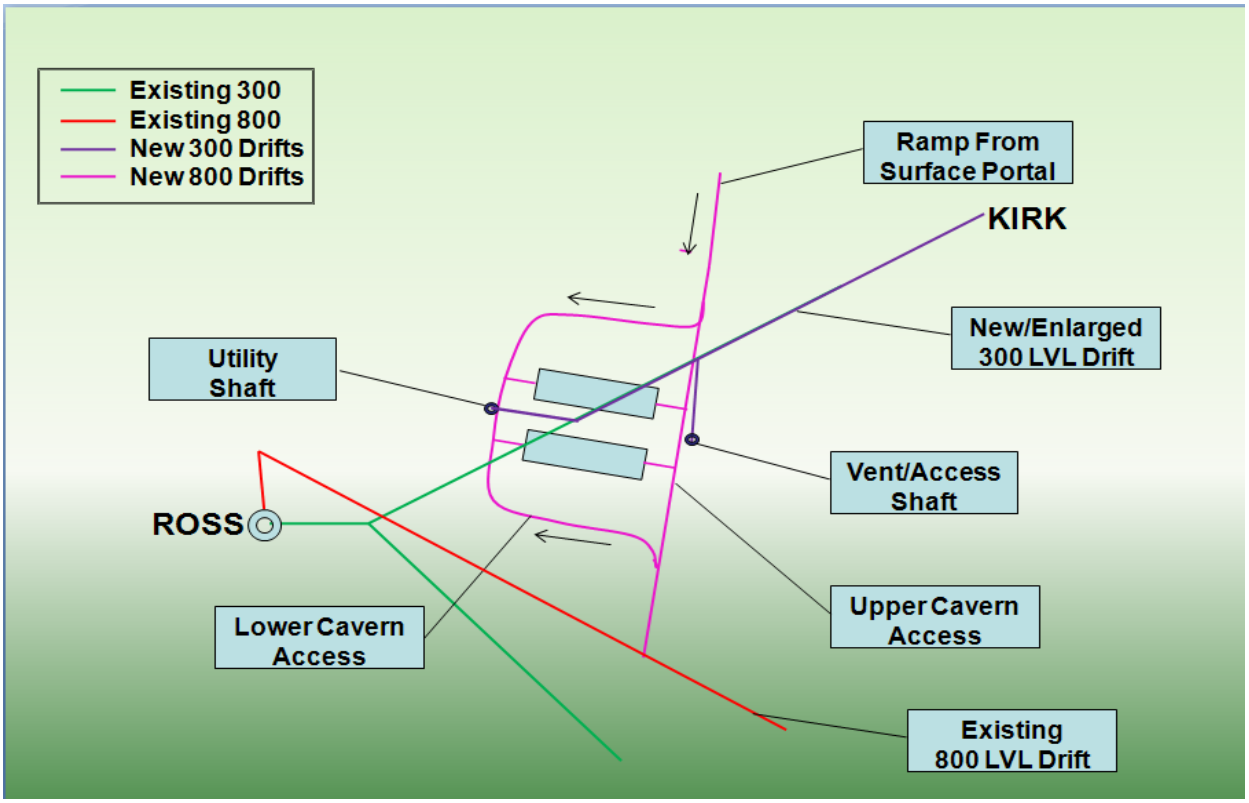

Fig. 2.8. Location of 800 cavern and access point from Kirk portal

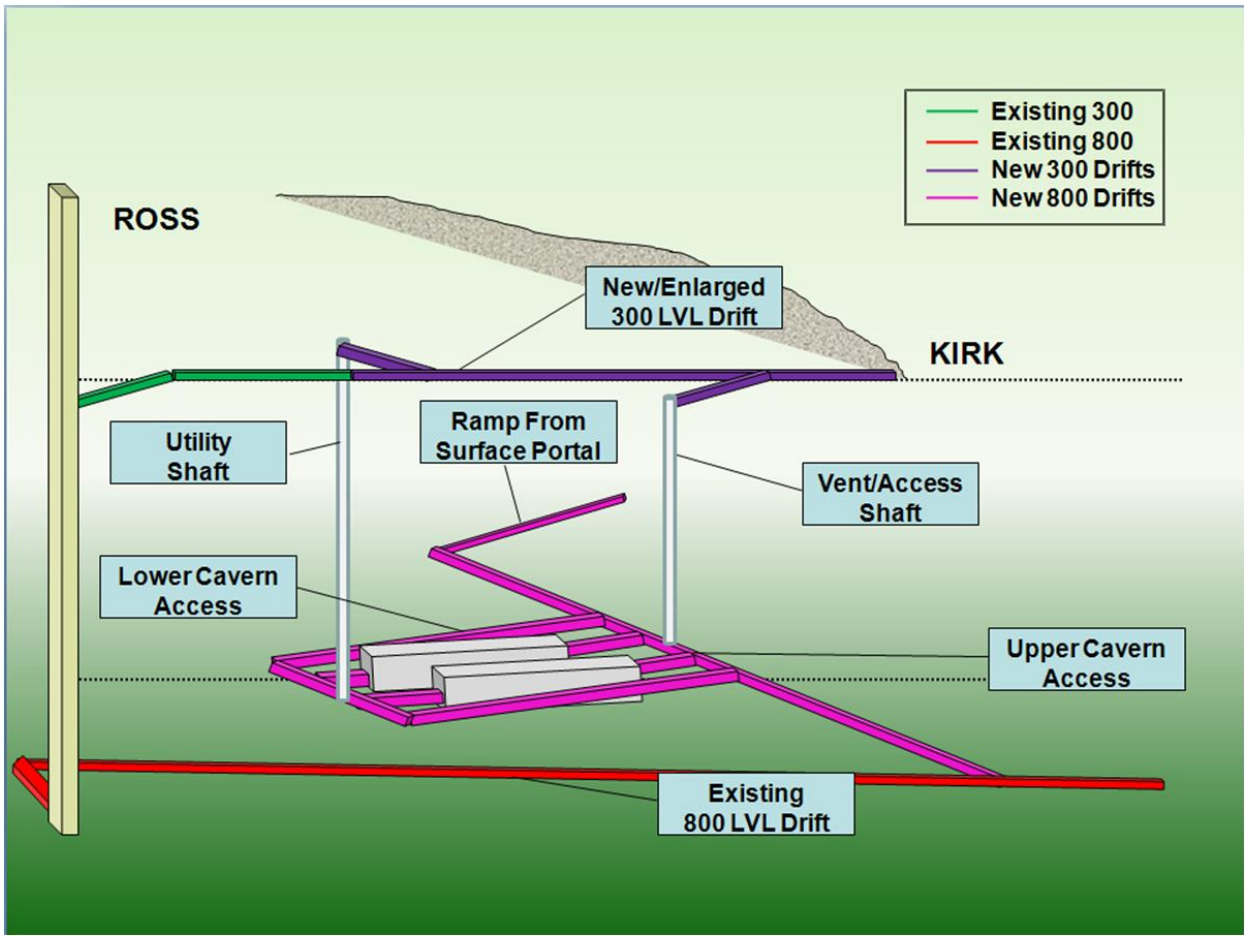

Fig. 2.9. Local layout of the LAr20 caverns with access

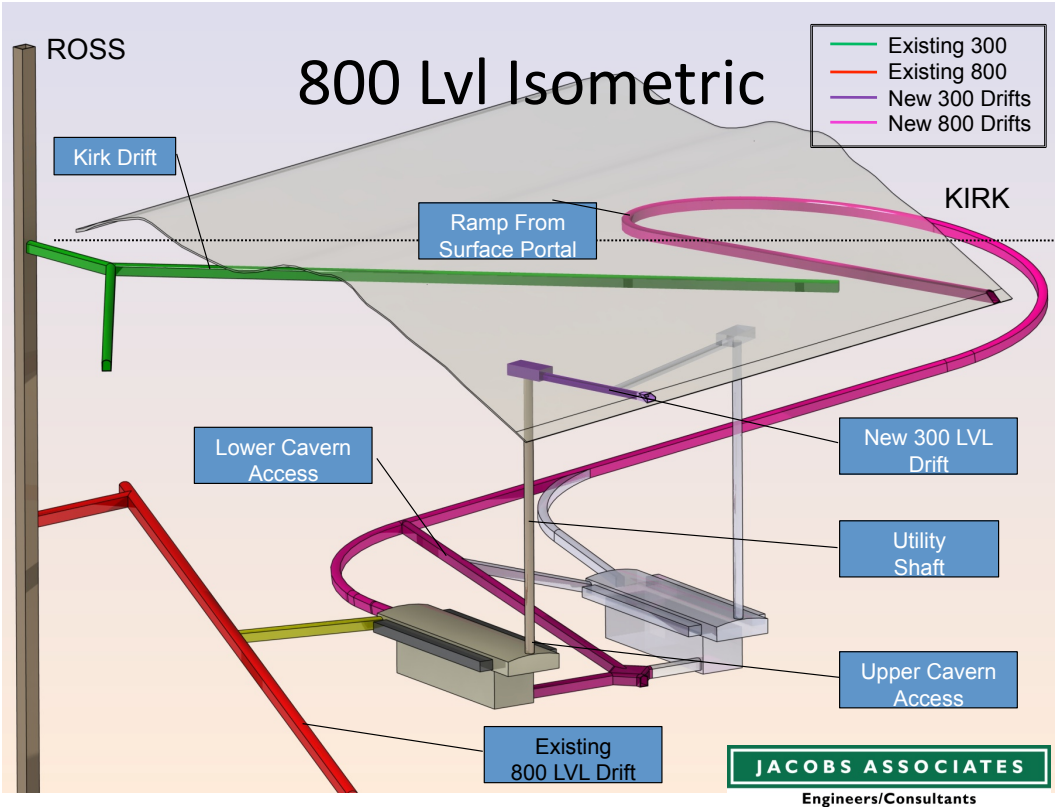

Fig. 2.10. 800L Isometric

Table 2.3. Cryogenic system equipment location for 800L siting

Equipment	**Location**
LAr receipt facility	surface
Optional L.Ar dewar (holding tank/emergency store)	surface
Argon recondensers	cavern
Argon refrigeration plants	cavern
LN receipt facility	surface
LN store	surface
Purification Plants (by FNAL)	cavern

2.4.1 Underground and Surface Components

Most of the cryogenic system components will be located underground, adjacent to the cryostat. A surface facility will be located immediately outside the new 300' level drift near the existing Kirk portal. The schematic, as shown in figure 2.11 delineates the services located above and below ground. The equipment is also listed in Table 2.3. The surface facility will include the liquid-argon receiving station, two 50 kW liquid-nitrogen refrigerators, and a 100 m^3 liquid-nitrogen dewar.

FIXME: *INSERT FIGURE E2. FLOW SCHEMATIC FOR CRYO PLANT HERE. AH: The text on this will be unreadable: need drawing redone appropriately for inclusion in CDR*

Fig. 2.11. Flow schematic for cryogenics plant

2.4.2 Cavern Components

Because of the large liquid-head pressures (and hence energy) required to push the liquid 500 feet to the surface, we will place the argon recondenser, the argon-purifying equipment and the cryostat overpressure-protection systems in the cavern. Four 34 m^3/hr circulation pumps will be placed within the membrane cryostat to circulate liquid from the bottom of the tank through the purifier. With the purifier in the cavern, these pumps each add about 6 kW of pump energy to the liquid. This number would increase by a factor of five if the purifier were located at the surface. By placing equipment with an eye towards efficiency, we aim to restrict the total system heat load to 50 kW.

We will place the following equipment directly on or within the cryostat, irrespective of the elevation or form of the cryostat:

- Circulation pumps to deliver LAr to purifiers

Table 2.4.

Start and End Points	**Duty**
LAr surface-to-cavern	commissioning only
LAr to purifiers	cryostat drain only
Purifier return to cryostat	continuous
Argon vent to surface	emergency relief
LN vent from recondenser to surface	backup operation or emergency
LN link from refrig plant to recondenser (and N2 link in opposite direction)	continuous

- "Commissioning" circulation pumps to deliver LAr to purifiers at an elevated rate during the initial purification period
- LAr return/fill line
- Boil-off gas line
- Cryostat pressure-control valves
- Cryostat pressure-relief valves
- Purge pipework
- Cryostat-monitoring equipment (pressure, temperature, density, depth, etc.)

All connections into the cryostat will be via nozzles or penetrations above the maximum liquid level and mostly located on the roof of the cryostat. Equipment located within the cryostat, such as monitoring instrumentation and pumps, will be installed within wells extending through the roof structure.

INSERT FIGURE OF PUMP TOWERS FROM GTT POWERPOINT**FIXME:** *Need an illustration*

2.4.3 Pipework between Surface and Cavern

Risers and other pipework linking the cavern to the surface will be routed through a 0.6 – 1.0 m-diameter vertical exhaust-ventilation shaft. The shaft will contain liquid-nitrogen-supply and return pipes, a liquid-argon pipe, vent piping and control-system wiring. Table 2.4 lists the lines, service duty and size of piping that will run between the surface and cavern.

The in-cavern cryogenic equipment will be located at the end of the cavern opposite the drive in access drift. This end will also be where the vertical utility shaft is located. Piping from the cavern will run vertically up the utility shaft 150 meters (500 feet) to the horizontal drift

located at the 300' elevation. The piping will then run horizontally along the horizontal drift for a distance of about around 100 meters (300 feet) to the cryogenic reciept facility located outside.

We will use metallic piping designed in accordance with the requirements of ASME B31.3 Process Piping and ASME B31.5 Refrigeration Piping and Heat Transfer Components. The piping material will be seamless Austenitic Stainless Steel in accordance with ASTM A312 Grade TP304 or TP304L. No corrosion allowance is required with this material in this service as stainless steel is resistant to corrosion. Cryogenic piping will be slightly inclined such that any boil-off vapor either vents through the dedicated vent system or returns to the cryostat, interim storage dewar, or another vessel designed for vapor recovery. We will use smaller-bore vents and drains as necessary to facilitate testing, commissioning and cool-down of the piping system, and minimize inclusion of flange type or bayonet type connections for the LAr systems in order to reduce the risk of leakage. Flanges may be required for the connection of the piping to proprietary equipment and vessels. When flanges are required, the minimum flange rating will be in accordance with ASME B16.5 class 150. All piping systems will be sized to limit liquid-flow velocities to a maximum of 2.5 m/s and gaseous flows to less than 20 m/s to prevent erosion on interior piping surfaces due to abrasion due to high flow velocities.

In addition to the minimization of flanges, all piping components and equipment will be selected and evaluated with consideration to contamination ingress to the system. The use of valves with bellows-sealed valve stems may be warranted on continuous-service lines. Where leak paths cannot be eliminated, for instance in rotating shaft seals, we will implement a guard atmosphere of gaseous argon so that any ingress into the system will be essentially pure argon rather than cavern air.

All pipe systems will be designed such that pipe sections and equipment may be isolated and removed from service for replacement or maintenance. All nozzles off the cryostat will include isolation valves in order to isolate the individual lines from the cryostat.

Wherever the pipe-system design leaves open the potential for isolated pipe sections to fill with cryogenic fluid (e.g., fluid trapped between valves) we will provide a means of relief to prevent over-pressure. All cryogenic lines, gaseous or liquid, will include insulation to minimize heat transfer to the fluid and to provide personnel protection. Vacuum-insulated pipe will minimize heat load and simplify pipe-support arrangements on straight runs. Internal-bellow arrangements are preferred to compensate for thermal length changes. For vacuum-insulated pipe, the outer pipe will be pressure rated for at least the design pressure of the internal pipe such that it is able to provide secondary containment in the event that the inner pipe fails. The use of foam insulation will be minimized. When foam insulation is used, a waterproof cladding will be applied to prevent water from entering the insulation and freezing.

In accordance with the requirements of ASME B31, all piping systems will need to be adequately supported to limit stress and vibration from thermal, mechanical and environmental sources, and from installation, long-term fatigue and seismic loads. Piping within the cryostat or within other vessels will require adequate support or guidance to minimize stress and to

accommodate differential thermal contraction as the various components cool.

2.4.4 Redundancy

We will implement safety-critical equipment, generally, on the basis of 'n+1' units. This will ensure continuity of operation and adherence to safety standards whenever a unit is unavailable for maintenance or other reasons. Items required short-term and those already present in multiple units are excepted; we assume a low probability of failure for the former and minimal impact to the performance of the overall system for the latter.

Where common function equipment could be used for alternate systems, interconnections will be provided to increase flexibility during operation. An example of this would be an interconnection between argon and nitrogen delivery lines at the surface facility and in the cryostat cavern. The argon piping will only be used during LAr delivery to the cryostat. Later during the lifetime of the experiment, if the LN delivery system had a problem such as excessive heat leak due to a degradation of vacuum, the LAr piping could be used in its place.

2.5 Cryogenic System Processes

2.5.1 Cryostat Initial Purge and Cool-down

After cryostat construction and following installation of all scientific equipment, the cryostat will be cleaned, purged and cooled. Construction procedures up to this time will ensure that the completed cryostat does not contain debris and is free of all loose material that may contaminate the LAr.

2.5.1.1 Initial Purge

Argon piping will be isolated, evacuated to less than 0.1 mbar absolute pressure and backfilled with high-purity argon gas. This cycle will be repeated several times to reduce contamination levels to the ppm level. The membrane cryostat will be flow/piston-purged, with the heavy argon gas introduced at the bottom of the tank and the exhaust removed at the top. The bottom field cage serves an additional role as a flow diffuser during the initial purge. A matrix of $\sim$ 10 mm holes in the field cage at a pitch of 50 mm provides a uniform flow.

The flow velocity of the advancing argon-gas volume is set at 1.2 meters/hour. This velocity is twice the diffusion rate of the air downward into the advancing argon so that the advancing pure argon gas wave front will displace the air rather than just dilute it. A two-dimensional ANSYS model of the purge process shows that after 20 hours of purge time and 1.5 volume changes, the

air concentration is reduced to less than 1% air. See figure **FIXME:** *3,4,5 below.* At 40 hours of elapsed time and 3 volume changes, the purge process is complete with residual air reduced to a few ppm. This simulation includes a representation of the perforated field cage at the top and bottom of the detector and heat sources due to the readout electronics. The cathode planes were modeled as non-porous plates although they will be constructed of stainless steel mesh.

FIXME: *INSERT FIGURES 3,4,5,6 from LBNE DOC-475 HERE - Air Fraction versus time for Purge Process*

The computational fluid dynamics (CFD) model of the purge process has been verified to predict purge results in an instrumented 1 meter diameter by 2 meter tall cylinder. Recognizing that obtaining the required purity levels by the flow purging method needs to be clearly demonstrated, a Liquid Argon Purity Demonstrator (LAPD) project is underway. The LAPD is a right cylindrical vessel 3 meters in diameter and 3 meters tall. The purge process has been modeled and will be compared to gas sampling measurements during the purge process. Data will be collected at varying heights and varying times to compare with the time dependent predictions of the computer modeling. The LAPD project is expected to start operations in the fall of 2010.

2.5.1.2 Water Removal

Water and oxygen will continue to be removed from the system for the next several days by flowing gas at the same rate, however the gas will now be filtered and recirculated. The detector contains $\sim$ 3 tons of FR4 circuit board material and a smaller inventory of polyolefin jacketed power and signal cables. These somewhat porous materials may contain as much as 0.5% of water by weight. Water vapor outgassing from these materials will be entrained in the gas flow exiting the top of the cryostat and will be removed from the gas stream by filters. Only adsorbed water will be removed from the inner surfaces of the cryostat and piping system however. Water deep within porous materials will remain since the water diffusion rate in FR4 at room temperature is quite low (0.3 $\mu m^2/s$) and the FR4 assemblies are relatively thick (1 cm).

2.5.1.3 Cool-Down

In this phase, gas will continue to be recirculated through the cryostat and filters however the gas temperature will be lowered to 120K over a period of $\sim$ 10 days. The cooling rate is determined by the maximum allowable stress that detector components can be subjected to. For example, the 150 μm APA wires will cool much more rapidly than the APA frames. A temperature control system will maintain a temperature difference of $\sim$ 20K between the input gas stream and the exhaust stream.

Water vapor outgassing is effectively stopped at 120K. The temperature dependence of the diffusion coefficient, D_T, follows Arrhenius equation: $D_T = D_o exp(-U/kT)$ where D_o is a

constant, U is the activation energy, k is Boltzman's constant, and T is the absolute temperature. For FR4, $D_{120K} = 6x10^{-10}\mu m^2/s$). This behavior has been confirmed by FR4 contamination tests in LAr on the Fermilab Materials Test Stand.

2.5.1.4 Traditional Method Alternative

The traditional method for removing water and oxygen from LAr TPC's is to evacuate the tank to $\sim 10^{-4}$ mbar and then backfill it with pure argon gas. The primary membrane of the reference design cryostat is not a vacuum vessel however. A membrane-cryostat vendor reports that evacuation of the insulation spaces is normally done during the construction and leak-checking phases. It has been demonstrated that a vacuum pressure of less than 200 mbar absolute in the insulation spaces can be achieved. We are currently researching how low a pressure is achievable. As long as the pressure-differential direction across the walls is kept outward, it is possible to reduce the internal membrane-tank volume to these pressures as well. This is considered an alternative rather than preferred option because we do not believe it will be necessary and designing the concrete cavern liner and cryostat roof truss for the additional loading due to external atmospheric pressure results in a higher cost.

2.5.1.5 Initial Purge and Cool-Down Design Features

Internal piping is positioned within the cryostat to support the purge and cool-down procedure. Heavy argon vapor will promote purging if it is delivered to the base of the cryostat and vented from the roof level. The LAr-supply pipework will have distributed nozzles along its length to uniformly distribute equal flow rates across the bottom of the cryostat. The flow nozzles will be directed downward or to the side so that the injection velocity will not cause local vertical gas plumes or turbulent mixing but will rather spread across the bottom of the tank and produce a stable upwardly advancing argon wave front. The vertical velocity of 1.2 m/hr includes a contingency for some level of turbulent mixing.

Main gas returns, used for pressure control, will be distributed along the cryostat roof. All nozzles and dead volumes located at the top of the cryostat will have gas-exhaust lines for the initial purge and for continuous sweep-purge of those volumes to the recondensor during normal operation. All purge gas will be contained and either vented outside of the cavern at a remote location, or recondensed using the refrigeration plant then reused. The temperature of the entering argon gas will be reduced and the gas recirculated after air removal is completed. The argon-gas to liquid-nitrogen recondensor will be used as a cool-down heat exchanger to enable decreasing argon supply gas temperatures and cryostat cool-down operations.

2.5.2 Cryostat Filling

Liquid argon will be delivered to the cryostat through the cryostat-filling pipework. It is anticipated that a number of small-diameter lines, nozzles and orifices will reticulate from the main fill line to distribute the LAr within the cryostat. To minimize any local disturbance within the cryostat caused by the LAr in- flow, we propose a reticulation system beneath the TPCs, with multiple outlets. The liquid argon filling line could be the same line that was used for distribution of the argon purge gas. Engineering calculations must be done to properly size the piping and nozzles for each function and a determination made as to whether one system or two are needed. The distribution piping will be located below a horizontal planar field cage that spans across the anode and cathode planes. The filling process will take place over many weeks due to the delivery schedule of liquid argon described in the next section. Liquid argon purification can begin once the liquid depth reaches about 2 meters in the bottom of the cryostat. At 2 meters depth, the recirculation pumps will be able to be turned on directing up to 136 m^3/hr (600 gpm) of liquid argon through the purification system.

2.5.3 Liquid Argon Reciept

The liquid argon detector will hold an inventory of 25 kton of liquid argon. Initial purge operations are expected to consume and exhaust about 0.25 kton. Considering that some product will be lost in transit, we assume that approximately 30 kton of liquid argon will need to be procured. The logistics and supply of LAr to the facility include the following considerations:

- The total capacity of commercial air-separation plants within freight distance of the facility (the peak delivery potential),
- The extent of boil-off that will occur in transit,
- The number of vehicle movements required,
- The costs and benefits associated with stockpiling LAr at the facility ahead of commencing the purge, cool-down and fill procedure,
- The provision of a temporary air-separation plant at the facility to generate liquid argon
- The availability and cost associated with the delivery of high-purity LAr as opposed to lower-quality, commercial-grade argon combined with on-site coarse purification.

Total argon production, considering all suppliers within the United States is currently approximately 3.6 kton per day. Argon is normally co-produced along with large volumes of oxygen, so any project that requires large oxygen quantities may also cause additional argon supply capacity. A 2013-2018 market-forecast report by the Freedonia group indicates that the demand for

Table 2.5.

Item	**Heat Load (kW)**
Insulation heat loss	32
Electronics power	9.7
Recirculation-pump power	6
Total	**47.7**

argon will increase at a rate of 3.4% per year whereas the demand for oxygen will increase 4.8%. Oxygen will register more rapid gains than will nitrogen, the latter driven by above-average growth in health-care markets. Also promoting growth will be greater use of nitrogen in food-packaging applications. Thus the conclusion we draw from the report is that the availability and pricing for argon gas will be on par or more favorable than current market conditions. The estimated 2010 cost for 30 kton of liquid argon is $30M.

The standard grade specification for argon is minimum purity = 99.995%; maximum O2 impurity = 5.0 ppm; maximum H_2O impurity = 10.5 ppm. This is designated as Grade 4.5 in the gas supply industry. Requiring higher-purity product would significantly reduce the volume of product available to the experiment, increasing cost and schedule duration. Therefore, we plan to procure standard product from multiple vendors. The typical mode of argon delivery is over-the-road tank truck with a maximum capacity of 18.7 metric ton (MT). We expect to need 1400 such deliveries over six months to fill the system. Rail delivery of liquid argon (in 177 MT quantities) is not cost-effective as there are no rail spurs leading to the site. A transfer of product from rail tanker to a tank truck would require infrastructure cost that exceeds the benefit.

Surface facilities are required for the offloading of LN and LAr road tankers. Vehicle access and hard surfaced driving areas are required adjacent to the LN dewar and LAr-supply piping. An interim LAr storage dewar will hold the contents of a road tanker in order to minimize off-loading time. Road tankers will connect to a manifold located close to the 300' access drift and will use their on-board pumps to transfer the LAr to the storage dewar. Each tanker will be tested to ensure that the LAr meets the purity specification. The liquid argon will be gravity-fed to the cavern where it will be routed through the purification system prior to discharging into the detector cryostat or underground LAr storage cryostat.

2.5.4 Argon Reliquefaction and Pressure Control

High-purity liquid argon stored in the cryostat will continuously boil due to the heat ingress into the cryostat. The argon vapor (boil-off gas) is to be recovered, chilled, recondensed and returned to the cryostat. A closed argon system is required to prevent the loss of the high-purity argon.

During normal operation the expected heat ingress of approximately 47 kW to the argon

system will result in the liquid Argon boiling at a rate of 1100 kg/hr and expanding in volume by a factor of 200 when it changes from the liquid to vapor phase. This increase in volume within a closed system will, in the absence of a pressure control system, raise the internal pressure. Argon vapor will be removed from the cryostat through the chimneys that contain the cryogenic feedthroughs, thereby cooling the feedthrough to minimize outgassing and sweeping any contaminants out of the cryostat.

Gaseous argon will be directed to a heat exchanger (recondenser) where it will be chilled against a stream of liquid nitrogen and condensed back to a liquid. The expected flow rate of gaseous argon is 1100 kg/hr. As the gaseous argon cools, the volume reduces and further gas is drawn into the heat exchanger, developing a thermal siphon. A pressure-control valve on the boil-off gas lines will control the flow to the recondenser so that the pressure within the cryostat is maintained at 0.113 MPa +/-0.003 MPa. The liquid nitrogen stream will be a closed-loop system. The system will be a commercially produced refrigeration plant based on compression/expansion and heat rejection that will continuously produce a liquid nitrogen from returning cold nitrogen vapor.

FIXME: *Could use an animation*

A duty and a standby refrigeration plant (2 x 100%) will be provided along with a duty and a standby recondenser. This will ensure high availability of the recondensing system and minimize any requirement to vent high-purity argon. The arrangement will permit maintenance of the recondensers and the refrigeration plants. The condensed stream of LAr will be combined with the LAr circulating stream and purified prior to being returned to the cryostat.

2.5.5 Argon Purification

Pumps are required to transfer LAr from the cryostat for the purposes of purification (or emptying) since the vessel is designed without penetrations below the normal liquid level. We plan to use vertical submersible pumps that can be inserted into pump wells extending down from the cryostat roof. The pump suctions must be located a minimum distance (normally ∼1.5 âĂŞ 2 m) below the lowest liquid level at which they are to pump in order to prevent cavitation and vapour-entrapment. The nominal plan calls for the pumps and pump wells to extend to the bottom of the cryostat. They could however be staggered at different elevations to allow flexibility in drawing liquid from different elevations.

Vertical, submersible, cryogenic pumps are supplied by manufacturers such as Ebara and Carter Cryogenic Products; see figure **??**. A description of their cryogenic electro-submersible pumps is provided by Ebara below for information.

The required flow rate of liquid argon to be sent for purification is expected to decrease over time. The initial maximum flow rate will be 136 m^3/hr (600 gpm). The liquid-argon volume

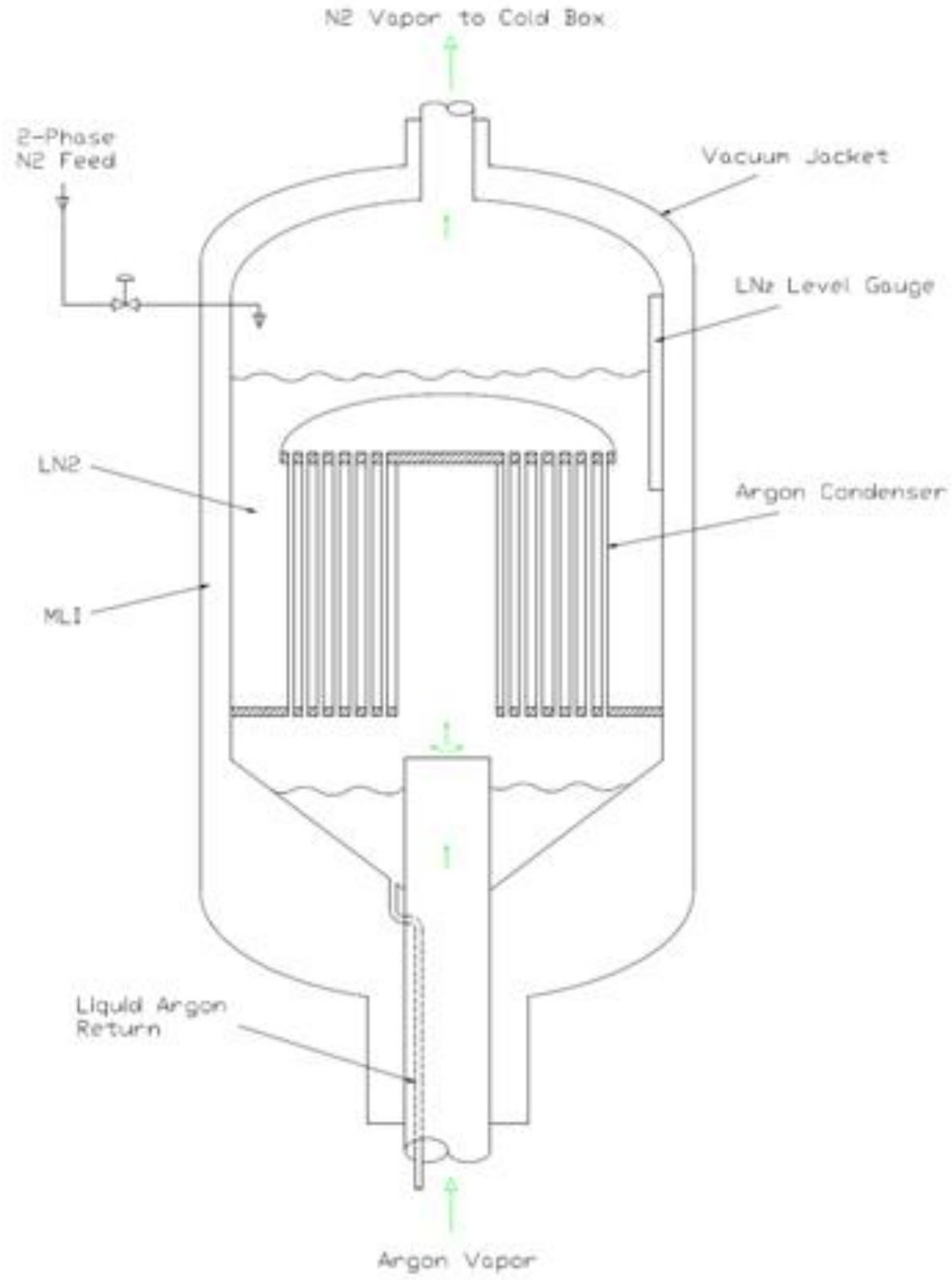

Fig. 2.12. Liquid argon recondenser

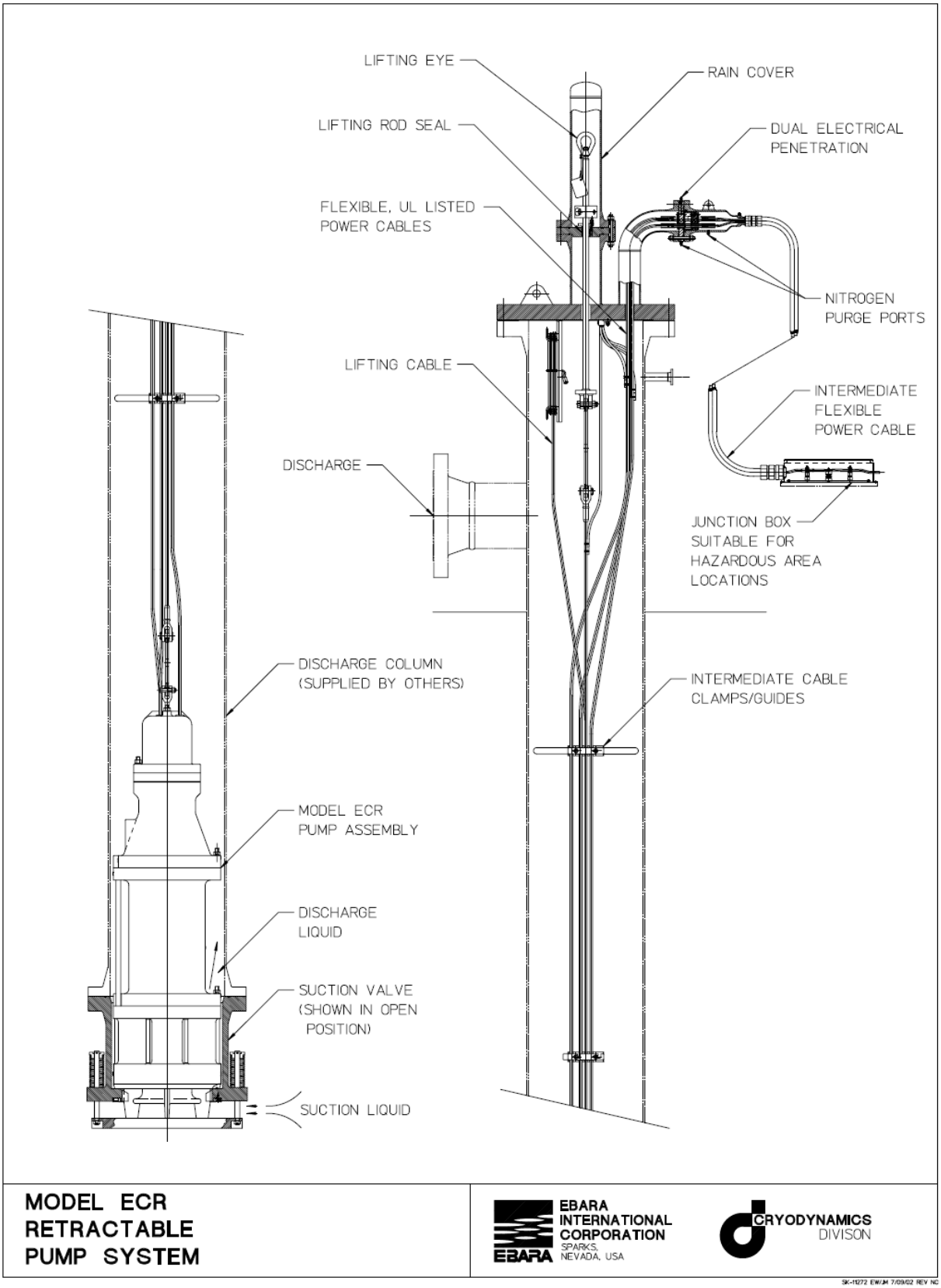

Fig. 2.13. Vertical submersible pump

will turn over every five days at this initial maximum rate. Longer term, the rate will decrease to 34 m^3/hr with a turn-over rate of 20 days. ICARUS T600, as point of comparison, has a maximum turn-over rate of eight to ten days. To achieve the turn-down required between the short-term commissioning flow rate (600 gpm) and the long-term operational flow rate (150 gpm) through the purifiers, 4 x 150 gpm pumps will be located within a 2 m space at the end of the cryostat. The multiple-pump arrangement will provide a very high level of redundancy, which will extend the cryostat operating period without maintenance. The heat load introduced to the cryostat for the initial circulation rate will result in a significant increase in the total heat ingress beyond the long term 50 kW refrigeration capacity. Therefore, additional refrigeration is required during the commissioning phase. However the refrigeration plant and recondenser have been provided on a fully redundant basis to ensure high availability. During the initial period the plants will be operated in parallel to provide the increased cooling capcity that will be required.

The purification plant will consist of a duty stream and an identical standby stream each consisting of a molecular-sieve column and a copper catalyst column.

Redundant equipment will:

- Allow regeneration of one system while the other is operating.
- Allow both units to operate in parallel during the initial cryostat filling period where a high throughput is required.
- Provide a maintenance contingency.

Key design parameters associated with the physical arrangement of the purifier columns include a molecular-sieve-bed column of size 2 m diameter x 6 m tall and a catalyst-bed column of size 2 m diameter x 6m tall. The pressure drop through each bed is 55 kPa (8 psi) for a total of 110 kPa. The purifiers will be located close to the cryostat to minimize the volume of LAr in the circulation pipework and the pump power required to achieve the desired flow rate. Locating the purifiers at the surface is unlikely to be viable due to the extended LAr flowlines, the associated heat gain and the pump-power requirements. Additional vertical excavation at the cavern end may be required to accommodate the column height.

2.5.6 Pressure Control

The pressure control valves are sized and set to control the pressure under normal operating conditions between two set points (50 and 200mbarg). Excursions above or below these levels will set off alarms to permit the operator to intervene. Further excursion may result in automatic (executive) actions occurring. These actions may include stopping the L.Ar circulation pumps (to reduce the heat ingress to the cryostat), increasing the argon flow rate through the re-condenser, increasing the LN flow through the re-condenser vessel, powering down heat sources within the

cryostat (detector, electronics) etc. Eventually if the pressure continues to rise the pressure relief valves will operate.

The ability of the control system to maintain a set pressure is dependent on the size of pressure upsets (due to flow changes, heat load changes, temperature changes, changes in atmospheric pressure, etc) and the volume of gas in the system. The reference design has 0.7 meters of gas at the top of the cryostat. This is 5% of the total volume and is the typical vapor fraction used for cryogenic storage vessels. Reaction time to changes in heat load are slow, on the order of one hour. At the expected heat load rate of 47 kW the rate of pressure rise in the cryostat if it was isolated or had no cooling is 200 mbar (3.0 psi) per hour. The pressure control valves will control the pressure between 50 and 200mbarg (0.75 psig and 3.0 psig). We plan to provide two redundant pressure control valves, each sized to handle at least 1500 kg/hr of argon flow to the recondenser.

A cryostat over pressure protection system is provided as a high integrity automatic failsafe system designed to prevent catastrophic structural failure of the cryostat due to excessive internal pressure. The overpressure protection system is in addition to the normal operational pressure control system.

The key active components are pressure relief valves (PRV) located on the roof of the cryostat. These monitor the differential pressure between the inside and the outside of the cryostat and open when the differential pressure exceeds a preset value. The PRVâĂŹs are self contained devices and are not normally part of the control system. They are provided for tank protection and open rapidly at the set point. The valves are typically pilot operated whereby the pressure within a small bore sensing line is used to trigger a pilot valve that delivers the power fluid (compressed air) to the actuator of the PRV. A pressurized reservoir of power fluid is provided to each valve to ensure that the valves will operate under all upset / shutdown scenarios.

The installation of the pressure relief valves is arranged such that each valve can periodically be isolated and tested for correct operation. The valves should be removable from service for maintenance or replacement without impacting the overall containment envelop of the cryostat or the integrity of the pressure protection system. This normally requires the inclusion of isolation valves upstream and downstream of the pressure relief valves and at least one spare installed relief valve (n+1 provision).

When the valves open, argon will be released and the pressure within the cryostat will fall. The valves are normally designed to close when the pressure returns below the preset level. The relief valves are arranged to discharge into the argon vent riser.

Vacuum relief valves are provided on LNG/LPG storage tanks to protect the structure from low internal pressure, for example if the discharge pumps are operating with the liquid return inlet valves shut.

Theoretically gaseous argon condensing in the re-condenser could result in a reduced pres-

sure in the cryostat (thermo-siphon) or a failure of the vent system when draining the cryostat could result in reduced internal pressure. The cryostat vacuum relief system is a high integrity automatic failsafe system designed to prevent catastrophic structural failure of the cryostat due to low internal pressure. The vacuum relief system should protect both the inner and outer tank. Activation of the vacuum relief system is a non-routine operation and is not anticipated to occur during the life of the cryostat.

The vacuum relief system is in addition to the normal pressure control system. The vacuum relief system is required to protect the cryostat during the initial purging operations when a controlled vacuum is to be created within the tank. The key active components are vacuum relief valves located on the roof of the cryostat. These monitor the differential pressure between the inside and the outside of the cryostat and open when the differential pressure exceeds a preset value. The relief valves will allow cavern air to enter the cryostat.

2.5.7 Liquid Nitrogen Refrigeration System

A duty and stand by commercially procured liquid nitrogen refrigeration plant will be provided. It will be a closed loop nitrogen system to supply approximately 50,000 W of refrigeration to the liquid argon re-condenser. The nominal rating of the quoted reference refrigerator is 59 kW. Two-phase nitrogen is delivered from the cold end of the refrigerator into a modest 4 cubic meter buffer tank. Liquid is pressure fed from the bottom of the buffer tank at a pressure of 2.0 bar and temperature of 84 K to the re-condenser to allow a 5 K temperature difference against the 89 K argon re-condenser temperature. The size of the buffer tank is chosen to allow for three hours of refrigeration time. This is suitable to span power outages, refrigerator performance problems, refrigerator switch overs, or to cool down the LN transfer line from the surface LN dewar.

The refrigeration system is based on the use of a centrifugal compressor and three turbo expanders for a clean, oil-free loop. This should ensure high reliability. It is expected that this system will run continuously for at least a year and then require only minor servicing. The system will be equipped with automatic controls and a remote panel so that no operator will be required during normal operation. Estimated maximum power requirement is 750 hp (560 kW) without credit for power generated by the expanders. Our reference design places the nitrogen compressor in the cavern. A chilled water heat exchanger removes heat from the refrigeation plant. Compression is carried out at close to ambient temperature. A compressor aftercooler is provided that will reject heat.

The cold box consists of four heat exchangers. These exchangers provide staged heat transfer from a cooling nitrogen stream to a warming nitrogen stream. The expanders are connected between the heat exchangers to progressively reduce the pressure of the cooling nitrogen stream. See

The physical dimensions of the compressor is 4.3 m long by 1.8 m wide and 2.7 m tall. The

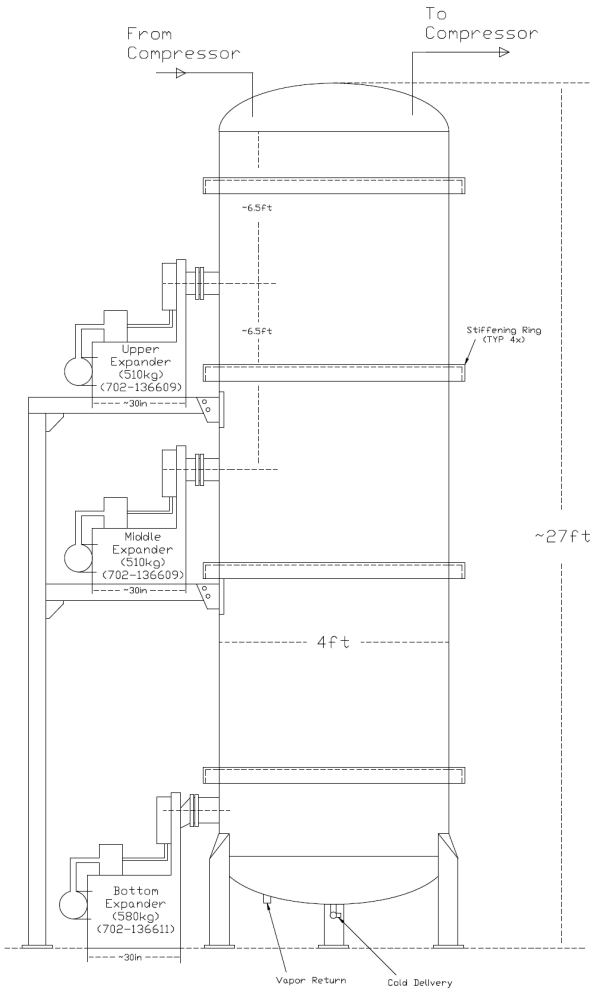

Fig. 2.14. Nitrogen refrigeration plant

compressor skid will weigh approximately 3630k. The physical size of the cold box is shown in figure xxx. The main cold box shell is 1.22 meters (4 feet) in diameter and 8.2 meters (27 feet) tall. The expanders are adjacent to the cold box at three elevations and extend about 1 meter to the side of the cold box shell. The cold box will weigh 5670kg.

2.6 Cryostat Prototyping Plans

The development of the liquid argon detector from a conceptual design to a preliminary design will include a prototyping program. A first prototyping project that will provide useful information is called the Liquid Argon Purity Demonstrator (LAPD). This prototype is actually off project. A second prototyping project is construction of a small membrane cryostat. There are two phases of testing that will be done with the membrane cryostat prototype cryostat. The individual prototyping programs are described in the following sections.

2.6.1 Liquid Argon Purity Demonstrator (LAPD)

This prototype is off project. It is being completed as part of the research and development program at Fermilab of scaling up liquid argon time projection chambers (TPC). As TPC detectors and vessels increase in size, the cost of providing a self supporting evacuable vessel becomes very expensive. The primary goal of the LAPD is to demonstrate that required electron lifetimes can be achieved without evacuation in an empty vessel.

FIXME: *INSERT PICTURE OF THE LAPD VESSEL FROM SLIDE 18, DUSEL DOC DB #72 HERE*

The LAPD vessel is a right cylindrical stainless steel vessel 3 meters in diameter and 3 meters tall and will hold 30 tons (30,000 kg) of liquid argon. The vessel is manufactured without special specifications to the welding or surface preparation. LAPD construction is expected to be completed in the fall of 2010 and operated shortly thereafter. The first phase of testing will be proving the effectiveness of using a slow 1.2 m/s argon gas purge to displace air upward and out of the tank. Residual air concentrations will be measured at varying elevations during the purge period. It is hoped that parts per million levels of residual air contamination can be achieved after three volume changes of gas. The gas will be further purified by use of recirculation and filtration. A comparison of the LAPD measurements to computer flow dynamic modeling will further validate using computational modeling to simulate the purge of large vessels. Later phases of the LAPD test will include filling with liquid argon and testing the liquid with ICARUS style argon purity monitors. Electron drift times will be measured. The LAPD vessel is passively insulated with 0.4 m of foam insulation. The heat load will be notably larger than a vacuum jacketed detector and about twice the expected heat load of our membrane cryostat reference design that has 1.0 m thick insulation. The fluid temperature gradients and convective fluid flows will be measured and

compared to modeling. A camera will be used to look for any bubbling or other surface effects. Finally, the LAPD will be used as a test bed for materials that would be used in a TPC detector. The effect of the materials on electron drift times will be made.

2.6.2 Prototype Membrane Cryostat Phase I - Purity

A prototype membrane cryostat will be procured and constructed on the Fermilab site. The purpose of the membrane cryostat prototype is to demonstrate that required electron lifetimes can be achieved without evacuation in a membrane cryostat. The testing program and phases will be very similar to the program described above for the LAPD prototype. We will in fact plan on using the refrigeration and system components from the LAPD test for the prototype membrane cryostat system. We hope to start design and planning in the fall of 2010 and start construction in 2011.

We envision that the prototype membrane cryostat will be approximately 6 m x 8 m x 8 m high. The insulation thickness will be 0.4 m rather than the 1.0 m chosen for our reference design. The construction techniques of membrane cryostat construction will be demonstrated to be fit for high purity TPC service. Welding of corrugated panels, removal of leak checking dye penetrant or ammonia activated leak detecting paints, and post construction cleaning methods will be tested for suitability of service. Residual contamination measurements at different elevations during the initial gas argon purge process will be compared to computational predictions and will validate the purge process modeling of a large rectangular vessel. The prototype membrane cryostat will be filled with liquid argon. Purification of the liquid with time and electron drift times will be measured. Heat load measurements will be made and compared to expectations. Eventually connectors and feed throughs, ports and other features that are planned for the reference design will be incorporated into the prototype. Materials and cold electronics testing can be done along with electron drift time measurements.

2.6.3 Prototype Membrane Cryostat Phase II - TPC

A second phase of the prototype membrane cryostat program described above will include adding a scale model of an anode plane, cathode plane, and field cage assembly to the vessel. Cold electronics and other instrumentation and features such as TPC frame supports will be incorporated. Detector readout will be accomplished.

Bibliography

[1] "Title", Month, year.

3 Time Projection Chamber

The Time Projection Chamber is located inside the cryostat vessel, completely submerged in liquid argon at 89K. This subsystem includes all mechanical components of the TPC: anode plane assemblies, cathode plane assemblies and the field cage. It also includes all in-vessel electronics, signal and power cables, their feedthroughs, as well as the low and high voltage power supplies feeding the electronics. This subsystem interfaces the cryostat and cryogenic subsystem through the TPC mounting fixtures, and it interface the DAQ subsystem through the signal feedthroughs.

The TPC's active volume (fig.3.1) is 14 m vertically and 15 m horizontally and 70 m long in the beam direction. It contains ∼20 ktons of liquid argon. It consists of 4 rows of cathode plane assemblies (CPA) interleaved with 3 rows of anode plane assemblies (APA). The distance between the cathode and anode is 2.5m. Both the cathode and anode plane assemblies are 2.5m wide and 7m high. Two 7m modules stack vertically to cover the 14m active depth. In each row, there are 28 such stacks in the beam direction, forming the 70m active length. There are a total of 168 APAs and 224 CPAs in each cryostat. Each pair of cathode and anode planes are surrounded by a field cage to ensure a uniform drift field.

On each anode plane assembly, 4 planes of wires cover both sides of a wire frame. The inner 3 planes of wires are oriented vertical, and ±45° respectively, and each wire is connected to a front end readout channel. The outer most plane of wires is a shielding plane. The wires are vertically oriented. They are biased with a specific voltage, but no signal readout. At a wire pitch of 3mm, the total number of readout channels is 645,120 in the entire detector.

The readout electronics are optimized for operation in the cryogenic environment. The front end ASIC chip has a mixed signal design. It has 16 channels of preamp, shaper and ADC in its analog section, followed by a 16 to 1 multiplexer at its output. 8 of such chips are mounted on a single readout board, covering 128 wires. A digital processing ASIC with an 8:1 multiplexer on this board further increases the multiplexing factor to 128:1, resulting in a single output channel. This output channel will be transmitted through two redundant optical fibers. On each APA, there are 30 output channels, with 60 optical fibers. The total number of output data fibers is 10,080. We are evaluating the options of implementing data compression and zero suppression to the data stream in the digital processing ASIC. With these features in place, we can add another stage of multiplexing (8:1) on the optical channels with redundant output at the APA level to

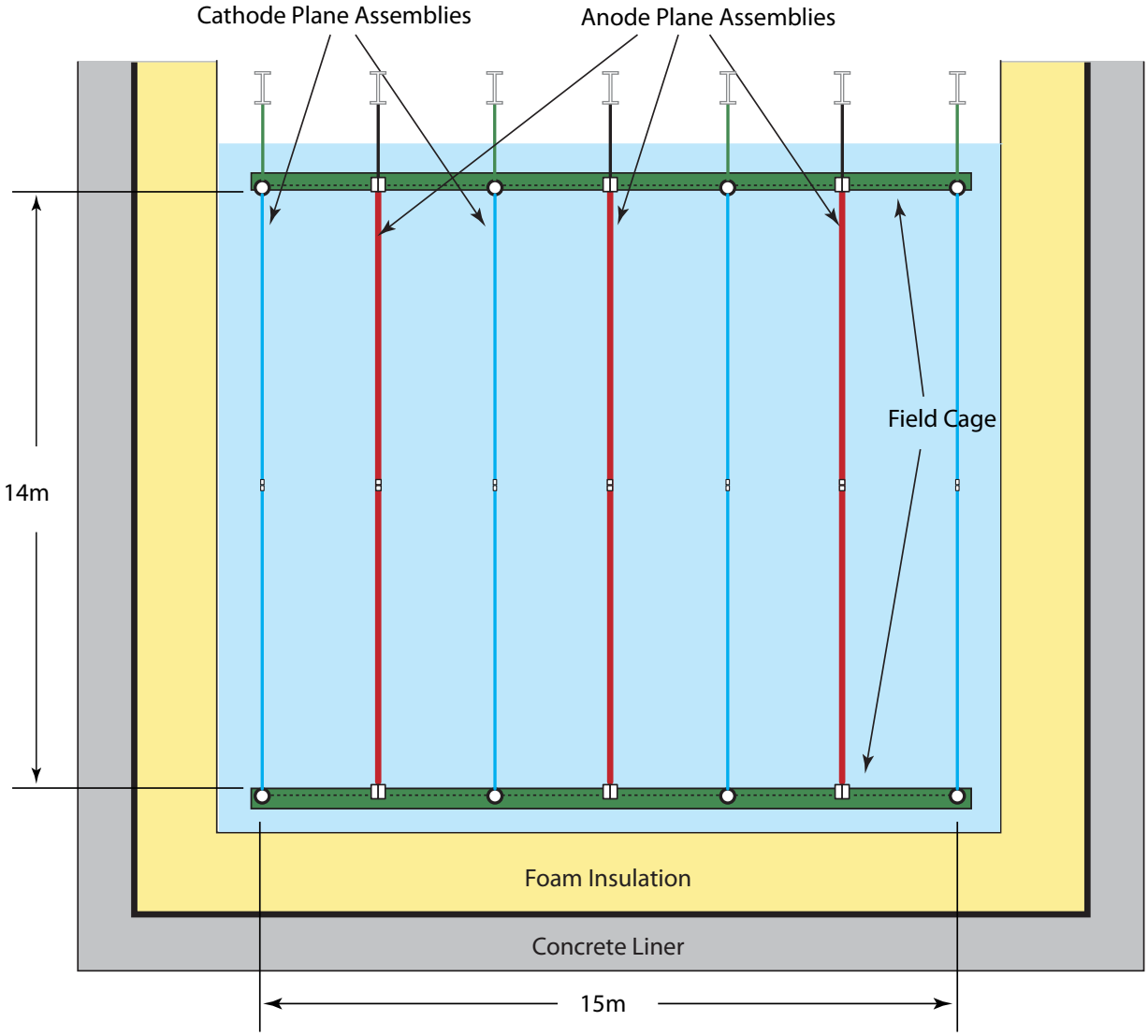

Fig. 3.1. Cross section of the TPC inside the cryostat (place holder)

further reduce the fiber count.

To get the signals out of the cryostat, we need feedthroughs for up to about 11,000 optical fibers. Additional redundant high voltage (for the cathodes), medium voltage (wire bias), and low voltage (ASICs) power feedthoughs are also needed. To reduce the DC current at the low voltage feedthroughs and the cables, DC-DC converters will be distributed inside the cryostat, above each APA stack.

3.1 Requirements and Specifications

The main requirements of the TPC are the followings:

- The fiducial volume enclosed by the TPC must reach 100 kton water equivalent.
- The TPC must be constructed from modules to minimize installation time and cost. Every module must be validated through thermal cycling to ensure compatibility with the LAr environment.
- 3 wires planes must be instrumented to provide redundant signal readout.
- The wire pitch should be between 3 – 5mm. The wire plane separation should be equal to that of the wire pitch.
- The maximum wire length is 10m, to minimize the readout electronic noise.
- The wire chambers must be designed and constructed to minimize the risk of wire breakage.
- The TPC must maintain a uniform electric field of 500V/cm, resulting in an electron drift velocity of 1.6 mm/μs. The field cage must keep the field uniform within 5cm of the field cage surface.
- The electric field must be kept below 100kV/cm in liquid argon, xxkV/cm in gas argon, throughout the cryostat to prevent high voltage breakdown.
- The readout electronics must provide a minimum signal to noise ratio of 10 for MIPs.
- The readout electronics must be designed to record the wire waveforms continuously without dead time.
- The readout electronics must provide redundant multiplexed data output to minimize the number of feedthrough penetrations.
- All materials used in the TPC must be tested and qualified to be compatible with high purity liquid argon.

3.2 TPC Chamber (WBS 1.5.4.2)

3.2.1 Anode Plane Assemblies (APA)

The anode plane assemblies are 2.5m wide, 7m high, and about 7cm thick. Each is constructed from a framework of light weight stainless steel tubes, with 4 layers of CuBe wires wrapped over both sides of the frame using automated winding machines. The front end electronics boards are mounted on one end of the wire frame and protected by a metal enclosure.

The wires used in the TPC must satisfy the following requirements:

- High break load to withstand the applied tension without breaking;
- Good conductivity to minimize noise contribution to the front end electronics;
- Comparable thermal expansion coefficient to that of the stainless steel frame to avoid tension change after cool-down.

Both stainless steel and copper beryllium wires are potential candidates. Stainless steel is the choice of Icarus, while a copper plated (to reduce resistance) stainless steel wire is chosen by MicroBooNE. Both experiments use a wire termination technique that is labor intensive and not practical for LBNE scale detectors. Previous experiences from FNAL have shown that a CuBe wire under tension can be reliably bond to a FR4 surface by a combination of solder and epoxy. This bonding technique greatly simplifies the electrical connection to the readout electronics, and it can be easily automated with commercial equipments. Since CuBe wire solders very well, it is selected as the wire of choice. At 150μm diameter, the break load of a hardened CuBe wire can reach to about 3kg. To ensure no wire breakage in the TPC, the nominal operating tension of the wire is set at 0.5kg. Periodic support structures on the wire frame limit the unsupported wire length to under 2m. No significant deflection due to gravitational or electrostatic forces is expected. The ends of a wire are soldered and then glued on to a printed circuit board made of FR4.

Four planes of wires are installed on both sides of an APA. The nominal wire pitch is 3mm and the distance between wire planes is also 3mm. The wires on the 1st and 4th planes (along the direction of electron drift) are vertically oriented, while the 2nd and 3rd planes are at $\pm 45°$. The wires on the first plane are not connected to the readout system. Their sole function is to shield the 2nd wire plane from seeing distant ionizations. The 4 wire planes must be bias in such as way that electrons from an ionizing track completely drift pass the first 3 planes, and are collected by the last plane. Preliminary calculation shows that the minimum bias voltages needed to achieve this goal are $V_S = -480$V, $V_U = -280$V, $V_V = 0$V and $V_X = 700$V respectively, with a grounded mesh plane 3mm behind the 4th wire plane. The V wire plane is directly connected to the FEE to simplify the coupling and reduce the maximum bias voltages on the other planes.

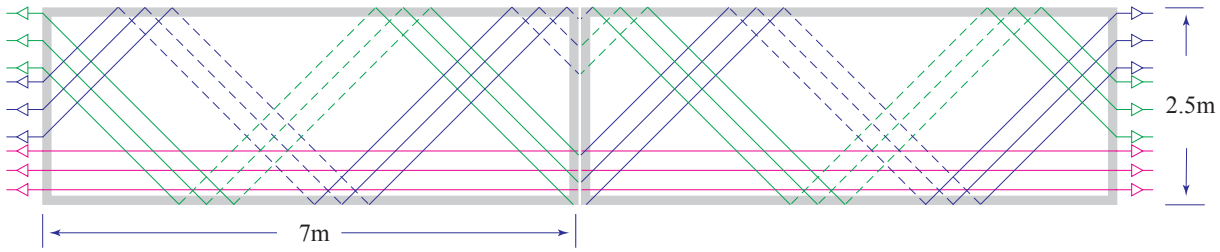

Fig. 3.2. Illustration of the wire wrapping concept. The wire frames are rotated 90° with a narrow end up in the TPC.

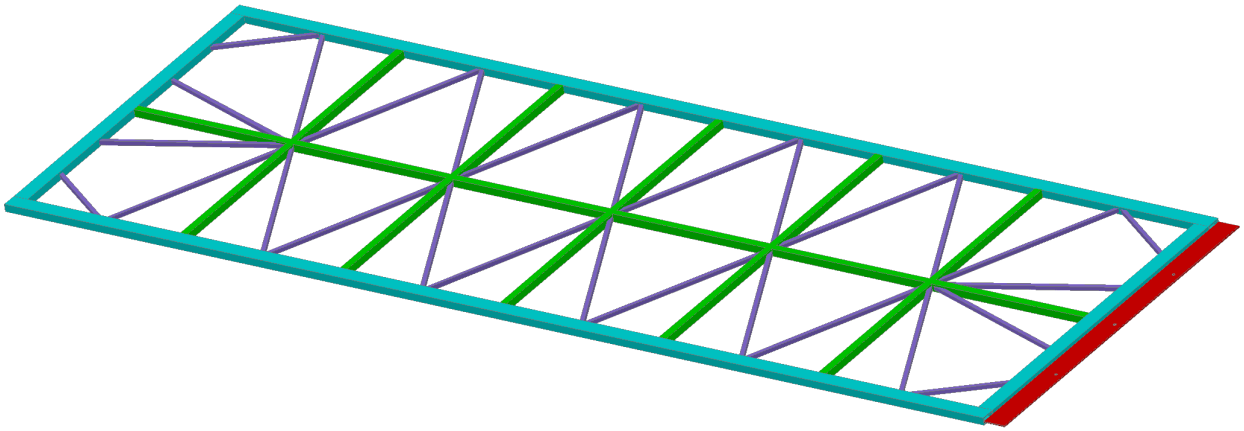

Fig. 3.3. Conceptual design of a wire frame.

The wires on the two induction planes (U & V) are wrapped at ±45° around the long edges of the wire frame (fig.3.2). This technique makes it possible to place readout electronics only at one narrow edge of a wire frame. It slightly complicates the track reconstruction because the U & V wires are sensitive to tracks on both sides of the APA. The upper APAs in the cryostat have their readout at the top edge of the frame (as shown in fig.3.2) , while the lower APAs mount their electronics at the bottom edge (a mirror image of fig.3.2).

At 3mm wire pitch and a 45° angle, the U or V wires intersect the readout end of the APA with a pitch of $3\sqrt{2}$ mm. Due to this $\sqrt{2}$ ratio between the U/V and the X wires, it is impossible to divide the readout end into regions with identical wire bonding patterns. To make the readout modular, we need to change the U & V wire pitch slightly. A convenient modularity is 128 readout wires, consisting of 56 X wires at 3mm pitch, and 36 U & 36 V wire at about 3.3mm pitch. These 128 readout wires span a width of 168mm. Using this modularity, the APA width is set to 2520mm. There are 1680 X wires, 1080 U wires, 1080 V wires, and 1680 shielding wires for each APA. The total number of readout channels is 3840 per APA. The total number of wires is 5520 per APA.

At a nominal wire tension of 0.5 kg, the 5520 wires exert a force of about 970 kg/m on

the short ends of the APA, and a 303 kg/m force on the long ends. The wire frame must be able to withstand the wire tension with a allowable distortion under 0.5mm, while minimizing the thickness of the frame to reduce the dead space occupied by the frame. A conceptual design of the wire frame is shown in fig.3.3. It is constructed from all stainless steel tubes welded in a jig. The total weight of the frame is about 250kg. All hollow members of the frame are vented to prevent trapped volume. The two long outer members of the frame are open-ended so that signal and power cables can be threaded through to reach the readout end of the lower APA.

Fig.3.4 shows 3 major cross sections of an APA.

The top figure is the cross section of the readout end of an APA. The four planes of wires are attached to their respective wire bonding boards through a combination of solder and epoxy. Copper traces on the wire bonding boards connect each of the readout wires to the front end readout boards. These readout boards (described in the next section) process the analog signals from the wires and transmit the digital information through optical fibers to the DAQ system outside the cryostat. The electronics on the readout boards dissipate of the order of 60W of heat per APA, generating a small amount of argon bubbles. Two stainless steel covers are placed over the readout boards to contain the bubbles and direct them to the gas volume of the cryostat.

The middle figure shows the cross section of the short, non-readout end of an APA. All wires are mechanically terminated on this end on the 4 layers of wire wrapping boards. No electrical connections are needed.

The bottom figure shows the cross section of the long end of an APA. Only two layers of wire wrapping boards are needed for the U & V wire planes along this edge of the APA. The wire wrapping boards are made from printed circuit boards. On each of the wire wrapping board, there are bonding pads for soldering and gluing the wires at the edges. Copper traces interconnect the wires from one side of the APA to those on the other side. This allows a more convenient placement of mounting holes through the center of the boards. As with the wire wrapping boards shown in the middle figure, precision grooves are machined onto the edge of the boards to guide the wires into the correction position, and to prevent sharp kinks forming on the wires. Fig.3.5 shows two examples of the groove design. The one on the right is for the X wires, and the one on the left is for the U or V wires. During storage and shipment, protective metal guards are placed on the three APA wrapped edges.

The left of fig.3.4b also shows the wire support structure mounted on one of the inner horizontal frame members. A detailed rendering of this concept is illustrated in fig.3.6. The support is made from strips of thin fiberglass boards, with notches machined at specific intervals. The support strip for X plane is directly mounted on the inner frame. After all X wires have been placed into the slits, the V support strip (shown in green) is glued onto the tips of the X strips, trapping the X wires in place. After the V wire are placed into the slits, the U support strip (identical to the V strip) is glued to the V strip, trapping the V wires... These structures are repeated 5 times along the 7m length of an APA, limiting the unsupported wire length on any wire plane to less than 2m, while introducing only millimeter scale dead regions. Such wire

supports play a key role in minimizing wire deflection due to gravity and electrostatic force, enable us to use a moderate wire tension, and reducing the risk of wire breakage. The support structure also make the wire frame much more stable against buckling along the frame length.

Two winding machines will be constructed to lay the 5520 wires on each APA. Their working concepts are illustrated in fig.3.7. For the X and the shielding wire planes, the wire frame will be standing on one of its long edges, while a wire is wrapped around the frame through the 3 axis linear stages. A wire tension controller maintains the wire tension and feed rate off the spool. Although the entire plane of wires can be wound in one pass, we'll pause the winding machine periodically and solder the last wire onto the frame to prevent large section of wires unravel due to a broken wire. For the U & V wires, it appears difficult to design a machine that can wind a entire plane of wires in one shot. The winding machine will wind a group of wires (~ 10) during each pass. A technician solders the ends of the wires before and after each pass of the winding process. An automated wire tension measuring device will scan the newly placed wires, record the wire tension of each wire. Any wire with abnormal tension will be replaced manually.

3.2.2 Cathode Plane Assemblies

Similar to the APAs, the cathode plane assemblies are also 2.5m wide and 7m high. Each is made of a stainless steel framework, with a layer of stainless steel wire mesh stretched over one side of the frame. To reduce distortion to the drift field, all surfaces significantly raised above the mesh, such as the stainless steel frame structure on the other side of the mesh, are covered with field shaping electrodes biased at the appropriate voltages. Fig.3.8 illustrates the concept of the cathode plane assembly.

To achieve a 500 V/cm drift field over a 2.5 m distance, the bias voltage on the cathode plane must reach -125 kV. A basic high voltage bias setup requires 4 HV power supplies, one for each CPA row in the cryostat. A more elaborate setup can limit the impact of a HV failure down to the extend of a few CPAs, with the expense of increased complexity in the CPA construction.

3.2.3 Field Cages

Each pair of facing cathode and anode rows form a drift volume. To maintain a uniform electric field inside this volume, a field cage is constructed to completely surround its 4 outer open edges facing the cryostat. To cover the entire TPC, we need about 170m $\times$ 2.5m $\times$ 6 of field cage material. Copper clad kapton film is a very attractive candidate. Manufactured in rolls, they can be easily processed in a reel-to-reel fashion. Parallel copper strips are etched on the kapton film, each strip is biased at a specific voltage provided by a resistive divider network. These strips provide a linear voltage gradient, ensuring a uniform drift field in the TPC's active volume. Fig.3.9 shows the results from an electrostatic simulation of a particular strip pattern. The drift field non-uniformity quickly drop below 1% roughly a strip pitch away from the field

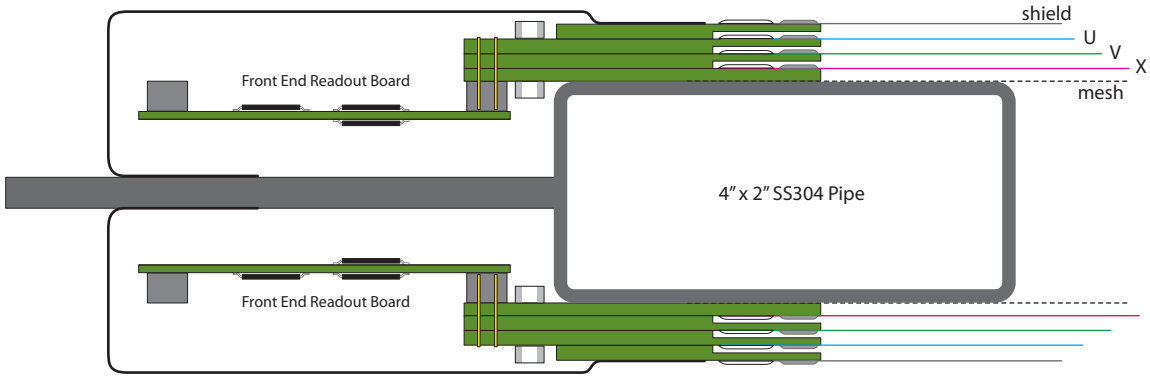

a) Cross section of the short, readout side of the APA

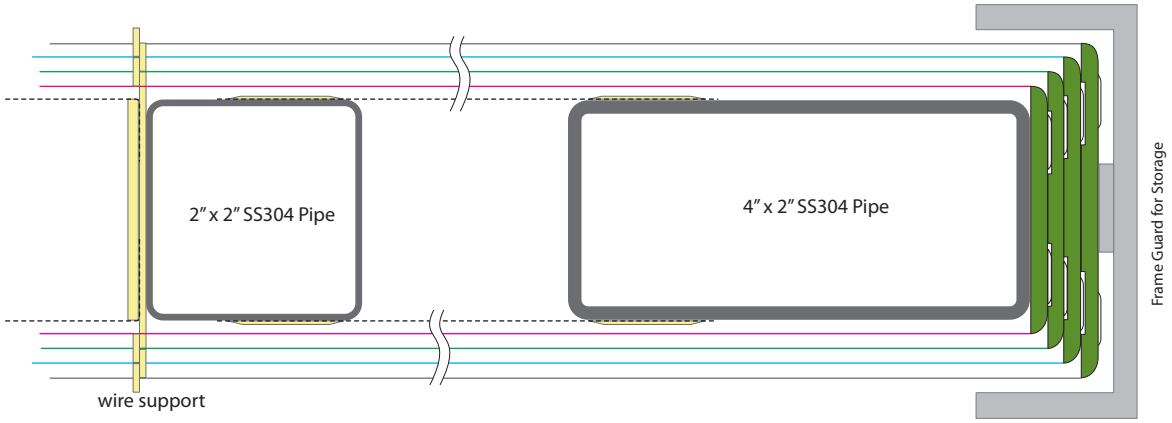

b) Cross section of the short, non-readout side of the APA

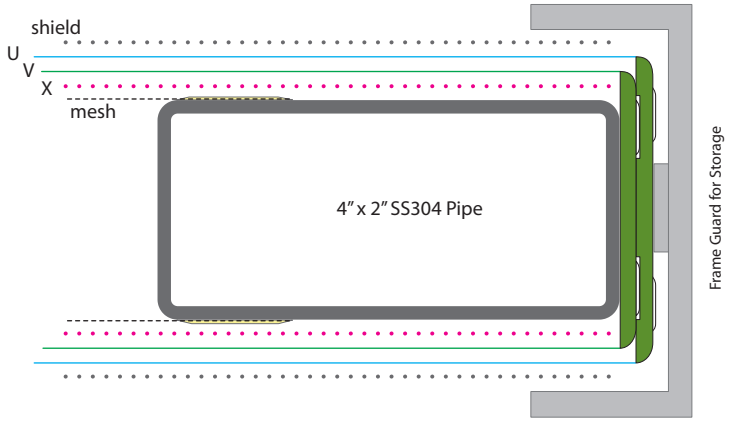

c) Cross section of a long side of the APA

Fig. 3.4. 3 cross sectional views of the APA.

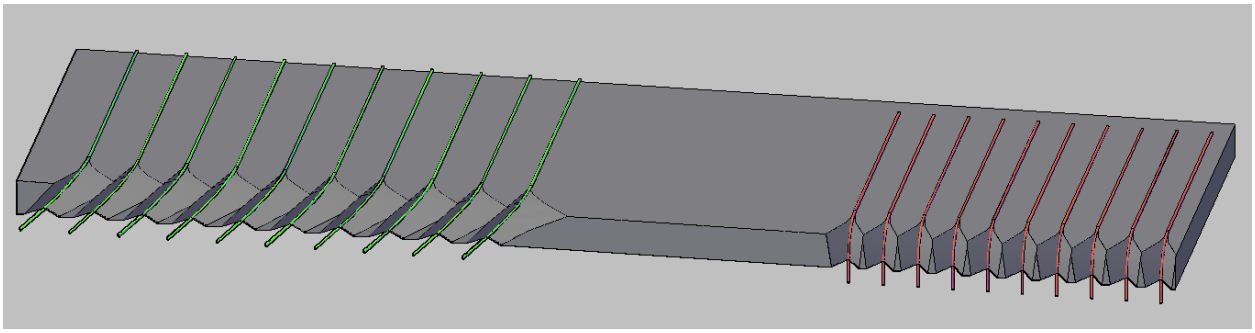

Fig. 3.5. Grooves on the edge of a wire wrapping board. The left group is for the U & V wires having a 45° angle. The right group is for the X and the shielding wire planes. These grooves not only allow precise placement of the wires, but also prevent kinking and consequently weakening of the wires.

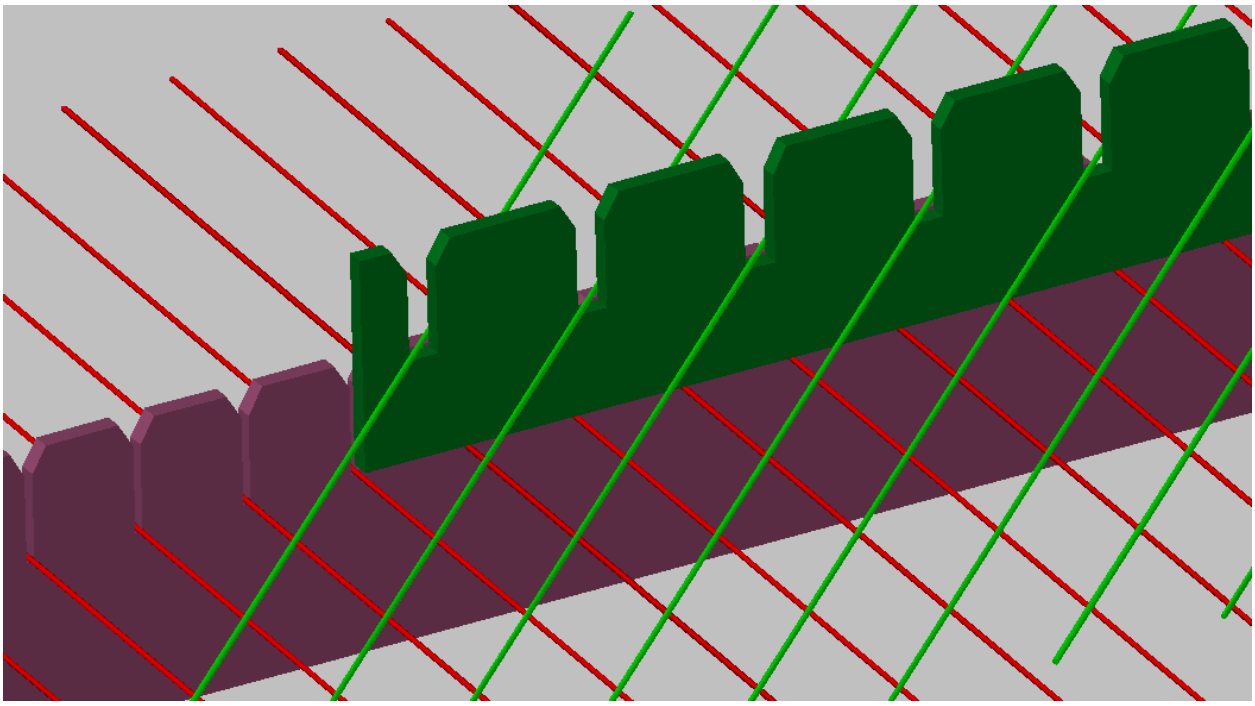

Fig. 3.6. Conceptual design of the wire support for the X and V wires. Similar structure can be built up to support the U and shielding wire planes.

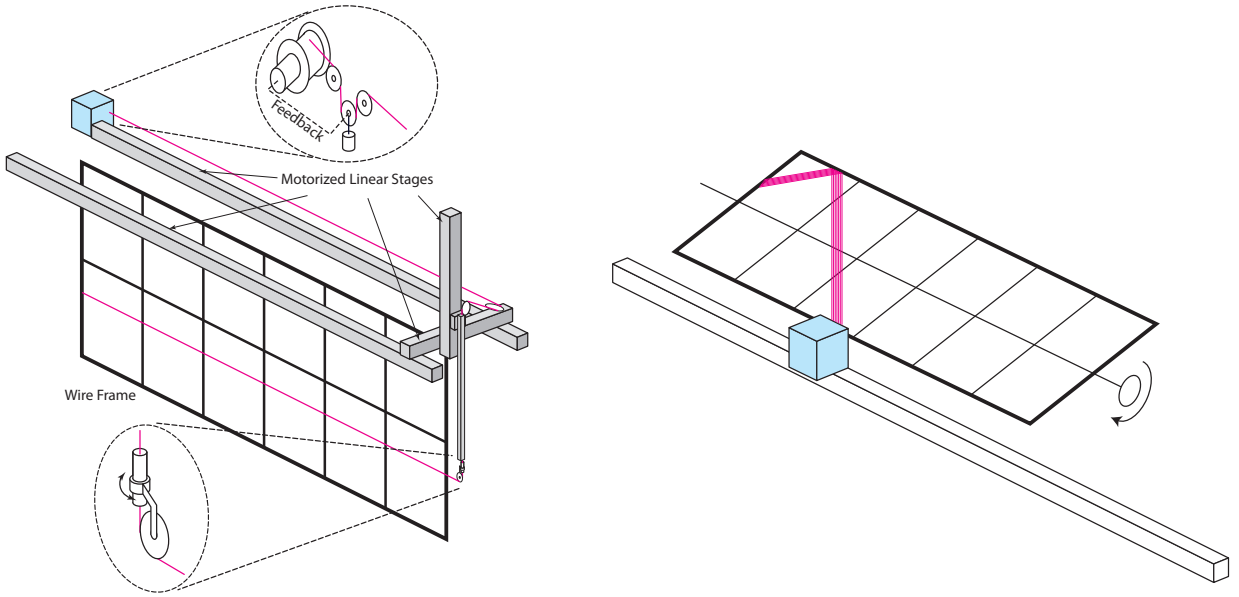

Fig. 3.7. Two winding machine concepts. The left figure is for the X and shielding wires, the right figure is for the U & V wires. The 'blue boxes' are wire spools with automatic tension control.

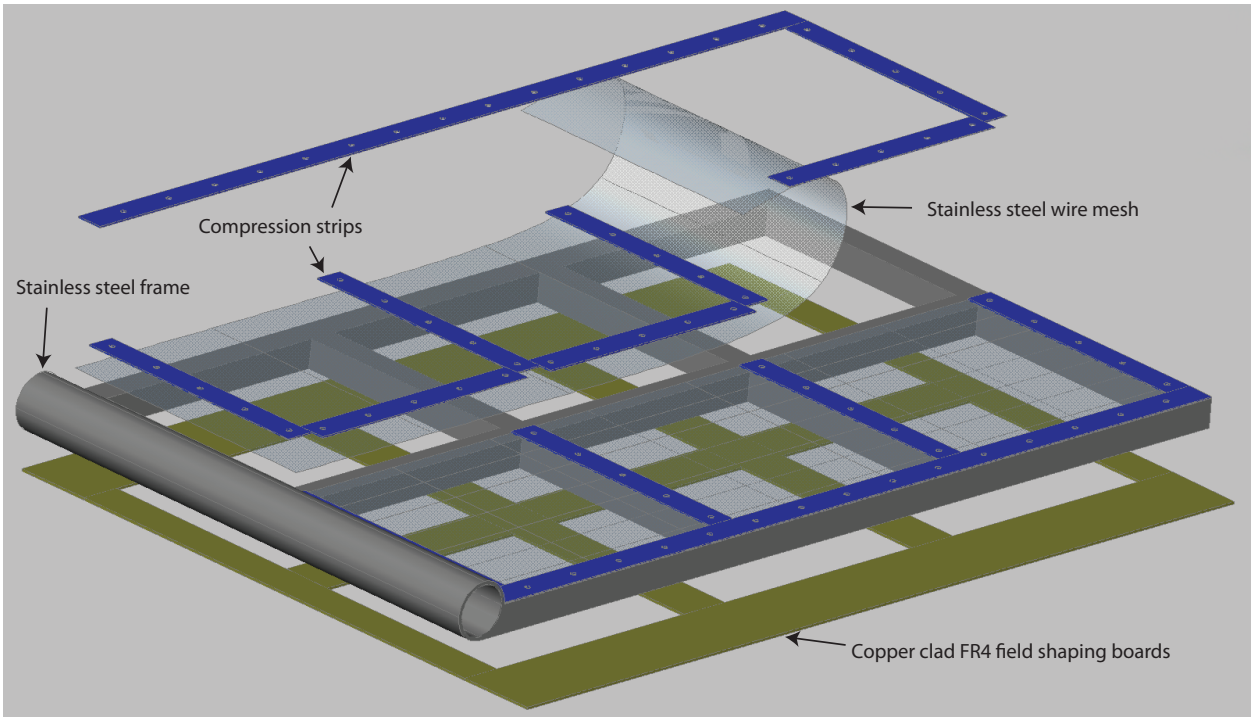

Fig. 3.8. Conceptual design of a cathode plane assembly (not to scale). The assembly is 2.5m wide and 7m tall.

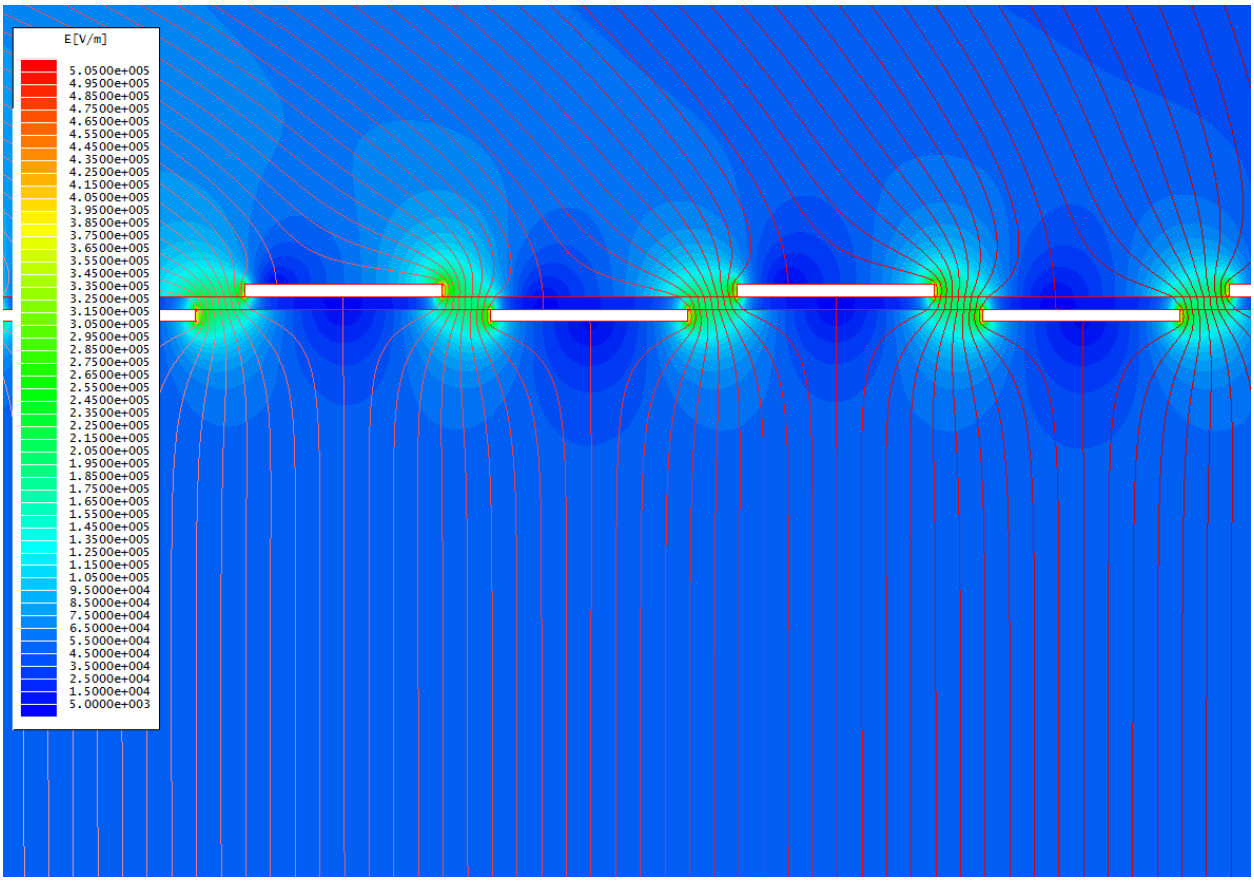

Fig. 3.9. Electrostatic simulation of the electric field near a section of the field cage. The filled color contours represent the electric field strength. The red line contours represent the electric potential at 50V intervals. The pitch of the electrodes is 1cm.

cage surface. Since the field cage completely enclose the TPC on 4 sides, the kapton film must be perforated to allow natural convection flow of the liquid argon. The "transparency" of the perforation will be determined by a detailed LAr convection study.

The resistor divider network is mounted on a printed circuit board, which is in turn soldered on to one end of the field cage kapton film. To minimize the impact of a resistor failure (open circuit), 4 resistors will be connected in parallel between any two taps of the divider. The combined value of the 4 resistors in parallel is in the order of 10 MΩ. These resistive divider boards will be attached to the top portion of the field cage, so that argon bubbles, if any, will not enter the active volume.

3.2.4 TPC Assembly in the Cryostat

Fig.3.10 shows a partial assembly of a section of the TPC. The finished cryostat has 7 rows of anchor points distributed along the ceiling. 7 mounting rails are attached to those anchor points. Under these mounting rails, rows of CPAs and APAs are suspended in an interleaved fashion. Due to the presence of high voltage on the cathode, the CPAs are attached to their mounting rails through G10 rods. The distance between the facing anode and cathode is maintained by a set of G10 beams, which also support the Kapton sheets forming the field cage. Detailed TPC installation procedure is discussed in Section **??**.

3.3 In-Vessel Electronics (WBS 1.5.4.3)

3.3.1 Requirements and Specifications

- The in-vessel electronics must be designed to operate at a liquid argon temperature of 89 K with a lifetime of 20 years.
- The front end electronics must have an ENC of $<1000e$ with an input capacitance of 200 pF, the equivalent of 10m wire.
- The total power consumption of all in-vessel electronics should not exceed $1/3$ of the total cryostat heat load through the foam insulation.
- The front end electronics must digitize the wire signal waveform at no less than 1 MHz and 11bits of resolution.
- The readout electronics must operate in a continuous mode with no dead time loss.
- The front end electronics must provide sufficient level of multiplexing to reduce the number of feedthroughs, and redundant output to ensure reliability.

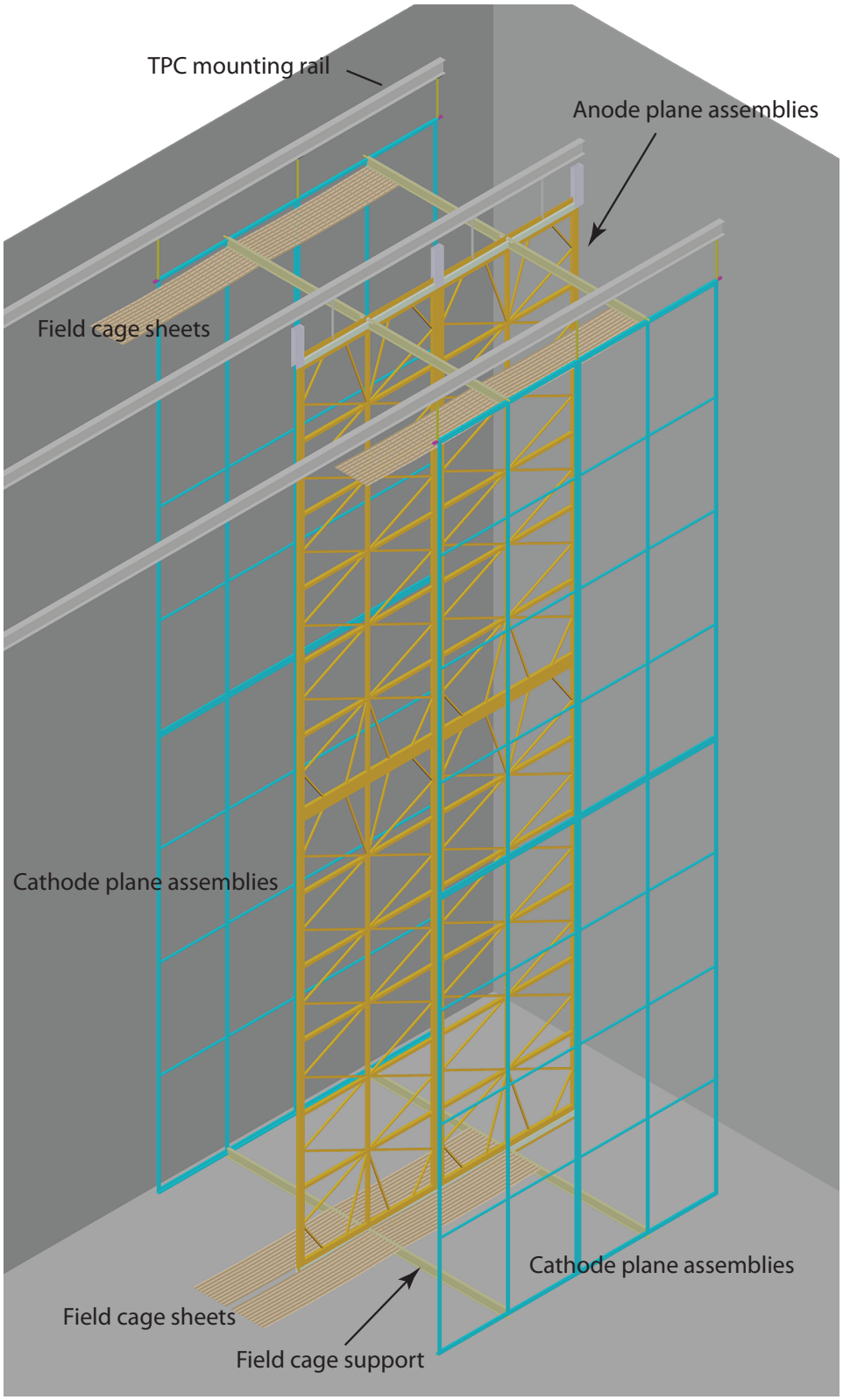

Fig. 3.10. A partial assembly of the TPC

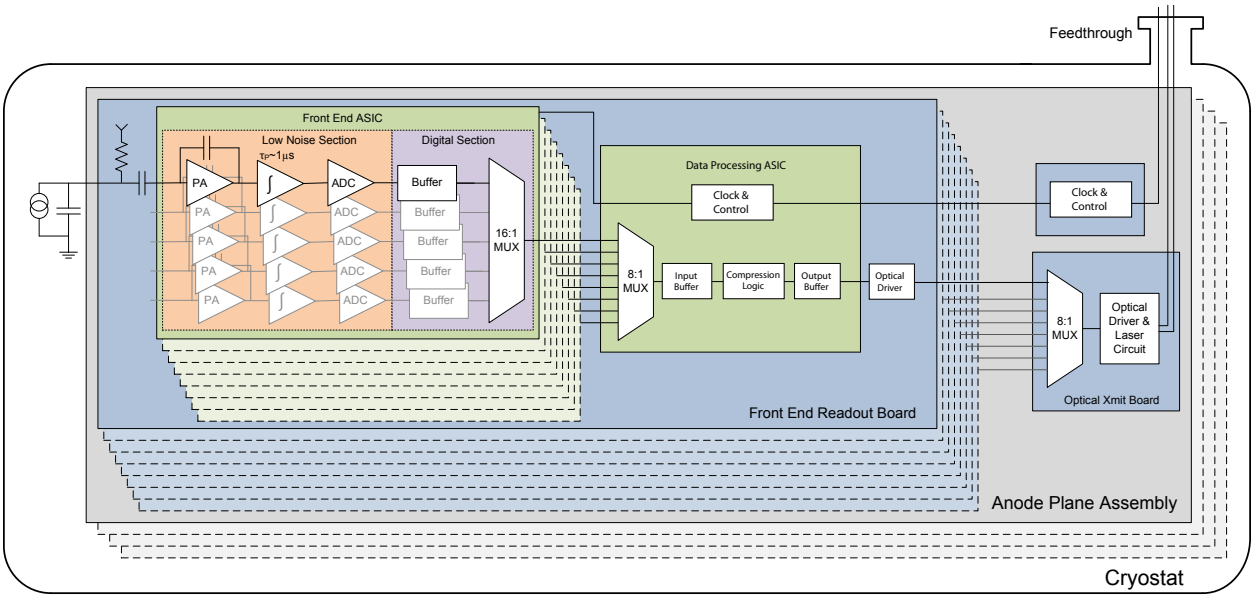

Fig. 3.11. Schematic diagram of the LArTPC front end electronics

- The in-vessel electronics must be able to reliably transmit the digital signal through fibers inside the cryostat to feedthroughs at least 100m away.

3.3.2 Description

The readout electronics are optimized for operation in the cryogenic environment. The front end ASIC chip is a mixed signal design. It has 16 channels of preamp, shaper and ADC in its analog section, followed by input buffer, compression logic, output buffer for each channel in the digital section, and a 16 to 1 multiplexer at its output. 8 of such chips are mounted on a single readout board, covering 128 wires. An 8:1 multiplexer on this board further increases the multiplexing factor to 128:1, resulting in a single output channel. This single output channel is connected to both a LVDS driver and a laser driver to generate redundant outputs on both copper wires and optical fiber. On each wire module, there are 32 LVDS output channels and 32 optical fibers. Further multiplexing (8:1) on the optical channels with redundant output at the module level is being considered. A schematic diagram of this layout is shown in fig.3.11. The total output signal connections per module with 4000 wires is 64 copper wires and 8 fibers.

3.3.3 CMOS at Cryogenic Temperature

With a wire capacitance approaching 200 pF, the resolution of 1000 rms electrons rms can only be achieved if the front-end electronics is located in close proximity to the wire ends, i.e. in the liquid Argon (89 K). Moving the front-end electronics in a warmer environment above the surface of the liquid (∼120 K) would require some meters of interconnect, and the associated

parasitic capacitance would make practically impossible to achieve the required resolution. Moving the front-end further outside the cryogenic environment (300 K) would require a prohibitive number of feedthroughs (one for each wire). In operating the CMOS technologies at the cryogenic temperature of 89 K, two critical aspects must be considered. The first is the reliability of the models in terms of operating point, signal response (transconductance, output resistance and capacitance), noise, interconnects and passive components (resistors and capacitors). The second is the long-term lifetime, since that the LAr TPC is required to operate for over 20 years without further access to the electronics for repair or replacement once the TPC is sealed.

Concerning the models, we have characterized a complete mixed-signal CMOS 0.25 μm ASIC, originally developed for room temperature applications, at temperatures down to 40 K, observing encouraging results (see for example fig.3.14. A comparison of the signal response to the simulation suggests that the models are to a first order reliable, and may need some minor adjustments. We have also fabricated in a CMOS 0.18 μm technology a dedicated analog front-end (described in the next Section) and a number of test structures.

With regards to the long-term lifetime, the major failure mechanisms like electromigration (EM), stress migration (SM), time-dependent dielectric breakdown (TDDB) and thermal cycling (TC) scale in favor of cryogenic operation [1]. The only mechanism that can affect the lifetime at cryogenic temperature is the degradation due to impact ionization, which causes charge trap in the MOSFET gate oxide [2]. Substrate current is a good indicator of the impact ionization. Accelerated tests and lifetime extrapolation enable us to develop design guidelines for the long-term analog and digital operation at cryogenic temperature.

3.3.4 Front End ASIC

In fig.3.15 a block diagram of the 16-channel front-end ASIC is shown. Each channel implements a charge amplifier with adjustable gain (4.7, 7.8, 14 and 25 mV/fC), a high-order shaper with adjustable peaking time (0.5, 1, 2, 3 μs), optional AC coupling, baseline adjustment for operation with either the collecting or the non-collecting wires, a 12-bit 2 MS/s ADC and a data compression stage. Shared among the 16 channels are the bias circuits, registers, a temperature monitor, the digital multiplexer (16:1), the FIFO and the digital interface. The first prototype has been developed in a commercial CMOS 0.18 μm technology, but the final choice will depend on the results from the characterization of several test structures.

The input MOSFET is a p-channel biased at 2 mA with a L/W ratio of 0.27 μm/10mm, followed by a dual cascode stage. The charge amplifier is composed of two stages and it provides a charge gain up to 20×16. In principle the charge gain could be arbitrarily increased, thus making negligible the thermal noise from the dissipative elements in the shaper and achieving an infinite dynamic range $\mathrm{DR} = \mathrm{Q_{max}}/\mathrm{ENC}$. However a limit is imposed by the maximum voltage swing V_{max} and capacitor value $\mathrm{C_{sh}}$ of the shaper. No matter how high is the power dissipated in the shaper and what shaper configuration is used (voltage- or current-mode, current-scaling, etc.),

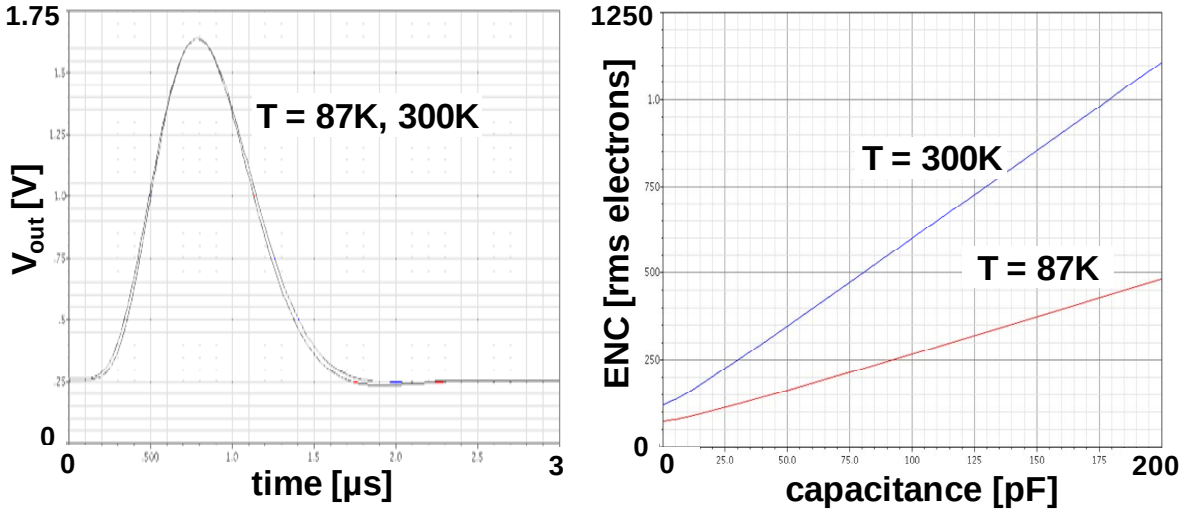

Fig. 3.12. Simulated response and ENC at 300K and 87K

the shaper imposes a limit to the dynamic range given by:

$$\mathrm{DR} <\sim \frac{V_{\max}}{\sqrt{4kT/C_{\mathrm{sh}}}} \tag{3.1}$$

From (3.1) it follows that the dynamic range is limited by the size of the capacitor and by the maximum voltage offered by the technology. In order to maximize the dynamic range large capacitors must be used, while the shaping amplifiers must operate rail-to-rail: we will use circuit configurations that allow so.

The analog section of the channel has been fabricated and it will be characterized. Fig.3.12 shows the simulated ENC and signal response at room and LAr temperatures.

The shaped signal which results from the induction in the TPC wires must be sampled and digitized in 12-bit words at a rate of 2 MS/s. This is achieved by integrating one Analog-to-Digital Converter (ADC) in each channel. The ADC, currently under design, aims at offering a 12-bit resolution and convert-ing in less than 500 ns, while dissipating about 2 mA (3.6 mW). The power can be reduced at expenses of the conversion time, which scales approximately with the inverse of the current.

The conversion occurs in two stages, the first occurring in about 150 ns, provides the six most significant bits (MSBs), while the second, occurring in about 250 ns, provides the six least significant bits (LSBs), for a total of 12 bits in about 400 ns. The residual 100 ns are used for

encoding and reset. Both stages are based on the current mode ADC concept described in ref. [3] where a number of matched individual cells are enabled in sequence.

3.3.5 Data Compression

The readout electronics is designed to sustain continuous waveform digitization without any deadtime loss. The ADC digitizes the shaper output at a rate of 2MHz and 12bits. The multiplexed output from the front end ASIC is 2MHz×16ch×12bits = 384Mbps. After another level of multiplexing at 8:1, the data rate jumps to 3Gbps. This data rate can be comfortably transmitted through optical fibers out of the cryostat. The minimum number of fibers required is 5,040, or 10,080 if we use two fibers per board for redundancy. Further reduction in channel count is possible by adding another level of multiplexing, say 4:1, raising the output data rate over 12Gbps. This is a brute force method, but it is simple and straightforward to implement in the cold electronics. The penalty is the high data clock on the readout boards, and the large number of optical fibers that must pass through the cryostat.

Huffman coding is a lossless data compression method commonly used in computer science. it uses a variable-length code table for encoding a source data. The variable-length code table is arranged based on the calculated probability of occurrence for each source data. In the TPC, the wire signal waveform is shaped with a 1μs peaking time and digitized at 2MHz. The incremental changes between successive samples are very small. For example, a large fraction of such changes are within ± 3. By using a much shorter bit pattern to represent the most frequently occurring numbers, we can greatly reduce the bit length required to represent a string of data. Fig.3.13 illustrates an implementation suitable for encoding data with little incremental changes. The compression ratio depends greatly on the smoothness of the digitized waveform. A conservative estimate is around 4?. Since this is a lossless encoding, we can get the original data back with no data loss. The compression works at its best when the incoming date stream is from the same ADC (wire) channel and consecutive in time, not immediately after a multiplexer when the data is rapidly switching from channel to channel. From this point of view, the best place to implement Huffman encoding is right after the ADC on the front end ASIC. However, mixing the data compression logic with low noise analog processing runs the risk of degrading the noise performance of the chip. The alternative is to include the compression logic in the high speed digital section of the data processing ASIC. We need to transpose the data coming from the multiplexer so the compression can be perform along the same waveform. Sufficient buffering is required to account for the worst case scenario when no compression is possible.

The background rate for this underground LAr TPC is very low. Even when a track passes through the TPC, only a small number of channels see signal during a brief time window. The TPC is designed to have a minimum signal to noise ratio of about 10 to 1. In most cases, the digitized wire waveforms are baseline noise, with no signal of interest. Zero suppression is a very efficient means to achieve data rate reduction. One thing we need to keep in mind is that "zero" is actually a meaningful data point on the induction wires due to their bipolar nature of the waveform. Zero

U(n+1)-U(n)	Code
-4 and others	Full 16 bits word
-3	000001
-2	0001
-1	01
0	1
+1	001
+2	00001
+3	0000001

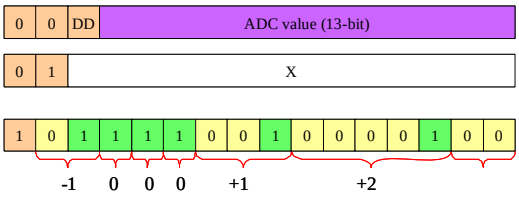

Fig. 3.13. Huffman coding

suppression should be applied under a threshold logic, or some other inputs. For example, if a localized light trigger is present in the APA, we can choose to record the full waveform only when a local light trigger is received. The rest of the time, the entire APA remains quiet. Another possibility is to use the collection signal waveform as a trigger: only transmit three planes of data when a channel on this APA has something beyond a threshold. Some buffering is required to ensure the leading edges of the induction signals, which occurs before the collection signals, are properly recorded. Another option is to make each channel self regulating: only transmit the waveform at full sampling rate upon the detection of a threshold pattern, otherwise, the waveform is smoothed and downsampled by a large factor. In either of these cases, Huffman encoding is applied to the zero suppressed data.

We will study the different scenarios to understand the implications in power consumption, data rate, cost, and design complexity and risk at the entire detector system level to reach our baseline design.

3.3.6 Data Transmission and Drivers

Besides the improved S/N ratio, the major advantage stemming from the placement of the front end electronics in close proximity to the sense wires, is the possibility of reducing the number of cryostat feed-through penetrations by multiplexing the digitized signals. This opens the possibility of placing the feedthroughs at the end of the cryostat since these connections carry digitized signals and do not impact any more the S/N ratio. This reduced number of feed-through connections not only improves the reliability of the cryostat by reducing the risk of leaks in the penetrations, but most importantly allows greater freedom in choosing the optimum shape and aspect ratio of the cryostat and the best mechanical structure for the top of the cryostat (which is not supported by the walls of the cavern and must withstand the overpressure inside the cryostat). One additional advantage is the reduction of the thermal load of >500,000 copper cables.

The table below summarizes the data rate at various points of the signal chain:

Data transmission between the front end ASIC and the data processing ASIC uses LVDS (Low Voltage Differential Signaling) at a maximum data rate of 384 Mbps, over a distance of

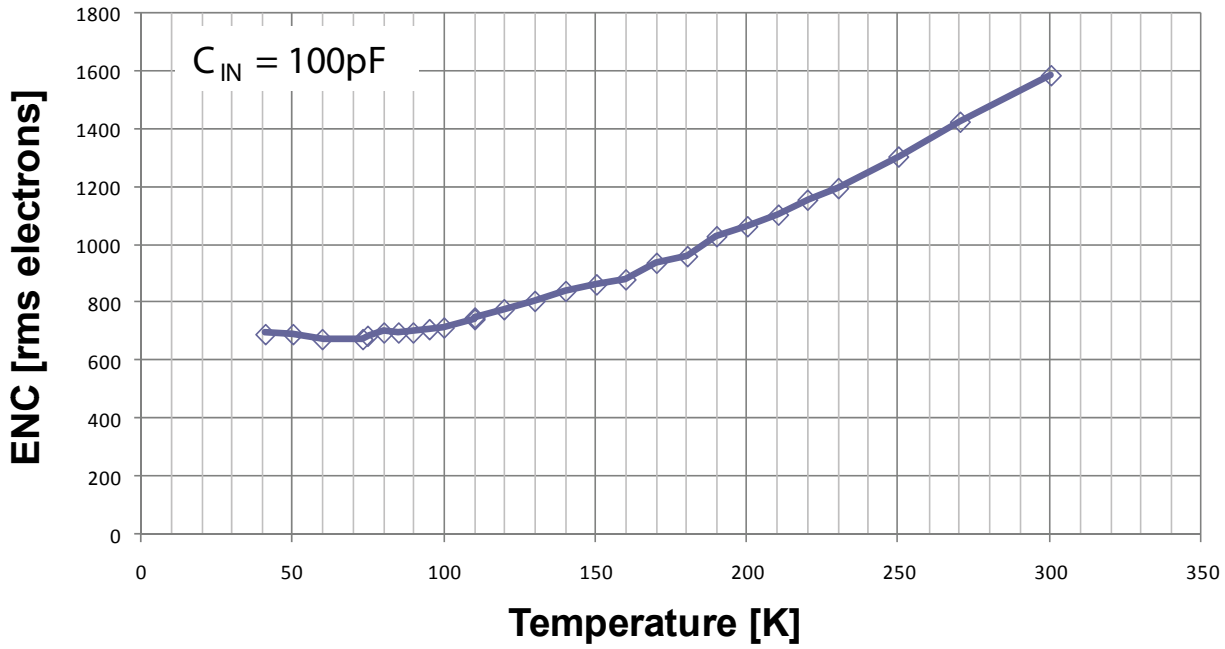

Fig. 3.14. ENC vs. temperature measured on a mixed signal ASIC designed for room temperature operation

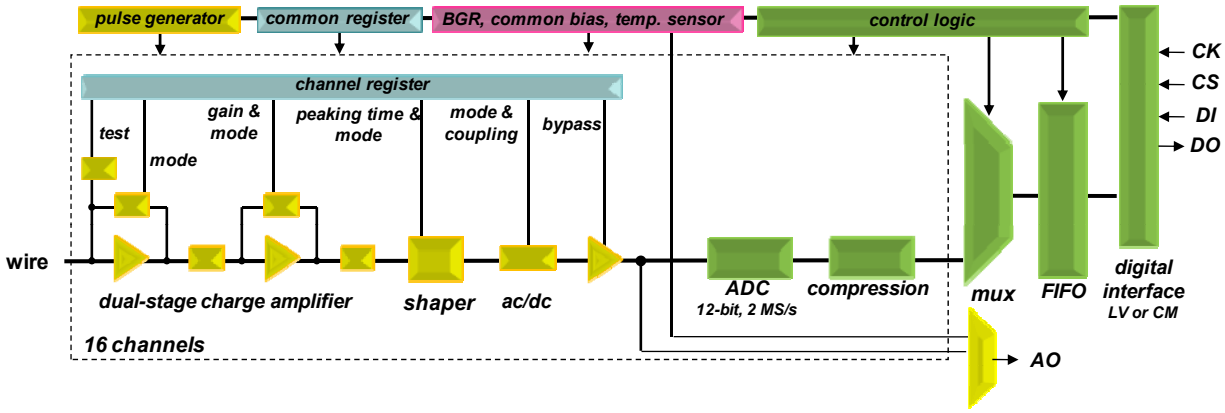

Fig. 3.15. Schematic diagram of the LArTPC front end ASIC chip

Element	Comment	Multiplexing Factor	Data Rate	Distance	Channel Count
ADC	2MHz, 12bits	1	24Mbps	0	645,120
FE ASIC Mux	LVDS	16:1	384Mbps	$\sim$ cm	40,320
FE board Mux	Optical or copper	8:1	3Gbps	$\sim$ 1 m	5,040
APA Mux	Redundant optical	4:1	12Gbps	50 m	2,520

Table 3.1. Data rate at various points of the cold electronics chain

a few centimeters. This is well within the specifications of the LVDS technology, and pose little technical challenge. At the output of the digital processing ASIC, the data rate will reach 3Gbps if no zero suppression is applied. This is beyond the capability of LVDS. With zero suppression, followed by data compression, and in conjunction with deep buffering, the data rate can be significantly reduces. Under these conditions, LVDS remains a viable choice between the front end readout board and the APA level multiplexer over a distance of 1m. If no further multiplexing at the readout board level, we'll need LVDS cables up to 50 m in length. Over this distance at room temperature, one must reduce the transmission speed to avoid data corruption. We are planning to study the LVDS data rate limit at LAr temperature.

Higher speed data links on copper are actively developed for data transmission on backplanes (over distances of $\sim$ 1m) or over short distances ($\sim$ 10 m over twisted pair). For example 10GBASE-T, or IEEE 802.3an-2006, is a standard released in 2006 to provide 10 Gbps connections over unshielded or shielded twisted pair cables, over distances up to 100 meters.

At this stage of development, we are also evaluating the option of an all-copper readout system. Assuming we can distribute the feedthroughs along the length of the cryostat, the length of the copper link could be less than $\sim$ 20m, which might be achievable without more complex drivers. This option becomes more feasible if data reduction by a factor $\sim$ 10 could be implemented.

One factor helping in achieving a high data rate in copper is the fact that copper resistivity decreases by a factor of five from room temperature to 87 K. This effect will reduce the copper link attenuation. It might be necessary to add a test connector on the readout board to transmit a full data rate stream during tests at room temperature. The âĂIJlow temperatureâĂİ data link could still be tested, albeit at lower data rate, at room temperature during installation.

Data links based on directly modulated laser diodes are commercially available for data rates up to 25 Gbps, and are being developed for higher data rates. The power required for a 10Gb/s link is less than 1W, or 2.5 mW/ch assuming a 24Mbps data rate (at room temperature). Assuming an optical link at $\sim$ 3Gb/s for each of the 128 channel front end board, a total of 5040 optical links (and vacuum proof optical connectors on the cryostat) would be needed.

If an additional level of 4:1 level of multiplexing is used, the required data rate would reach 12Gb/s. With these higher level of multiplexing, it would be prudent to add redundancy in the system to avoid the possibility that a a single point failure in the link would disable a large section of the detector.

Several semiconductor technologies currently used in the optical communication market are capable of cryogenic operation, including

- CMOS
- SiGe Bipolar

- InP HEMT
- GaAs
- SOI-CMOS (Silicon-on-Insulator CMOS)

We will evaluate these technologies and select the one based on cryogenic reliability and low power consumption.

3.3.7 Readout Board

Each readout board has 128 input channels, connecting to 128 wires from three wire planes. These 128 channels are divided into 56 X wires, and 36 U and 36 V wires. At 3mm wire pitch, the board will cover a 168mm section of the wire frame. 15 boards are needed to read out each side of the APA. The total number of readout boards needed is 30 per APA, 5040 in one 20 kton module.

8 front end ASIC chips, one digital multiplexing chip, and the optical drivers are mounted on the readout board. Due to the 128 multiplexing factor on the front end chips and the required redundant output, the readout board will have only optical fibers for data output. Power to the electronics, and the pass-through bias voltages to the wires are supplied to the board. Additional digital control lines for the ASICs, as well as a distributed clock signal are also routed to each board.

The interconnect between the wires and the FE ASIC inputs will be arrange in such a way that adjacent wires from the same plane will always be routed to different ASICs. This scheme saves us from being totally blinded by a failed ASIC.

3.4 Power Supplies, Feedthroughs, and Cabling

3.4.1 Requirements and Specifications

- All power supplies must be able to be monitored and controlled both locally and remotely through the DAQ system. They must have over-current protection circuits.
- The power supplies for the TPC cathode planes must be able to provide -150 kV at 1mA current. Its ripple voltage must be less then $10^{-}5$ peak to peak. They must be programmable to trip (shutdown) their output at certain current limit. During power on and off, including output loss (for any reason), the voltage at the feedthrough must be controlled to not exceed xxV/s to prevent damage to the in-vessel electronics through charge injection.

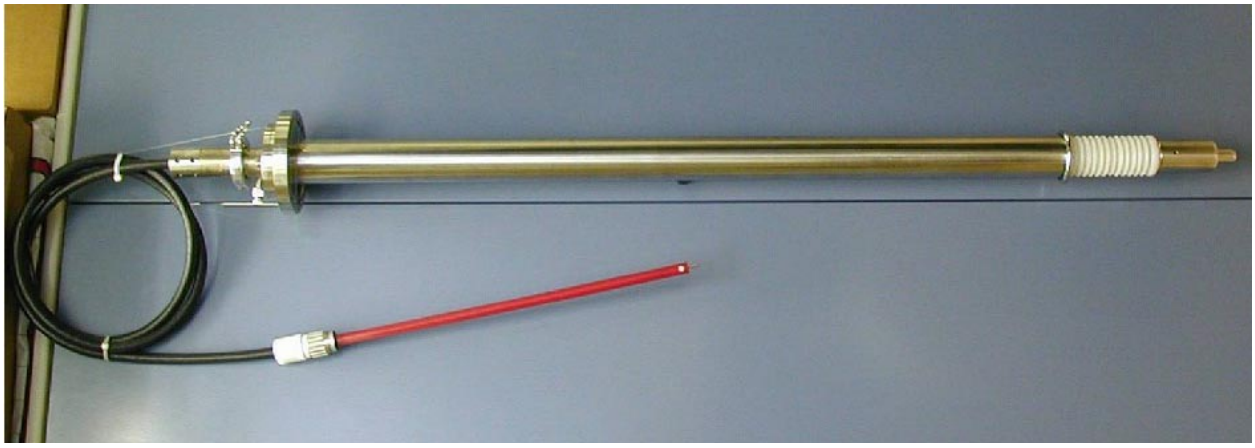

Fig. 3.16. A high voltage feedthrough developed by the UCLA group for the Icarus experiment. It was tested up to 150 kV.

- The power supplies for the wire plane biases and the purity monitors must provide up to xxmA of current with less than xxmV of voltage ripple.

- High voltage feedthroughs must be able to withstand −250 kV at their center conductors and in 1 atm air or argon gas environment.

- Medium voltage feedthroughs must be able to withstand ±1kV with leakage current less than xx nA in 1 atm argon gas;

- Low voltage power feedthroughs must be able to deliver a total of xxxx A of current.

- In cryostat DC-DC converters must provide redundancy in case of failure.

3.4.2 Description

There are 4 types of power supplies and the matching feedthroughs in the cryostat: TPC high voltage, purity monitor high voltage, wire bias voltages, DC power. There are two additional types of feedthroughs carrying signal: LVDS and optical fiber.

With the exception of the TPC high voltage links, all other cables inside the cryostat will be bundled and attached along the 3 mounting rails of the APAs before the installation of the TPC modules. All cables for a APA stack branch off from the bundle and connect to the respective APAs at specific points.

3.4.3 TPC High Voltage

The cathode planes are biased at -125kV to provide the required 500 V/cm drift field. At a minimum, we will use 4 high voltage power supplies, through their own feedthroughs, connect to the 4 rows of the cathode plane assemblies.

The current candidate for the high voltage power supplies is the Heinzinger PNC*hp* series, which is used by the Icarus experiment, and is also the candidate of MicroBooNE.

To ensure safe and reliable operation, the feedthroughs will be tested at a much higher voltage ($\sim$ 250 kV) in air and in 1atm argon gas environment. The 4 feedthoughs will be mounted in a group at one end of the cryostat with sufficient separation between them to allow any one of the feedthrough to be grounded. The feedthroughs are mounted on the ceiling of the cryostat, their cold ends reaching through the gas ullage space and submerge into the liquid argon. The center conductor on the cold side of a feedthrough is insulated and shielded by a grounded shroud at least 50cm below the liquid. Connections between the feedthroughs and the CPA rows are made through stainless steel pipes in the liquid argon. Fig.3.16 is an example of a feedthrough made by the UCLA group for the Icarus experiment.

3.4.4 Purity Monitor High Voltages

Each argon purity monitor requires 2 bias voltages, one for the cathode at ~ -100 V, the other for the anode at $\sim$1 kV. Typical wire chamber power supplies with low ripple voltage should satisfy the requirement for the purity monitors. There are SHV type feedthroughs readily available commercially. Inside the cryostat, SHV cables connect the feedthroughs to the purity monitors. Additional signal cables will be needed for the purity monitor readout. These signal cables will be routed through the LVDS feedthroughs to the DAQ system.

3.4.5 Wire Bias Voltages

Each anode plane assembly requires 3 bias voltage connections at +700V, −200V, and −480V. The current on each of these voltages is expected to be under xx mA. However the ripple voltage on the supply must not exceed xx μV to avoid noise injection into the front end electronics.

The power supplies for the wire bias will be those used for MWPCs. Additional filtering network will be needed to further reduce their ripples. The default feedthroughs are commercial SHV type. However, we are evaluating other higher density multi-channel feedthroughs capable of withstanding the maximum voltage. Each cable trio will connect to an APA stack (2 APAs). This arrangement requires 84×3 SHV feedthroughs.

3.4.6 Power for the Cold Electronics

The 645,120 channels of in-vessel electronics in the cryostat consume up to 10kW of power. With an operating voltage less then 2V, this requires more than 5,000A of current through the cryostat. Significant amount of copper is needed to provide this current with negligible voltage drop. High current feedthroughs also results in large heat losses. An internal study has shown that the heat loss at the feedthrough and in the cables in such a scheme will add up to more than 60% of the total power of the cold electronics.

A more efficient arrangement requires the use of in-vessel DC to DC converters. With a 50V supply voltage, for example, the input current through the cryostat will be reduced to a moderate 200 A. With a conversion efficiency of 85% or better, the heat generated by the converters is in the order of 1.5 kW. For reliability reasons, we will use 2 DC-DC converters for each APA. Naturally, the 1.5kW heat released from these 300+ converters will cause significant bubbling, if the converters are installed in the liquid. Therefore we will mount the converters on the TPC mounting rails in the gas space, with their output connectors lowered into the liquid together with the other cables to connect to the APAs. This mounting scheme should help the converters to spread the heat quickly and reduce their temperature rise to limit potential outgassing.

3.4.7 Optical fiber feedthoughs

The number of optical fibers in the cryostat can reach up to 10,000, if no data compression is employed in the cold electronics. Unless a commercial high density optical feedthrough is available, we will need to develop our own. A straightforward method is to encapsulate a group of optical fiber cables with connectors at both ends onto a flange. A few special feedthroughs may be needed to transmit high intensity UV light to the argon purity monitors.

3.4.8 LVDS feedthoughs

The number of LVDS connections through the cryostat varies depending on the availability of data compression in the cryostat. If data compression makes it possible to readout the electronics with LVDS, there will be about 10,000 redundant output channels through the cryostat. The channel count in this scheme similar the that of the MicroBooNE (8,000+). Commercial high density feedthroughs meet this demand.

Additionally, LVDS connections will be made to each APA to distribute clock signal and control data. These information can be transmitted at a lower bit rate where LVDS is capable of. The number of channels for these signals are in the order of hundreds.

3.5 TPC Instrumentation and Monitoring

The TPC Instrumentation and Monitoring system consists of a distributed array of temperature sensors, argon purity monitors and liquid level monitors. Information obtained through these sensors guide the operation of the cryogenic plant, and provide calibration data for the TPC.

3.5.1 Requirements and Specifications

- The temperature sensors must have an accuracy of 0.1K at 90K.
- The liquid argon level must be measured with an accuracy of ∼1 cm. An interlocking system must ensure the cathode bias voltage be enabled only when the liquid level is above a threshold.

3.5.2 Liquid argon purity monitors

Multiple purity monitors are located inside the cryostat in order to monitor the electron lifetimes. Developed by the ICARUS Collaboration [4], these purity monitors are essentially miniature TPCs with the cathode and anode enclosed in a field cage. A UV light pulse knocks of a bunch of electrons from the photocathode surface. These electrons drift under the influence of the electric field, pass through two sets of wire grids separated by a known distance. Induction signals are measured at the grids. By comparing the amplitudes of these two signals, one can measure the attenuation of the electron cloud traversing this distance.

3.5.3 Temperature sensors

Several temperature monitors located at various depths in the argon measure the temperature of the argon as well as any gradients that may develop.

3.5.4 Liquid level monitors

Liquid level monitors are installed near the liquid gas interface to record the level of the liquid argon. The cathode high voltage power supplies must be interlocked with the level monitors in order to shut down the high voltage when the liquid level drops below a threshold to prevent high voltage discharges in the argon gas.

3.6 TPC Prototyping, Test, Checkout

3.6.1 Requirements and Specifications

- All TPC modules and assemblies must undergo at least one thermal cycle down to liquid nitrogen temperature to verify their mechanical and electrical integrity.
- Electronic calibrations will be performed on all readout channels at various stages to identify and correct for any defects.

3.6.2 TPC Prototyping

Several prototype TPC modules will be constructed during the design phase. The initial prototypes will be fraction scale or partial models of the APA and CPA. The CPA prototype will be used to evaluate the wire mesh tension and field shaping electrode attachment techniques. The APA prototype will be used to study the placement of the wire wrapping boards and wire support structures. It will also be used in to develop the prototype winding machines. The prototypes will undergo numerous thermal cycling down to the liquid nitrogen temperature to test the integrity of the bond between the wires to boards, and boards to frame.

The second set of prototypes will be full scale models of the APA and CPA. They will be used to to validate the designs, and to evaluate production procedures. Prototype front end electronics boards are expected to be available at this stage. A partial or completely instrumented APA can be assembled and tested in the prototype cryostat.

3.6.3 Assembly Testing

Front end readout boards:

- A small number of the ASICs will undergo a complete suite of tests, including thermal cycling to determine the batch yield.
- If the yield is high ($>$ xx%), all ASICs will be mounted on the front end boards. Tests will be performed on each board. Replace bad chips as needed.
- If the yield is low ($<$ xx%), an automated test fixture will be fabricated to validate every ASIC chip before mounting on the readout boards. Repeat tests at the board level.

APAs:

- The tension and electrical continuity of each wire are measured after the plane of wires is bonded to the frame;
- After the frond end electronics boards have been installed on to the APA, an initial calibration of all electronic channels is performed. The electronic gains and noise levels of all channels are recorded in a database;
- A cool down stress test is performed on each completed APA in a liquid nitrogen environment. Electronic calibration on all channels is performed while the APA is cold, and after warmed up. Significant changes in the calibration results will be investigated, and remediated.

CPAs:

- A cool down stress test is performed on each completed CPA in a LN_2 environment. After warming up, check the tension of the wire mesh.

Field cage:

- Measure the resistance along each copper strip, and between each strip pairs. The resistance between two strips should exceed 1 GΩ.

3.6.4 Checkout

After passing the tests at the assembly level, the APAs are put into storage, and later transported to the LBNE site. Prior to installation, another round of electronic calibration is perform on the APAs to validate their health. As each stack of APAs are being connected to its power and data connections, we will repeat the calibration process to ensure the connections are made properly. Repair or replacement at this stage is still straightforward.

After the entire TPC is assembled, a system wide calibration is performed at room temperature and again at cryogenic temperature in argon or nitrogen gas. Repair or replacement requires partial disassembly of the TPC, and should be avoided unless absolutely necessary.

Bibliography

[1] J. Srinivasan, S. V. Adve, P. Bose, and J. A. Rivers, âĂIJThe impact of technology scaling on lifetime reliabilityâĂİ, IEEE The International Conference on Dependable Systems and Networks (DSN-04), June 2004.

[2] T. Chen, L. Najafizadeh, C. Zhu, A. Ahmed, R. Diestelhorst, G. Espinel, and J. D. Cressler, âĂIJCMOS device reliability for emerging cryogenic space electronics applicationsâĂİ, IEEE International Semiconductor Device Research Symposium, 2005.

[3] G. De Geronimo, *et al.* âĂIJASIC for small angle Neutron scattering experiments at SNSâĂİ, IEEE Trans. Nucl. Sci., vol. 54, no. 3, pp. 541-548, 2007.

[4] S. Amerio *et al.*, "Design, construction and tests of the ICARUS T600 detector," Nucl. Instrum. Meth. A 527, 329 (2004).

4 Data Acquisition (WBS 1.5.4)

The data acquisition subsystem (DAQ) for the LBNE Liquid Argon TPC will serve the functions of (1) controlling configuration, operation and data read out of the detector (including generating timing and control signals), (2) receiving raw data from the front-end electronics system and from ancillary hardware, (3) filtering that data and constructing event records to be logged to persistent storage media, (4) monitoring detector and environmental conditions as well as data quality/integrity, and (5) performing online calibrations of the detector as required. Receiving and handling the beam spill signal is also part of the DAQ system scope. The DAQ system will comprise a combination of custom and commerical hardware and firmware, commodity computing hardware, and both commercial and internally developed software. The development of a DAQ system conceptual design is guided by experience gained in the development of relevant systems for the NOvA [1] and MicroBooNE [2] experiments.

The scale of the main task of handling digitized data from the TPC is determined by physics considerations, both directly and indirectly through their influence on the design of the TPC and front-end electronics systems. As described in Chapter 3, achieving sensitivity to signals that occur independently of the LBNE beam spill, such as those from nucleon decay or supernova neutrino bursts, requires a free-running transmission of data from the full detector at a 2 MHz sampling rate. Data transfer is enabled by multiplexing and data compression/zero-suppresion in front-end ASICs in the liquid, and by redundant copper and optical links that provide connection to data acquisition hardware outside the cryostat. Event building and triggering/filtering will thus be accomplished outside the cryostat.

In detail, the DAQ system design will depend on several key factors yet to be determined: for example, on detector depth (and hence atmospheric muon rate), and on the inclusion of a system to detect prompt scintillation photons. For the reference design described in this chapter, we assume the detector will be sited at the 800-ft level of the Homestake mine. We also assume that the photon signal, if present, will not be used to trigger the readout of data from the front ends, but rather will be employed in the event building and filtering stages of the DAQ. We are considering the implications for the DAQ system of alternative detector configurations.

This chapter is organized as follows. In Section 4.1, we summarize the requirements that must be met by the DAQ. Where appropriate we list basic specifications for the system that follow

from these requirements as well as from aspects of the TPC and front-end electronics design. In Section 4.2 we introduce a conceptual data acquisition architecture, and briefly summarize its main features. In Sections 4.3 through 4.8 we provide some detail on possible implementations for the various DAQ subsystems.

4.1 System Requirements and Working Assumptions

4.1.1 DAQ System General Requirements

General requirements of the LArTPC DAQ system are summarized here:

1 Signals to and from detector elements:

- 1.1 The DAQ system must be capable of providing configuration and control signals to the TPC and auxiliary detection systems such as the atmospheric muon veto detectors.
- 1.2 The DAQ system must be able to receive the raw detector data provided by a freely running readout from the TPC front-end electronics system located within the cryostat. To achieve required space-point precision, the TPC sampling rate is expected to be 2 MHz. (Although beam spill signals and prompt scintiallation photon signals may be available, we require that any event triggering functions be carried out on data after readout to the DAQ system. This will ensure a high trigger efficiency even for physics events that do not have information from these sources.)

2 Timing system:

- 2.1 Synchronized clock signals must be distributed to the front-end electronics throughout the detector.
- 2.2 The DAQ system must be able to provide accurate time stamp information to the data stream for each (set of) digitized samples from the TPC and auxiliary detector elements.
- 2.2 The DAQ system must be able to provide to the data stream information regarding the time of a beam spill signal originating at Fermilab.

3 Event building, filtering and storage

- 3.1 The DAQ system must be able to unpack, assemble, and otherwise process collections of data signals coming from the entire TPC and auxiliary detector channels into data blocks that can be logged to persistent storage.
- 3.2 These data blocks are required to be of a format and size so as to be amenable to physics analysis tasks that could be run on- or off-line. In addition to spanning the detector geographically, the data block should correspond to a time interval sufficient

to contain the full data from a physics event, taking into account the maximum ionization drift time (1.6 ms).

3.3 The DAQ system must be able to carry out data compression and event filtering functions, within the constraints of physics requirements for the event data. It must be able to retain samples (via random or prescaled selection) of data blocks that are deemed not to contain physics of interest.

3.4 The DAQ system must provide a means for logging detector data to persistent storage, including transfer off-site (to Fermilab).

4 Calibration:

4.1 The DAQ system must be able to initiate, collect and record data for detector calibration.

5 Run control system:

5.1 The DAQ must provide a run control system. This system must be able to allow experimenters to configure and ready the detector for operation. It must also provide functionality to monitor the integrity of data collection as well as the quality of the data being collected.

6 Slow controls systems:

6.1 The DAQ must provide and manage slow controls systems. This system will interface with hardware (such as power supplies) needed in support of the detector systems. It must be able to configure and read back data from these hardware components.

6.2 The DAQ slow controls systems must include necessary hardware that is not already being supplied as part of a detector system. (Currently, the high and low voltage power supply systems needed by the TPC and front-end electronics are being specified and will be provided through the TPC WBS.

6.3 The slow controls tasks must include collection of relevant environmental and hardware conditions data.

6.4 The DAQ system must make provision for persistent storage of some portion of the slow control data.

4.1.2 Working Assumptions

Physics considerations and nominal detector characteristics provide the critical context for the development a reference DAQ conceptual design. Some of these inputs are described here.

Signals associated with beam events will be localized within the TPC and synchronous with discrete ($\mathcal{O}(1\,s)$ rep rate) beam spills intervals spanning approximately $10\,\mu s$ (assuming fast extraction of the primary beam). However other physics events of interest will occur at random

times, and can be dispersed throughout the TPC volume as in the case of neutrino bursts from supernovae. Other specific signatures, such as very slowly moving magnetic monopoles ($\beta < 10^{-3}$) may involve signals spanning sample times exceeding the $1.6\,ms$ maximum ionization drift time.

As described earlier in this report, the cold electronics for a single Anode Plane Assembly will consist of 32 128-channel front-end boards, each board providing a single digital output channel for the multiplexed signal. Assuming 2 Msps and a 12-bit ADC, this output line will carry 384 Mbps. For the 168 APA's in the full detector this corresponds to 5,376 front-end boards, and hence that many lines. Redundant LVDS and optical signals will be generated to carry these lines out of the cryostat to the DAQ system. Data compression and zero suppresion will reduces the data rate as described in Chapter 3, so this throughput represents an upper limit.

It is expected that the rates of physics and calibration events of interest are low enough that – in comparison with more typical higher rate experiments in particle physics – the challengess of triggering and transfering data out of the DAQ are modest. At the 800-foot level, the highest-rate natural source of events in the detector is atmospheric muons, which will generate signals in the TPC at a rate of order 100 Hz. (An accurate evaluation of this rate remains to be carried out.) These events are of critical importance as a calibration source, and the DAQ system will need to be able to identify and log the signals needed to study them. It is also expected that 'random trigger' data records will need to be recorded at a rate that allows understanding of noise in the detector.

4.2 Reference Data Acquisition Architecture Summary (WBS 1.5.5.2)

The reference design of the data acquisition system is summarized in block diagram form in Fig blah. The architecture employs elements of the NOvA and MicroBooNE DAQ systems. The main components include:

1. a "Data Receiver" system to receive and unpack (demux) the continuously arriving stream of compressed digitized signals,

2. a "Buffer Farm" and associated network hardware in which to buffer the output from the data receiver system

3. an "Event Builder" system of computers to form event records from data received within a specified time interval (frame), and to apply trigger algorithms to determine which frames to log.

4. a "Timing System", including hardware that handles the beam spill signal and the distribution of timing and control signals to the front-end electronics.

5. a "Slow Controls" system to configure/ready the detector for operation and to readback detector and environmental conditions.

6. a "Run Control" system that provides the operator interface and data quality/DAQ/conditions monitoring capability.

These components are described in the sections that follow, on: data exchange with the cold electronics (Sec. 4.3), event building and triggering (Sec. **??**),

4.3 Data Receiver: data transfer from cold electronics (WBS 1.5.5.3)

With their similar signal sampling rates in the front ends, the NOvA and MicroBooNE components provide a useful template for LAr20. Thus, the LAr20 Data Receiver system is envisioned to incorporate the functionality of NOvA's "Data Concentrator" system and the digital portion of MicroBooNE's "Front End Module" (FEM) cards. Namely, the Data Receiver will provide an interface for the LVDS and optical input signals carried out of the cold volume. It will packetize and transmit the data to the "Buffer Farm" for event building. It will also provide the interface for transmitting timing and control signals to the cold electronics.

4.3.1 Data unpacking: demuxing, rotation to time-ordering and zero suppresion

As described in Chapter 3, compressed digitized signals from a single APA will arrive on 32 LVDS lines and, for redundancy, on four 'primary' optical lines and four 'backup' optical lines. Thus, for example, each LVDS line will carry a serial stream of data with a common timestamp from 128 wires once every $0.5\,\mu s$. As is the case for MicroBooNE, analysis of the complex time structure of the ionization signature for a given induction or collection wire requires that data be 'rotated' into a time-ordered data set, spanning a specified time frame. In the case of MicroBooNE the nominal time frame is a $4\,ms$ interval; it remains to be determined what interval is appropriate for LBNE. The deserialization and rotation of the data can be accomplished in an FPGA as is the case in the MicroBooNE FEM. It also remains to be determined whether (further) zero suppression can/is desired take place at this stage.

4.3.2 Output data

As described below in Section 4.4, the output of the Data Receiver system will be transfered to a disk farm ("Buffer Farm") for event building and triggering. NOvA achieves this with Gigabit Ethernet links, and a processor on the Data Concentrator that forms the packets. The viability

of a similar scheme for LAr20 will depend on the degree of data reduction upstream of this step. (**Need some numbers here!**)

4.3.3 Timing, control and configuration signals

The Data Receiver will provide the interface for the transmission of timing, control and configuration signals to the TPC/front-end electronics. More detail on these signals is given in following sections.

4.4 Event building and triggering (WBS 1.5.5.4)

The event building and triggering function of the LAr20 DAQ system will be performed by the "Event Builder" and "Buffer Farm" components.

4.4.1 Physics Triggers

4.4.2 Event Model

An Event Data Model will need to be developed. Experience with MicroBooNE will be helpful is optimizing the design for this.

4.5 Timing System (WBS 1.5.5.5)

Again, similar requirements and conditions suggest a timing system similar to that being implemented for NOvA. That system meets the requirements of deterministic timing and coherence of signals distributed across the entire detector. It consists of a Master Timing Unit (MTU), in which a main task is generation of GPS-based timing packets, and an array of Timing Distribution Units (TDUs). The TDU's are geographically distributed: they compensate for propagation delays before transmitting timestamp packets to the front ends. Such a system could work well for the LAr20 system and may be able to be adapted with only minor design modifications.

4.6 Run control (WBS 1.5.5.6)

4.7 Slow control systems (WBS 1.5.5.7)

4.8 DAQ Infrastructure (WBS 1.5.5.8)

4.8.1 Networking

4.8.2 Data Archiving

Bibliography

[1] "The NOvA Experiment Technical Design Report", October 2007.

[2] "The MicroBooNE Conceptual Design Report", February 2010.

5 Installation and Commissioning (WBS 1.5.5)

LAr20 construction and installation will occur in several distinct phases:

- Installation planning and prototyping.
- Surface storage identification and operation.
- Excavation and outfitting of the cavern. This activity is the responsibility of WBS 1.6.
- Construction and installation of the cryogenics system and cryostat at DUSEL by a contractor. The contractor will provide construction management. This activity is the responsibility of WBS 1.5.2.
- Construction of LAr20 detector components at collaborating institutions and shipment to DUSEL. This activity is the responsibility of WBS 1.5.2 - 1.5.7
- Installation of detector components at DUSEL. Installation management is provided by this WBS (1.5.5).
- Commissioning of LAr20 with management provided by this WBS (1.5.5).

The Installation and Commissioning system will accept responsibility for the LAr20 cavern, associated tunnels, infrastructure and above-ground facilities from WBS 1.6 upon completion of the excavation contract. The cavern will be outfitted with the following utilities upon receipt of beneficial occupancy:

- Ventilation in accordance with OSHA standards and independent of the existing DUSEL facility.
- Electrical power sufficient for the HVAC, cryogenics-plant cooling, electronics and general 110 V service.
- Communications consisting of 3 copper-pair telephone lines and a multi-strand, fiber-optic cable for data transmission.

- Cavern lighting in accordance with OSHA regulations for industrial use.
- Tunnel lighting with battery-powered backup or emergency-circuit backup.
- Environmental monitoring of oxygen, carbon monoxide, smoke and temperature.
- Dual isolation bulkheads separating the cavern from the existing DUSEL facility.
- Sump pumps for ground water removal.
- A light monorail crane located over the cryostat **FIXME:** *confirm this with JA*

Area responsibility will immediately be transferred to the cryogenics and cryostat contractor **FIXME:** *at what point? This seems in contradiction to pgraph above the above list*, who will retain responsibility for the site during construction. The Cryogenics & Cryostat WBS will provide oversight during this phase. Upon completion of this contract, the facility will be in the following state:

- The LN2 refrigeration system will be constructed and commissioned with liquid nitrogren. **FIXME:** *confirm this*
- The LAr systems and cryostat will be constructed and tested without the introduction of cryogens. The personnel-access hatch on the cryostat and the cryostat chimneys will be temporarily sealed.
- The APA- and CPA-installation monorails will be in place.
- The temporary floor in the cryostat will be left in place.

The Installation and Commissioning system will be responsible for all LAr20-related activities at the far-detector site from this point in time until the start of routine operations of the LAr20 Detector (CD-4). Close coordination is clearly required between the I&C WBS, provider systems and other DUSEL construction activities.

On-project commissioning activities include the coordination of system-checkout activities, culminating in the approval to introduce liquid argon into the detector, and managing the subsequent steps required to meet the CD-4 goals.

5.1 Installation Prototype (WBS 1.5.5.2)

An installation and integration detector mock-up will be constructed at Fermilab to confirm that interfaces between detector systems are well-defined and to refine installation procedures.

A mechanical mock-up of several APA's will be constructed. The APA mock-ups will include all mounting points and interface points, such as optical-fiber readout cables and power cables. A mock-up of a section of the cryostat will also be constructed in a suitable location at Fermilab **FIXME:** *Do we want this?* (e.g., CDF or DZero). The cryostat section will include a representation of the roof hatch, APA supports and feedthroughs.

5.2 Surface Storage Facilities

A surface-storage facility on the DUSEL site will be identified and an agreement made for its use during construction. The surface-storage facility may be segmented for use by both the project and its various contractors. Responsibilities will be clearly assigned for each part of the storage facility for specific time intervals. The cryogenics-system contractor will likely require the largest portion of the storage facility. The cryostat insulation will comprise the largest bulk of material; approximately 5500 m^3. Figure 5.1 shows membrane-cryostat components staged in the hull of an LNG tanker under construction. Control of all contractor areas will revert to the Installation WBS, as each contract is completed.

Detector components will be delivered to DUSEL over a period of many months and will be stored in the surface-storage facility. APAs will be constructed elsewhere, electronics installed and cold testing performed. They will be shipped in sealed shipping containers as shown in figure 5.2. No significant preparation or testing of APAs is expected prior to installation.**FIXME:** *are they tested in situ?*

5.3 Below-ground Pre-Installation (WBS 1.5.5.6)

This WBS will provide minor improvements to the below-ground infrastructure such as signage, installation tools and cavern access controls. Access controls will include a mechanism for checking the training status of personnel, badge-in/badge-out procedures and closed-circuit television monitoring of the entrance portal.

Only trained personnel will be allowed below-ground. Members of the installation crew will be trained on both general underground safety and working procedures, and on specific installation tasks. Assessment tests will monitor the effectiveness of training procedures. The training will likely use mock-up APAs constructed for the installation prototype described above. The training program will be modeled after the Fermilab "NuMI underground training" and will be developed in collaboration with DUSEL ES&H personnel.

This WBS will also develop and implement the procedures for monitoring the integrity of the membrane-cryostat primary liner during installation. The space between the primary liner and the secondary liner will be held under vacuum during installation. The vacuum level will

be automatically monitored and will alarm if a dropped object has punctured the primary liner. **FIXME:** *what happens if it's punctured?*

5.4 Below-ground Installation Activities (WBS 1.5.5.7)

The installation sequence will proceed as follows:

1. Move installation and access equipment into the cryostat.
2. Install cryogenic feedthroughs and dress cables.
3. Install protection on (or remove) existing cryogenics instrumentation in the cryostat.
4. Install purity monitors and other instrumentation.
5. Construct the far-end field cage.
6. Transport APA and CPA shipping boxes into the cavern.
7. Install detector cells:
   (a) Install three APAs and four CPAs.
   (b) Connect power and signal cables.
   (c) Test each APA wire for expected electronics noise. Spot-check electronics noise while cryogenics equipment is operating.
   (d) Install top and bottom field-cage sections.
   (e) Perform electrical test on CPAs and field cage.
8. Install the near-end field cage.
9. Temporarily seal the cryostat and test all channels for expected electronics noise.
10. Seal the access hatch.
11. Final-test all channels for expected electronics noise.

5.4.1 Cryostat Cleaning & Purging

The cryostate cleaning and purging procedure is described here. **FIXME:** *But it's not... still to come?* I am assuming that no cryogens will be introduced to the detector prior to commissioning. Some thought needs to be given to the optional LAr storage system and how this system would be approved for use with cryogens.

5.5 Detector Commissioning (WBS 1.5.5.8)

FIXME: *We need to have an idea of the CD-4 goals before this section can be written.*

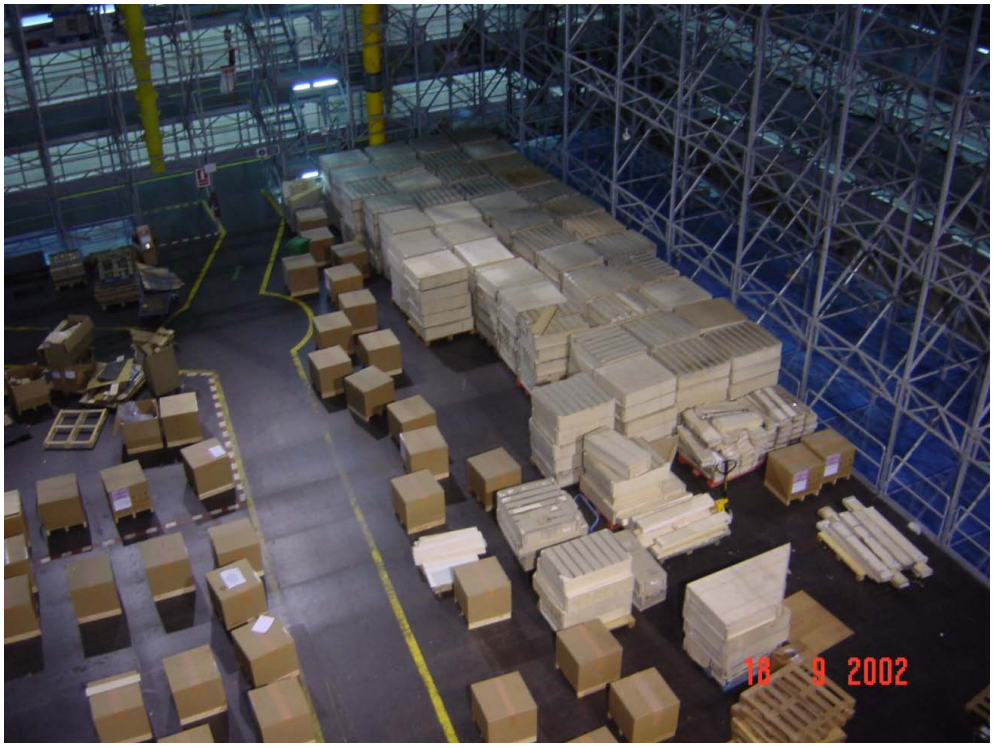

Fig. 5.1. Membrane cryostat components staged in a LNG transport ship under construction.

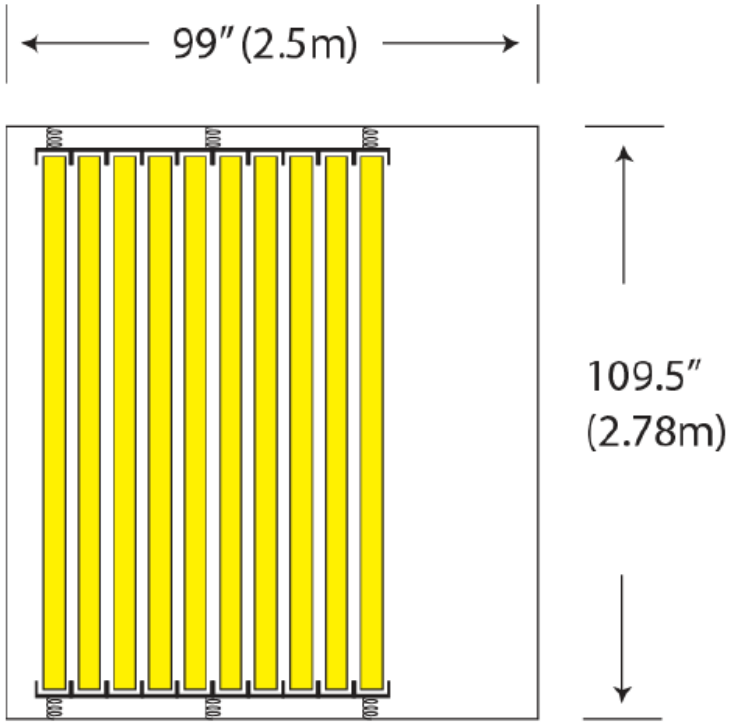

Fig. 5.2. APA shipping container concept.

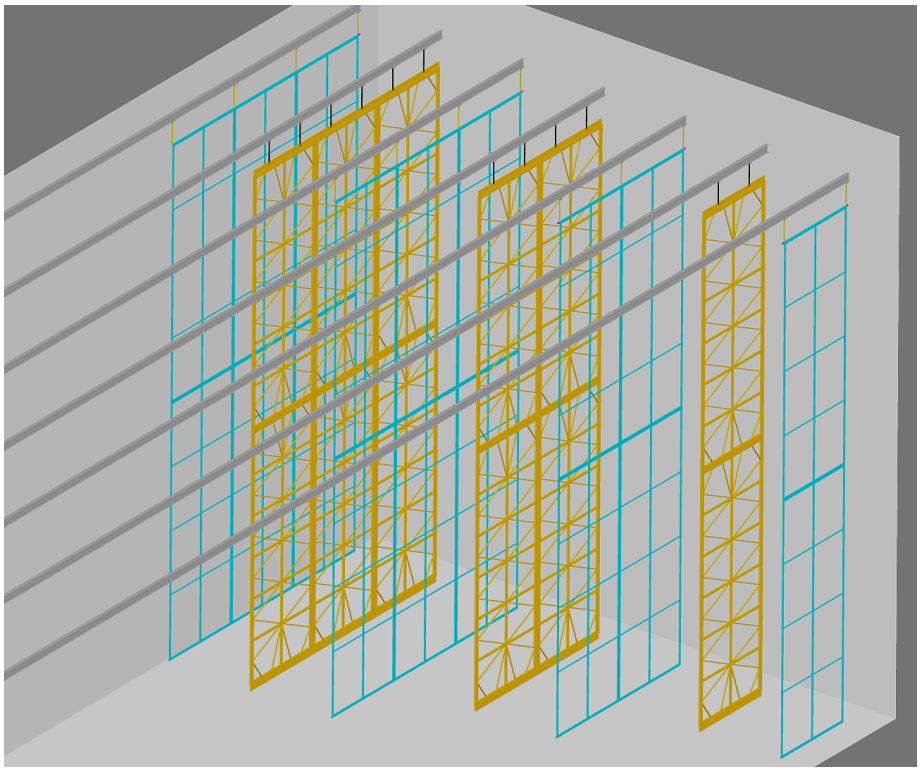

Fig. 5.3. TPC Installation scheme

Bibliography

[1] "Title", Month, year.

6 Photon Detector (WBS 1.5.6)

Ionization electrons produced along a particle trajectory, Q_o, are lost due to impurities as they drift to the wire planes. The ionization charge seen on a wire plane, $Q = Q_o e^{-t_e/\tau}$ where τ is the lifetime of the ionization electrons. The lifetime is measured directly by the purity monitors. Q_o can be calculated if the time of passage of the particle, t_e, is known.

The event time is known to within a few nano-seconds for accelerator-produced neutrino interactions by using a GPS locked beam spill signal from the accelerator, so no photon detection system is required for this analysis.

We note that knowledge of Q_o is not required to perform particle identification. Particle identification for stopping tracks is performed by comparing the track length with the ionization behavior along the track length. The red arrow in figure 6.1 shows that a 105 MeV kaon, presumed to be produced in proton decay, will lose $\approx$ 4 MeV/cm when it is created and will lose approximately three times that amount when it stops. The kaon stops after 13 cm of travel in liquid argon. If the kaon travels parallel to the wire plane, all of the ionization electrons arrive at the wire plane at the same time and no electron lifetime calculation is required to determine dE/dx along it's length. If the kaon travels directly towards the wire plane, ionization electrons at the end of the track arrive $13\ cm/v_{drift}$ before the ionization electrons at the beginning of the track, where v_{drift} is the electron drift velocity. A lifetime correction can be made between these end points, but knowledge of the actual position of these points is not required.

This can be shown more generally in the following calculation. Let $t_{1(2)}$ be the drift time for ionization electrons from the start (end) of the track, and $Q_o 1(2)$ be the true ionization charge on the start (end) of the track. The ionization charge measured on the wires is $Q_{1(2)}$. The true charge at the track start is $Q_{o1} = Q_1/e^{-t_1/\tau}$. The true charge at the track end is $Q_{o2} = Q_2/e^{-\delta t/\tau}$, where $\delta t = t_2 - t_1$. It is straightforward to show that Q_{o2}/Q_{o1}, the charge ratio used for particle identification, is equal to $Q_2/Q_1 e^{-\delta t/\tau}$.

Also note that if a track passes through a cathode plane into an adjacent APA cell, ionization electrons will appear as truncated track segments in each cell. The value of t_e is determined when the track is "glued" back together during track reconstruction. This technique cannot be applied to tracks in APA cells at the edge of the detector however. The purpose of the photon detection

Fig. 6.1. Energy loss as a function of particle kinetic energy for muons, kaons and protons. The red arrow depicts the energy loss behavior of a 100 MeV charged kaon that stops in the detector. Reproduced from **FIXME:** *ICARUS reference here*

system is to determine t_e for the edge APA cells.

The primary proton decay background is cosmic ray spallation. A potential drawback of this concept is that the there is a 1.5 ms uncertainty in the time of passage of cosmic rays passing through the central cells of the detector. This is the maximum drift time for ionization electrons in the 2.5 m APA cell. The cosmic ray rate at the 800 level is $0.06 Hz/m^2$. We assume that a proton decay candidate event would be rejected if a cosmic ray passes within 7 m of the event. There is a 1.3% probability of a random cosmic ray passing within this area, resulting in a negligible loss of fiducial mass.

6.1 Requirements and Specifications

The main requirements for the Photon Detection system are:

- The system must be capable of detecting an energy deposition of at least 10 MeV within the edge drift cells.
- The system must not compromise the operation of the TPC under any circumstances.
- The readout electronics must provide a minimum signal to noise ratio of 10 for a 10 MeV energy deposition.
- The readout electronics must record photon signal waveforms continuously without dead time.
- The signal waveforms must be sampled at the same frequency as the wire electronics.
- All materials used in the photon detection system must be qualified for used with high purity liquid argon.

6.2 Photon Detection Description

The PMT assembly shown in figure 6.2 was developed by MicroBooNE. The MicroBooNE photon detection system uses 30 PMT's located behind the 11.5m x 2.5m anode plane, or roughly 1 PMT$/m^2$. LAr20 will adopt the same PMT coverage and will require 18 PMT's/APA or 2016

PMT's in total. MicroBooNE estimates that 2.2 photo-electrons/MeV will be collected with this photocathode coverage, observing to a depth of 2.5 m. This estimate does not consider internal reflections from the MicroBooNE cathode plane which would increase the detection efficiency. Reflections from the LAr20 APA's will be negligible. We propose to locate the PMT's behind the cathode plane and provide them with electric field shielding.

The unit consists of a Hamamatsu R5912-mod suspended loosely between PEEK posts, with an acrylic plate above which is coated with wavelength shifter. The input HV and the output signal share a single 93 ohm cable (not shown). The tube is designed for operation at cryogenic temperatures, with a K2CsSb+Pt photocathode. The wavelength shifter is Tetraphenyl-Butadiene (TPB) which absorbs light in the UV and re-emits it at 425 nm. A mixture of 50% TPB and 50% polystyrene is used for the coating. This coating is less efficient than a coating of 100% TPB, but has very good scratch resistance and is immune to the effects of humidity. All of the design elements are qualified for use in LAr. The design has passed the MicroBooNE CD-2 internal technical review.

Fig. 6.2. Mechanical mockup of the MicroBooNE PMT assembly.

Construction and installation of the photon detection system will be similar to the CPA's. Eighteen PMT assemblies will be constructed, tested and mounted on a 2.4 m x 7 m frame which comprises a Photon Detection Assembly (PDA). The 112 required PDA's would be shipped to DUSEL and installed using the same technique that has been developed for the CPA's.

The Photon Detection readout will use conventional commercially available electronics.

FIXME: *There is a considerable amount of text from the MicroBooNE TDR describing on-going and planned R&D that could be added here.*

Bibliography

[1] "Title", Month, year.

7 Veto System

Of all the ingredients in the cosmic shower that constantly bathes the Earth, only cosmic-ray muons and neutrinos penetrate to significant depths underground. The goal of the underground laboratory is to reduce such sources of backgrounds by shielding the detectors under rock. The shielding is commonly expressed as either feet of standard rock (with density of 2.65 gm/cc) or in meters-water-equivalent (mwe). As muons penetrate underground they lose energy by ionization and by radiative processes.

FIXME: *Add something about "Since we prefer the 800L to the 4850L for reasons x, y and z, we will have less natural shielding above the detector and will need to supplement background-rejection with a veto counter." or some such*

7.1 Background-Rejection Requirements for Physics

7.1.1 Accelerator Neutrinos

The rate of cosmic muons in the detector at the 800L is 0.06 Hz/m^2 or $\approx$ 1 Hz/APA cell. During a drift time of 1.5 ms, 0.003 cosmic rays will pass through the active volume of one APA cell, resulting in a timing rejection factor of $\approx$ 800. The high granularity of the detector will allow identification and removal of the cosmic muons from the data, introducing only a small ($< 0.1\%$) inefficiency to the active detector volume, so that most of the accelerator-induced events will remain unobscured. In short, a cosmic ray veto is not required to study accelerator-neutrino interactions at the 800L.

7.1.2 Nucleon Decay

The depth requirement for proton-decay experiments is dominated by the livetime loss due to event overlap with cosmic muons **FIXME:** *in other words when you reject a cosmic muon, you're cutting out a time slot (decreasing livetime)?*. A liquid argon detector will have much less deadtime loss at shallow depths than a water Cherenkov detector since the fine segmentation in

space and drift time allow exclusion of the regions of the detector **FIXME:** *immediately?* around each passing muon **FIXME:** *i.e., allow one to exclude only small regions around the muon as opposed to larger regions and hence you keep more data?*. With mountainous overburden of only 200 m and a veto counter, Bueno et al.[12] **FIXME:** *need reference* estimate an effective loss of detector mass of less than 4% for a 100-kton liquid argon detector (GLACIER).

The most serious source of nucleon-decay background for the νK^+ mode are K^0_L mesons produced by spallation of cosmic-ray muons in the rock surrounding the detector. The effective interaction length of these K^0's in liquid argon is 86 cm. These neutral kaons may enter the detector and produce a K^+ via charge-exchange **FIXME:** *which causes what kind of problematic signal?*. The cosmic muons that pass through the rock near the cavern wall at small zenith angle as shown in figure 7.1 produce the largest contribution to the K^0 background. Muons traveling at a larger zenith angle are unlikely to produce a forward-going K^0 that is unaccompanied by the interacted muon. **FIXME:** *Do we need the last sentence, since these don't seem to be an issue?*

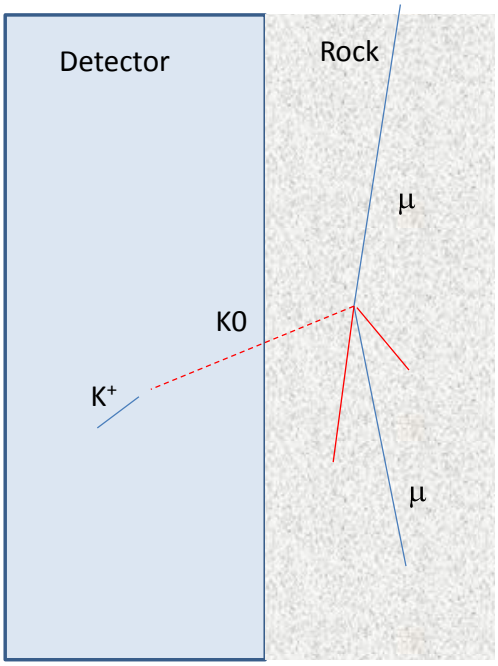

Fig. 7.1. Cosmic-ray spallation background to proton decay in the p $\rightarrow \nu K^+$.

The veto described in the following section is designed to reduce the background in the νK^+ mode to a negligible level based on these arguments. Monte Carlo simulation of the proposed

veto system is clearly required.

FIXME: *Other physics topics? snova, atmos, dnsb etc? I guess you've covered the DOE big ones.*

7.2 Veto System Description

The 800L cavern will be constructed with 3194 veto tubes embedded in the cavern walls as shown in figures 7.2 and 7.3. The design and the cost estimate are adapted from the NOνA detector. The veto system WBS 1.6 **FIXME:** *not 5.x?* provides veto counters for insertion into each veto tube. Each veto tube consists of a 4-in square steel tube, 7 m long.

The aforementioned GLACIER detector concept is an upright cylindrical tank of 20 m height and 70 m diameter, surrounded by annular veto detectors that extend 3 m into the surrounding rock. An additional 3 – 5-meter fiducial cut was made inside the detector to reduce the spallation background in the νK^+ channel to 0.1 event per year. In contrast, we propose to extend the veto counters 7 m into the rock to obviate the need for a fiducial cut. The interaction length of rock is roughly half the interaction length of liquid argon, so each meter of rock should provide twice the neutral-kaon attenuation as each meter of liquid argon.

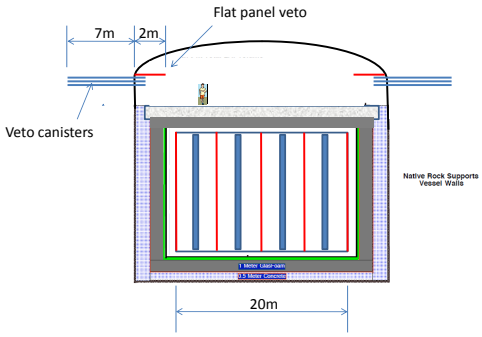

Fig. 7.2. End view of the cavern wall showing veto tubes embedded in concrete in the walls of the cavern.

FIXME: *Supply missing volume-5/figures/chapter-03_vetotube*

Fig. 7.3. Conceptual layout of the veto tubes.

An LAr20 veto counter will consist of a 9-m-long × 8.4-cm-square PVC extrusion containing liquid scintillator and a loop of wavelength-shifting (WLS) fiber. The inside dimensions of the

PVC extrusion are 7.8 cm square × ??? long?. **FIXME:** Both ends of the WLS fiber are attached to a single-channel Avalanche Photo-Diode (APD) mounted on the extrusion end-cap.

For comparison, each NOνA module consists of 32 detector cells extruded in one piece. The NOνA detector cell is 3.7 cm × 5.9 cm **FIXME:** *3rd dimension is 15.9 m?*. Each cell contains liquid scintillator and a looped WLS fiber that is routed to a single APD channel. Cosmic ray tests, summarized in figure 7.4, have shown that 21 photo-electrons are observed at the APD from a minimum-ionizing particle at the far end of the 15.9-m-long cell. The RMS width of the cosmic-ray signal is eight photo-electrons, as shown in figure 7.5, or 38%. NOνA has set a threshold of 15 photo-electrons **FIXME:** *i.e. twice as high so as to not record them?*, resulting in a 23% inefficiency for minimizing-ionizing particles. **FIXME:** *I (Anne) don't see how 38 and 23 % follow, but maybe ok – gotta look at the figures*

FIXME: *Supply missing volume-5/figures/chapter-03_nova_pe*

Fig. 7.4. The average number of photoelectrons in a NOνA cell as a function of distance d from the APD. The cell is broken up into 1-m-long sections. Note the fiber has to exit the cell and run a short distance to the APD, so the effective length of the cell is longer than the physical 15.7 meters filled with scintillator.

FIXME: *Supply missing volume-5/figures/chapter-03_nova_pehist*

Fig. 7.5. Histogram of pulse heights observed in cosmic ray data with a NOνA test cell. **FIXME:** *ref nova cdr*

We estimate the performance of the proposed veto design by scaling the number of photo-electrons expected in a NOνA cell at 9 m (41 photo-electrons) by the ratio of the cell inner dimensions for the two cell configurations (1.32 = 7.9 cm/5.9 cm). We therefore expect 54 photo-electrons and will set the threshold at 15 photo-electrons with a resulting inefficiency of $\approx 10^{-7}$. **FIXME:** *can we compare apples to apples? How does this compare with nova's 23%?*

The two rows of veto counters are arranged parallel to each other, and offset, to provide full geometric coverage for cosmic rays at all angles. This configuration does not provide any stereo angle information **FIXME:** *Is this like triangulation?* to determine the distance from the cavern wall to the cosmic ray. Pulse-height information can conceivably be used for this purpose with an accuracy of a few meters. **FIXME:** *So, how good is that? Sufficient? Way better than sufficient?*

The veto system also provides veto tubes and veto counters for coverage at the ends of the cavern. We propose to set two layers of end-wall veto tubes on the cavern floor before any other equipment is set in place. Approximately 866 veto tubes and veto counters are required to cover both ends of the cavern floor. The veto-tube layer would be covered with 1/2-in steel plate to provide a means of securing equipment and to prevent inadvertent drilling into a veto counter.

The veto will be implemented in the data acquisition as an additional detector system. The veto detectors will be sampled by ADCs operating at 2 MHz and merged with the TPC data stream. The veto system will be used to reject a reconstructed K^+ as a proton-decay candidate if a nearby veto counter has a pulse height consistent with a minimum-ionizing particle.

Bibliography

[1] "Title", Month, year.

8 Alternatives

Alternative detector configurations and design parameters are discussed in this chapter.

8.1 Detector Configuration

8.1.1 Double Phase Readout

The European GLACIER collaboration is pursuing a novel double phase readout detector technology that has potential advantages. In this scheme, ionization electrons are drifted upwards under the influence of an electric field towards the liquid-vapor interface. The electrons are extracted from the liquid into the vapor by an electric field of 2.5 kV/cm. The electrons then drift to two stages of Large Electron Multipliers (LEM). Electrical signals are induced on segmented electrodes on the LEM.

This method requires far fewer readout channels than the preferred design, however significant R&D is required to demonstrate the viability of this technique for a large detector. This design requires very long electron drift lengths ($\sim$20m) in order to be cost effective.

8.1.2 Cryostat Shape

Storage tanks can be classified by shape (upright cylinder, horizontal cylinder, rectangular parallelepiped) and means of support (self supporting, externally supported).

A horizontal cylindrical tank would require significant structural support to withstand the gravitational load. On the other hand, upright self-supporting cylindrical tanks are commonly used for surface storage of cryogenic liquids. The proposed above ground LAr TPC experiment FLARE utilized a tank of this configuration. An upright cylindrical tank is also proposed for the 100 kton GLACIER underground detector. In contrast, the 600 ton ICARUS detector is a rectangular parallelepiped.

A study was performed to compare the cost for three configurations of equivalent active mass: upright cylindrical cryostat (soup can), rectangular parallelepiped externally-supported cryostat (membrane) and the rectangular parallelepiped self-supporting cryostat (modular). The study considered the cost of rock excavation, the cost of the total inventory of LAr required for a detector for an "active mass" of 16.7 kton and a rough estimate of the cryostat cost. The "active mass" is defined as the volume of LAr that is sampled by the readout electronics. (Note that the "fiducial mass" of the detector is less than the "active mass".)

The active/total mass fraction for the three configurations varies between 70% and 74% and is therefore not a significant factor in the cost difference. The major cost factor is the volume of rock that must be excavated for these configurations. There is a significant amount of unused cavern space if an upright cylindrical tank is located within a rectangular parallelepiped cavern. The amount of unused space can be reduced by excavating a cylindrical cavern but the excavation cost would increase significantly ($\sim$30%).

The study results show a cost range of 10% - 20% for the different configurations. This is within the uncertainty of the estimates ($\sim$50%) so none of the options can be rejected purely on economic grounds given our current state of knowledge. Given sufficient resources, all configurations could be more fully developed to make a more informed decision however any potential value would be offset by the cost of pursuing multiple design paths.

The study results also indicate that a membrane cryostat is the most cost effective solution. It clearly maximizes the use of the excavated rock volume. A membrane cryostat is also inherently more cost effective that a self-supporting cryostat since the hydrostatic pressure of the liquid is constrained by the cavern walls and not the cryostat walls, thereby reducing the amount of structural steel required.

8.1.3 Modular Cryostat

The modular LANNDD detector concept is a viable alternative to the preferred design. The detector, shown in Figure xxx, consists of a cubic matrix of drift cells.

FIXME: *Include lots of text from the Ref Design 1b document*

8.2 Depth Options

FIXME: *If these are rejected, move to VE chap*

8.2.1 300 level

This section should describe the physics and cost issues for the 300 level

8.2.2 4850 level

This section should describe the physics and cost issues for the 4850 level

8.2.3 Deep Cavern Considerations

The vertical distance between a deep cavern (4,850âĂŹ) and the surface will necessitate the inclusion of pressure control stations within the LAr riser. The static liquid head pressure in a full argon line routed between the surface and the cryostat would be 202bar (2,930psi). A design pressure to accommodate this operating pressure would require heavy wall piping and high pressure pumps and fittings. This would result in a high capital cost for equipment which is utilized only for a short duration and an increased hazard in the event of leakage.

A piping system with a pressure rating in accordance with ASME B16.5 Class 300 would provide a design pressure up to 51bar (740psi). Pressure control stations would then be included in the risers to limit the static head to approximately 600psi. This would then allow a margin for friction losses in the system when fluid is being pumped from the cavern to the surface.

Six pressure reduction stations are proposed. Each pressure reduction station will include a vented break tank, level control valve and level controller fitted to the break tank.

The arrangement of the pressure control stations is shown on the Process Flow Diagram for the 4,850âĂŹ level cryostat. The vented break tanks should be sized to provide a 2 minute reaction time to the peak flow rate through the riser. This occurs during reverse flow when the cryostat is being drained. They should therefore each have a capacity of $1.2m^3$ to provide ample time for control purposes.

The break tank vent will be connected into the cryostat over pressure protection system vent (discussed below) and released / recovered at the surface.

8.3 Cryogenics Plant

8.3.1 Refrigeration

FIXME: *7/23 AH took from 2.4.1 Cryostat Purges and Cool-downs (before hearing back from Russ on fixmes)* A possible alternative to the flow/piston-purging discussed in section **??** is evacuating the membrane tank **FIXME:** *How?* and then backfilling with argon. This is a more traditional approach. A membrane-cryostat vendor reports that evacuation of the insulation spaces is normally done during the construction and leak-checking phases. A vacuum pressure of less than 200 mbar absolute in the insulation spaces is typical. As long as the pressure- differential direction across the walls is kept outward, it is possible to reduce the internal membrane-tank volume to these pressures as well. This is considered an alternative rather than preferred option because the concrete cavern liner and cryostat roof truss have not yet included loading due to external atmospheric pressure as a design requirement.

8.3.1.1 Alternative Nitrogen Cool-down Procedure

As an alternative to cooling the cryostat with liquid Argon a more cost effective procedure may be to cool the cryostat with liquid nitrogen and purge the cold cryostat with argon.

The procedure would be as follows:

- Purge with warm dry nitrogen (gas) to remove moisture
- Cool with liquid nitrogen
- Evacuate N2 using vacuum pump
- Purge with pure cold gaseous argon
- Repeatedly evacuate and replace argon to achieve purity close to LAr supply purity
- Fill with LAr
- Circulate LAr through purification plant to achieve purity required

The availability of large quantities of liquid nitrogen is substantially better than that of liquid argon and the cost is far lower. The viability of this procedure has not been proven.

8.3.1.2 LAr Supply using Temporary Air Separation Plant

We have considered whether the provision of a temporary dedicated air separation plant could be justified based on the elimination of LAr losses due to boil off during transportation, elimination of vehicle movements and the potential increase in the supply reliability. These advantages must be offset against the net capital cost of the temporary plant, the operating cost of the plant and the relative inefficiency of the âĂŸsmallâĂŹ temporary plant as compared to a large commercial plant.

8.3.2 LAr Storage

It is desirable to provide temporary storage of liquid argon to decouple the delivery schedule from the detector construction schedule. Ideally, temporary storage could reduce the LAr20 schedule by 6 months since argon deliveries can occur in parallel with detector construction. This is only possible if construction of the temporary storage facility occurs concurrently with other activities.

Temporary storage also mitigates the risk of a detector failure necessitating access to the cryostat. If this occurred and temporary storage were not available, the argon would be vented to the atmosphere and the $25M investment of LAr would be lost.

FIXME: *Stick the Arup NPV calculation in here somewhere*

A rough estimate for the cost of above-ground LAr storage and associated infrastructure is ∼$25M. This estimate was found independently by Arup and by application of a cryogenic tank cost scaling formula given in lbne-docdb #54.

It would be advantageous to provide underground LAr storage in a cryostat that has the same configuration as the detector cryostat. This second cryostat could be converted into a second detector in the future. The cost of this option is explored below.

FIXME: *Need costing information from Arup to complete this section. We have something from Jacobs already*

8.3.2.1 Optional LAr Surface Dewar

The outline project requirements provided included a LAr storage facility to be located above ground. This surface dewar was to be capable of storing the full liquid inventory of the underground cryostat. The proposed dewar would be an above ground or in ground cylindrical insulated tank with an available storage volume in excess of 26,400m3. It would be constructed as a double wall, perlite insulated storage tank. The dewar would:

- provide interim storage for consolidating delivered LAr prior to cryostat fill,
- offer emergency storage of LAr,
- provide buffer for Argon boil off vented from cryostat in upset condition (although, concerns were raised over surface refrigeration capacity for this condition),
- and could be used as a buffer for multiple cryostats (for the future condition).

An associated refrigeration plant would be required to recovery the gas which would boil off from the stored liquid. The dewar would be maintained at cryogenic temperature for the life of the cryostat so that should a cryostat leak occur then the dewar would be immediately available. This would require a long term inventory of LAr and continuous operation of the refrigeration plant. It is estimated that a 30,000m^3 dewar with 50kW of refrigeration plant would be required.

The dewar would be filled by the pumps located on the delivery tankers or the offloading facility pumps. An electro-submersible in-tank pump would be required to transfer fluid from the dewar to the cavern.

There will therefore be a capital cost and an operational cost associated with provision of the dewar.

The capital cost of the dewar, associated transfer pumps, circulation pumps and refrigeration plant has been estimated as follows.

Item	Cost
Dewar structure	\$15M
Pumps	\$2M
Minimum argon inventory	\$3M
Refrigeration Plant (50kW)	\$3M
Capital Cost	**\$24M**

The operating cost of the storage dewar has been estimated as follows:

Item	Cost
Refrigeration plant power (200kW)	\$190k
Maintenance (2% of capital cost)	\$400k
Annual Opex	\$590k
Net present cost	**\$7.7M**

The cost of providing and maintaining the surface storage facility should be compared to the benefits that may accrue.

The Net Present Cost of providing the dewar is estimated to be \$32M.

In terms of the value of the argon that may be recovered from the cryostat in the event that a significant leak occurs the benefit is less than $26.4million per incident.

The current cost of the dewar exceeds the current cost of replacing a single inventory of LAr.

This cost comparison ignores:

- the low probability of a significant leak developing due to the design of the cryostat containment system,
- the quality controls that are applied during construction,
- the testing that can be undertaken after construction, and
- the diminishing cost (in current terms) of the replacement argon.

It has not been possible to fully evaluate the benefit that may accrue during the cryostat filling procedure from the presence of the surface dewar. The dewar provides the capability to stockpile LAr at the facility prior to filling the cryostat. This will only be of benefit if the dewar filling procedure is significantly less onerous that the cryostat filling procedure.

8.3.2.2 Combined LAr and LN risers

The potential for the replacement of the two liquid cryogen risers (LAr and LN) with a common cryogenic riser should be considered during later design phases. The lines are not normally used during operation. After initial filling of the cryostat the argon line is not planned to be used unless the cryostat is to be drained. The common line would be configured in standby mode for LN service in case of unplanned outage of the refrigeration plant.

8.3.2.3 Common Vent Lines

A common vent system could be adopted that would be suitable for both nitrogen and argon. It would need to be sized for the peak combined flow rate. The probability of either argon or nitrogen being vented under normal operations is low but a Simultaneous Operations Study (SIMOPS) would be required to demonstrate that cross contamination could not occur during commissioning, normal or emergency operations. A greater level of design detail is required to support this study than has been possible to date and therefore separate vents have been included at this stage

8.3.3 LAr Circulation Pump Configuration and Operation

FIXME: *reference the ref design, section 2.5.5 with 4 pumps, each 150 gpm, run all during commissioning, but only 1 (at full power) during normal operations*

An arrangement with multiple pumps could be provided. Four pumps would operate as 4 x 25% during the commissioning phase and 4 x 100% during the long term operation. **FIXME:** *this is opposite of what I understood from Russ* This would provide a more flexible pump configuration. The progressive reduction in required flow rate as the LAr purification increases would be met by incrementally reducing the number of pumps operating. An appropriate number of pumps would be operated at any one time to match the required flow rate with minor throttling occurring at the pump header if required. Individual pumps would therefore be able to operate more closely to their Best Efficiency Point, BEP (optimum flow rate). Long-term, the multiple pump arrangement would allow the pumps to be specified with their BEP closer to the desired long-term continuous flow rate. Expensive VSDs **FIXME:** *What's vsd?* are less appropriate in this arrangement due to the associated capital cost and the low utilization rate that would occur on individual VSD units (i.e., when only one pump is required). The multiple pump arrangement will provide a very high level of redundancy which will extend the cryostat operating period without maintenance. **FIXME:** *Fit in argument: this would allow wider range of operational flow rates (as the advantage)*

8.4 Cryostat Insulation

[Describe the pros and cons of passive vs active insulation. Can use the results of the May 17 mini-review here. Something about vacuum-jacketed vs not – Russ said he'd provide info from Arup rpt 8/5]

8.5 TPC

8.5.1 TPC Configuration

8.5.1.1 Reference Design 1a

Reference Design 1a relies on a minimal extrapolation of the MicroBooNE TPC module design. The detector would be installed in a cavern with drive-in access and would consist of a rectangular stack of TPC modules that have been constructed above ground.

CD-1 level cost and schedule information is available for the MicroBooNE TPC module. A modest extrapolation of the module design parameters will not introduce large cost uncertainty

if done properly. The extrapolations are in dimensions that do not challenge the limits of the technology. For example, the result of increasing the width of the MicroBooNE TPC wire frame size will increase the length of the longest wire and increase the number of wires by a small amount. The increased capacitance due to longer wire lengths will increase the electronics equivalent noise charge, but the signal to noise level will remain above the minimum required. The drift distance of this Reference Design is the same as that of MicroBooNE TPC module (2.5m) since additional R&D would be required to demonstrate that a longer drift is feasible.

The technical requirements for this reference design are determined in part by the construction model. We assume that the construction steps are as follows:

1. Fabrication of components and sub-assemblies at vendors, universities and national labs and shipment to DUSEL.
2. Final assembly of TPC modules in a surface building at DUSEL.
3. Transport of the TPC modules by truck to the cavern.
4. Rigging of the TPC modules into the cryostat using a cavern crane.

The height of one TPC module is determined by the minimize size constraint of these steps. The limit is found to be ∼7m. The limiting factor is the maximum transverse size for an economical access drift into the cavern. Each LAr20 TPC module would be constructed similarly to ICARUS; with the cathode plane in the middle and anode wire planes on each side. Figure 8.1 shows the detector concept consisting of 42 TPC modules arranged in a stack 3 wide x 2 high x 7 deep.

This detector configuration suffers from a poor fiducial/total mass fraction. Only 56% of the LAr in the detector is useful for physics. The cost of this TPC design is ∼3x the cost of the preferred design.

8.5.1.2 Reference Design 2a

Reference Design 2a is similar to the preferred design. The major difference is the use of room temperature accessible electronics. The concept is shown in Figure 8.2.

Short low-impedance cables route wire signals from the Anode Plane Assemblies (APA) to a cold feedthrough which is kept at ∼120K. The readout electronics are located within the feedthrough. The benefit of this design is that the electronics boards can be replaced without removing LAr from the detector.

There are a number of disadvantages to this concept however. The cable lengths must be kept to ∼1m, the wire spacing must be increased to 5mm and the wire angle reduced from 45^o to 30^o in order to achieve a marginally acceptable signal to noise ratio. As a result, the track resolution in the vertical direction is ∼1cm. A large number of feedthroughs are required in order to keep the cable lengths short. One feedthrough containing 576 electronics channels is required for every 53cm along the top of each APA. Each feedthrough would be 34cm x 22cm in cross section and would be ∼2m long.

8.5.2 Wire Spacing

There is a clear benefit to having the smallest wire spacing possible. The distinguishing feature of the LAr TPC is the ability to distinguish one MIP electrons from 2 MIP electron-positron pairs close to the interaction vertex. A wire spacing smaller than the preferred design (3mm) would have smaller Signal-to-Noise ratio (S/N) commensurate with the wire spacing. The design S/N ratio could be restored by decreasing the noise. The most direct means of accomplishing this would be to reduce the wire length, thereby increasing the number of electronics channels. Reducing the wire spacing below 3mm will only offer minimal return since the background from NCπ^0 events is already quite small (∼1%).

We now explore the cost savings by increasing the wire spacing from 3mm to a larger value (5mm). This is a reasonable value engineering option to consider if the savings are significant. A study of the detector cost estimate shows that the dominant factors are the incremental cost for the electronics readout and the labor required to wind the wires.

The electronics readout cost defined here includes design labor, IC masks, ASIC chips, boards, cables, cryogenics feedthroughs and cold testing. The electronics cost can be split into fixed and incremental costs and can be parameterized as \$3.7M fixed cost + \$4.60/channel incremental cost. These costs are fully burdened without escalation or contingency.

The incremental labor cost to wind the detector wire planes is \$0.9M for three wire planes with a 3mm wire spacing, or \$1.50/wire.

In total, the incremental cost of adding one wire of readout is \$6.10. The cost of the LAr20 detector could be reduced by ∼\$1.6M by increasing the wire spacing to 5mm. This is <1% of the LAr20 Total Project Cost. We judge that the potential benefit of having the highest possible granularity greatly outweighs the cost savings.

8.5.3 Number of Wire Planes

The results of the cost exercise described in the previous section can be applied to the question of the optimal number of wire planes.

The preferred design includes three instrumented wire planes and one un-instrumented grid plane. Reducing the number of instrumented planes to two would reduce the detector cost by ∼$1.3M with a minor loss of ν_e identification efficiency. This would also reduce the readout redundancy however and potentially affect the long term reliability of detector operations. We do not consider this a credible value engineering option.

The un-instrumented grid plane could be eliminated, saving ∼$1M. As described in section xxx, the grid plane is used to create equal signal levels in both induction planes. The signal level in the first induction plane would be reduced by ∼2x if the grid plane were eliminated. We do not consider this a credible value engineering option.

8.5.4 Drift Length

As shown in Figure 8.3, an electron lifetime of ∼5ms will result in a 25% loss of signal for a 2.5m drift.

The specification of the 2.5m drift is based on a judgment that considers experience from historical and currently operating detectors and test stands and the purification techniques used to achieve an acceptable lifetime.

An electron lifetime of 10ms is routinely achieved on the Fermilab Materials Test Stand. The ICARUS detector is now in operation and has achieved a lifetime of xxx ms. The Liquid Argon Purity Demonstrator (LAPD) will (has?) achieved a lifetime of xxx ms without relying on vacuum evacuation for initial cleaning.

LAr20 R&D includes a study of argon purity in the 30 ton membrane prototype. The LAr20 2.5m drift length specification will be revisited when this R&D is completed. A longer drift length may be specified in the future as a value engineering option if the R&D results are supportive.

8.6 Trigger & DAQ

We need to define the Trigger DAQ first...

8.7 Installation & Commissioning

8.7.1 Drive-in/Shaft Access

We can't write this section until we have made a decision on the preferred option.

FIXME: *More thought needs to go into alternatives...*

8.8 Photon Detection

Photon detection is not required to address the primary scientific goal of LBNE - the study of accelerator neutrino oscillations. A beam signal from the accelerator complex is sufficient to reduce cosmic ray backgrounds to a negligible level.

Photon detection is also not required for non-accelerator physics studies if data is read continuously from the detector. **FIXME:** *Mention the resulting data rate at the 800 level here?*

There is no ambiguity about the location of an event in the detector if at least one track crosses an interior cathode plane. The transverse position of an event is unknown if it is fully contained within one drift cell and there is no photon detection to define the event time. It is impossible to determine if the event is fully contained if the event occurs in the drift cells at the edge of the detector however. As a result, the edge cells cannot be used for non-accelerator physics studies, reducing the fiducial mass by 33%. The photon detection system allows the entire fiducial mass to be utilized for these physics analyses.

Most LAr TPC's use TPB coated PMT's to detect scintillation light. Light emitted more than a few meters from a PMT is not detectable however due to Rayleigh scattering, so PMT's would need to be placed between drift cells. This configuration is not readily compatible with the anode plane assembly concept. Conceptually, each interior cathode plane can be replaced with two cathode planes separated by sufficient space for an array of PMT's. This would increase the width of the detector and the cavern by $\sim$1m and result in a lower fiducial mass.

A variety of options were considered for the wave length shifting scheme and the light guides. These options suffer from lower light collection efficiency and result in higher cost for the same performance.

8.9 Veto

The original veto concept shown in Figure 8.4 is a more conventional option than the preferred design. The 3m width of the veto panels shown in the figure requires a 31m cavern span which would require significantly more roof support and rock excavation, and thus higher cost, than the preferred design.

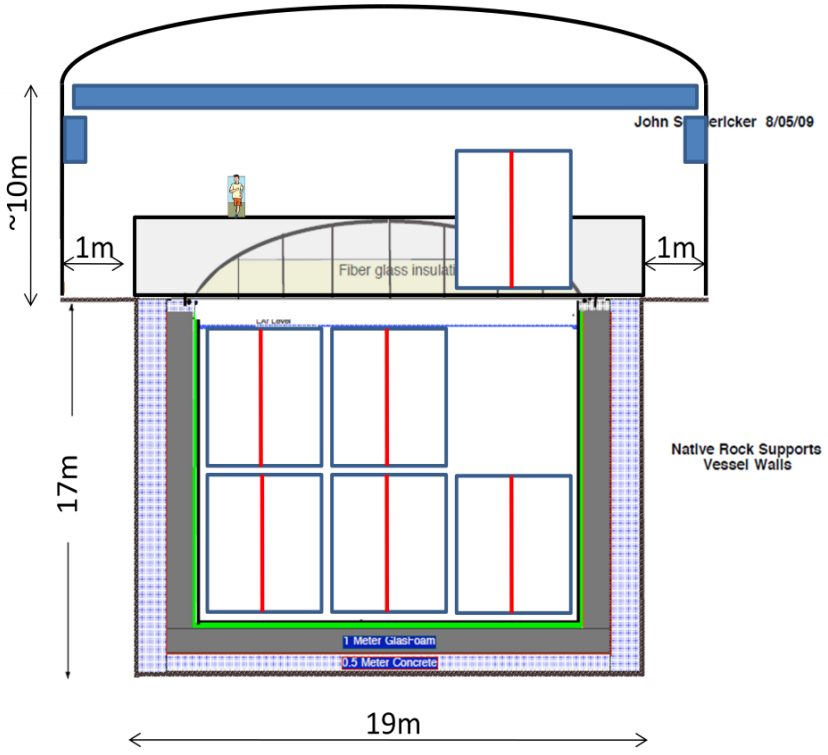

Fig. 8.1. Reference Design 1a cryostat pit and cavern concept showing one 5m x 7m TPC module as it is being rigged into position. Cathode planes are shown in red.

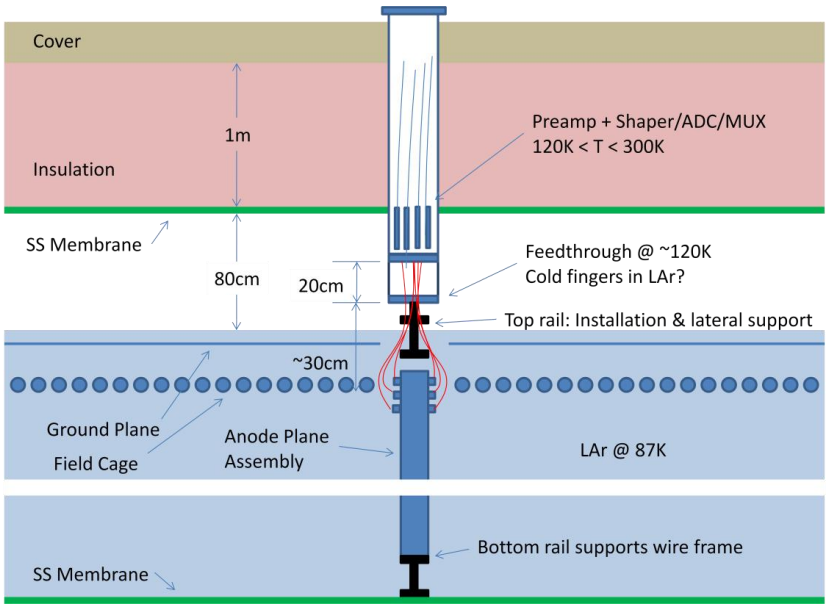

Fig. 8.2. Reference Design 2a, showing cable routing from an Anode Plane Assembly to a cold feedthrough. The warm readout electronics are located within the feedthrough.

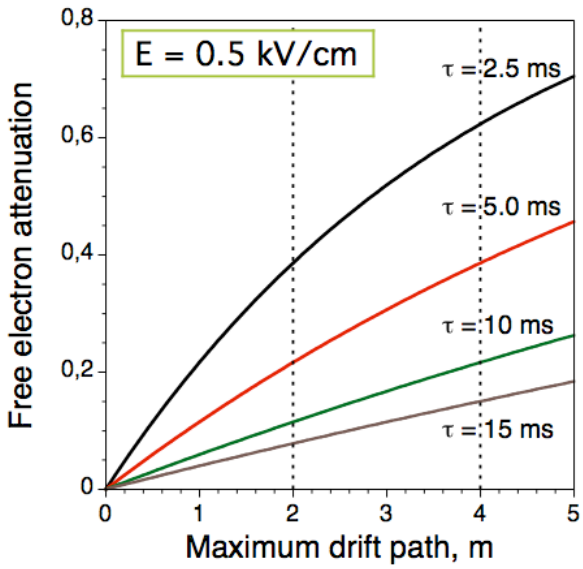

Fig. 8.3. Signal attenuation vs electron lifetime and drift distance

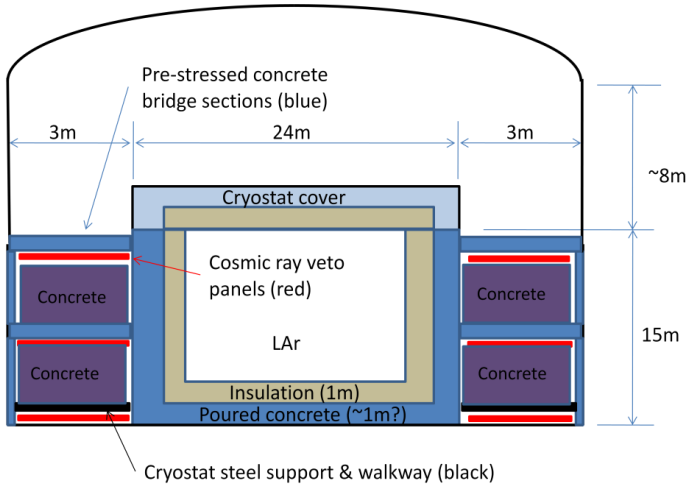

Fig. 8.4. Alternative veto concept

Bibliography

[1] "Title", Month, year.

9 Value Engineering

9.1 Cryogenics System

9.1.1 Boil Off Gas Options

Alternative arrangements with regard to handling the argon boil off gas that have been considered include venting the boil off gas and replacing the lost volume with fresh LAr and re-condensing the boil off gas using an open LN system A coarse whole life cost estimate was prepared to compare the two optional schemes with the selected closed loop LN refrigeration plant.

9.1.2 Argon Venting

Venting the argon gas that boils off from the cryostat was considered as the minimum equipment and minimum capital cost option. Argon would be released from the cryostat to a well ventilated, remote area above ground. A make-up stream of LAr would be provided to maintain the gross volume within the cryostat.

Concerns raised by this system were:

- Ability to achieve required cryostat purity with a continuous stream of commercial grade argon entering the cryostat
- Reliability and availability of liquid argon supplies in the vicinity of Lead, SD.
- Continuing cost of supplying LAr throughout the life of the cryostat.

9.1.3 Argon Re-condensing by LN boil off

To recover the boil off gas emitted from the cryostat it is necessary to extract heat from the gas so that it cools and recondenses. The LAr can then be returned to the cryostat.

Cooling using an open liquid nitrogen system was considered. This system included a recondenser supplied with liquid nitrogen. Within the recondenser the boiling LN (at -196ÂřC extracts heat from the warmer argon stream (at -186ÂřC) and evaporates. The nitrogen is then vented. In cooling the argon gas it condenses and can be drained from the vessel.

A proposal was obtained for a suitable recondenser which has provided the details illustrated in figure 9.1:

A number of potential suppliers of bulk LN were also contacted. Cost estimates were requested for the supply of 20tons of LN per day and a stock holding on site of 80tons. A wide variation in price was received as the supply of LN is highly dependent on the cost of transportation to the site from commercial air separation facilities.

Storage tank costs were typically quoted as a rental rate. Most large users contract for a long term supply of LN and the supplier provide and maintain the necessary facilities at the customer's plant. This includes monitoring inventory levels, determining restock schedules, undertaking deliveries and undertaking all necessary inspections and maintenance of on-site equipment. The lowest costs were provided by Praxair supplying LN from their air separation plant in Loveland, Colorado.

A whole life cost comparison estimate was undertaken of the two options and the selected arrangement with a closed loop nitrogen refrigeration plant. The analysis is included below:

Option	Estimated Capital Cost	Annual Operating Cost	Total Discounted Opera
Argon boil off and replace	$1.6M	$9.5M	$92.4M
LN open loop	$1.2M	$2.1M	$20.8M
LN refrigerated cycle	$4.0M	$0.6M	$5.5M

Notes:

1. The Estimated Capital Cost" includes engineering, equipment cost and installation in current fiscal year dollars.

2. The "Annual Operating Cost" includes utilities and maintenance (3% of capex).

3. The "Total Discounted Operating Cost" was calculated using a 20 year operation at a 5% annual discount rate.

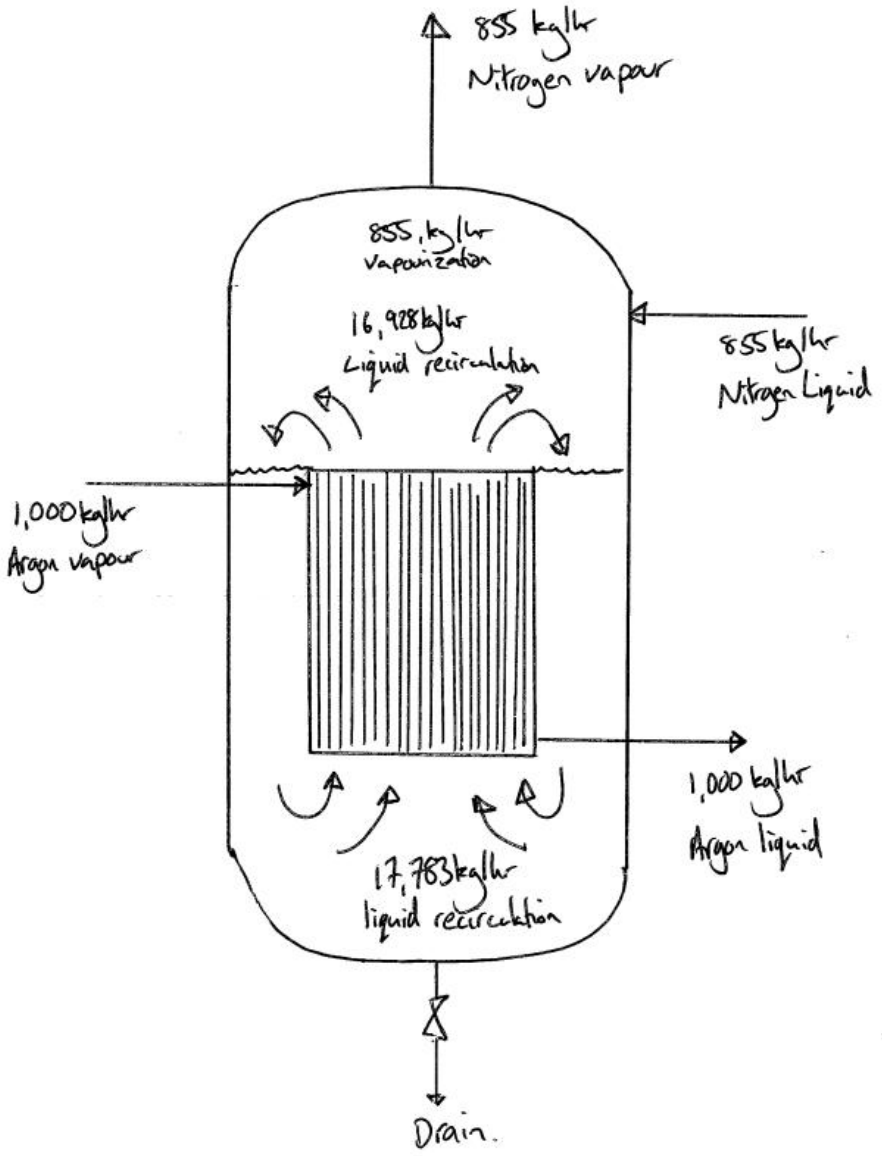

Fig. 9.1. Alternative argon re-condenser

The analysis was undertaken during the concept engineering phase of the study and therefore the costs should be considered as indicative only. However the analysis clearly demonstrate a significant cost benefit from selecting the refrigeration plant based recovery system. The higher capital cost is offset by operational savings over the 20 year design life.

However as a back up to the refrigerated closed loop nitrogen system a LN supply has been provided. This assumes that a relatively small supply of LN would be maintained on-site and would only be used when the refrigeration plant was unavailable. The on going cost of this provision is low due to the low cost of LN, the smaller inventory on site and the ability to control boil off by adopting vacuum insulated storage tanks.

1 text

Bibliography

[1] "Title", Month, year.

10 Environmental Safety and Health

FIXME: *Pgph is general, not LAr20-specific* Because of DUSEL's unique nature, environmental safety and health is a mission-critical concern. Many DUSEL activities will be located deep underground, a condition that may increase both the probability of occurrence and the consequences of an adverse incident. DUSEL will house large detectors with multiple safety risks, including falls, electrical incidents and oxygen deficiency hazards (ODH). A programmatic strength of DUSEL is the interelationship of the various scientific initiatives. However, this interdependence could become problemmatic. A serious accident involving one detector may well have an adverse effect on the entire suite of current and future DUSEL experiments.

The LAr20 Detector, particularly its proposed cryostat and the associated cryogenic systems, will form a unique facility within DUSEL, one that must be subject to rigorous health, safety and environmental assessments during the detector's entire life cycle — design, engineering, construction, commissioning and operations. As with many unique projects, the LAr20 Detector will apply extensive experience gained on similar previous projects, both in the U.S. and around the world. In particular,

- Fermilab has extensive experience working with liquid argon and other cryogens in a laboratory environment, albeit at a smaller scale.
- Fermilab has eight years of experience with the development and operation of underground laboratories, including the NuMI facility at Fermilab and the MINOS and CDMS Detectors in Soudan, MN.
- The deep underground Gran Sasso Laboratory (LNGS) in Assergi, Italy, has more than a decade of experience with the design, installation and operation of large underground physics detectors, including the 800 ton ICARUS liquid-argon detector.
- Some LBNE Collaboration members have successfully worked on underground experiments for as many as 30 years in several laboratories around the world and have extensive experience with underground procedures and safety.
- The engineering and construction industry has more than 20 years experience in the fabrication and maintenance of very large cryogenic storage tanks, such as liquified natural gas (LNG) storage tanks with volumes up to 185,000m^3)

- The mining industry has extensive experience working underground and the Mine Safety and Health Administration (MSHA) and state mining regulators have a well-developed body of regulatory and best practice protocols.

A major challenge for the LAr20 Detector project is to ensure that all of this relevant experience is consistently applied, during design, construction and operation. This includes enforcing industry standards, relevant building and other regulatory codes and Fermilab and DUSEL standards. LAr20 Detector features to ensure environmental safety and health will include secondary containment, appropriate ventilation, oxygen sensors, alarms, signs and training.

10.1 Underground Cryogenic Storage Tanks

10.1.1 Cryostat Design

The LAr20 Project strategies for environmental safety and health start with a desgin process that includes safety as a principle design criterion. The LAr20 cryostat design has no connections or penetrations below the maximum liquid level. This configuration ensures that should pipework or associated equipment fail, pumps can be switched off so as to limit the maximum release to the pipework volume. No liquid will be released from the cryostat as a result of a failure in the cryogenics systems.

10.1.1.1 Containment

The liquid-contaminant capabilities of the cryostat are comparable to those of cryogenic liquefied-gas storage tanks used for storing products such as LNG, LPG and ethylene. The level of containment provided by these tanks is defined in regulatory codes, including BS 7777, BS EN 14620 and NFPA 59A. BS EN 14620, the most recent code, defines three levels of containment:

- *Full Containment - A full-containment tank shall consist of a primary container and a secondary container, which together form an integrated storage tank.*
  - *The primary container shall be a self-standing steel, single-shell tank, holding the liquid product. The primary container shall either be open at the top, in which case it does not contain the product vapors or equipped with a dome roof so that the product vapors are contained.*
  - *The secondary container shall be a self-supporting steel or concrete tank equipped with a dome roof and designed to combine the following functions:*

1 * *In normal tank service: to provide the primary vapor containment of the tank*
2 *(this in case of open-top primary container) and to hold the thermal insulation*
3 *of the primary container;*
4 * *In case of leakage of the primary container: to contain all liquid product and to re-*
5 *main structurally vapor-tight. Venting release is acceptable but shall be controlled*
6 *(pressure-relief system).*
7 – *The annular space between the primary and secondary containers shall not be more*
8 *than 2.0 m.*

9 ◦ *Double Containment - A double containment tank shall consist of a liquid- and vapor-*
10 *tight primary container, which itself is a single containment tank, built inside a liquid-*
11 *tight secondary container. The secondary container shall be designed to hold all the liquid*
12 *contents of the primary container in case it leaks. The annular space, between the primary*
13 *and secondary containers, shall not be more than 6.00 m.*

14 ◦ *Single Containment - A single containment tank shall consist of only one container to*
15 *store the liquid product (primary liquid container). This primary liquid container shall be a*
16 *self-supporting, steel, cylindrical tank. The product vapors shall be contained by:*

17 – *Either the steel dome roof of the container;*
18 – *Or, when the primary liquid container is an open top cup, by a gas-tight, metallic,*
19 *outer tank encompassing the primary liquid container, but being only designed to*
20 *contain the product vapors and to hold and protect the thermal insulation.*

21 The LAr20 membrane-cryostat design (the reference design), by virtue of the primary steel
22 membrane and the secondary polymeric barrier within the insulation, are able to provide full
23 containment.

24 A modular cryostat design (an alternate design) also provides double containment with the
25 cavern pit providing the secondary containment. A failure (significant leak) of the primary barrier
26 in the modular cryostat will result in a release of argon and a subsequent ODH in the cavern.
27 However, the primary barrier is manufactured from high-quality 9% nickel steel, is tested during
28 construction and is of robust design and construction. The probability of failure is therefore low.

29 The primary barrier in the membrane cryostat is manufactured from thin, flexible sections
30 of stainless-steel plate. This is inevitably less robust than the primary barrier within the modular
31 cryostat. However the design of the barrier system and high-quality control during construction
32 has resulted **FIXME:** *in what instance?* in an excellent service performance with only anecdotal
33 evidence of pin-hole leakage which was understood to have been detected during testing. A failure
34 of the primary barrier in the membrane cryostat will not result in the release of argon.

A published risk assessment **FIXME:** *ref geostock* of a pilot plant for underground storage of LNG utilizing the GTT membrane cryostat has estimated that the probability of failure is approximately once in 110,000 years.

In summary, the membrane (reference design) system may have a slightly higher probability of failure but with low ES&H-related consequences, whereas the modular cryostat (alternate design) has a lower probability of primary barrier failure but a higher resulting consequence.

10.1.2 Construction

The processes involved in the construction of the cryostat have been well developed over many years. The LAr20 cryostat's unique aspect is its underground location. World-wide there is limited experience with the construction of large-scale, underground cryogenic storage tanks. The two ICARUS Detector cryostats, each holding 400 metric tons of LAr, are likely the largest cryostats ever installed deep underground. The very large cryogenic tanks (volumes greater than $10^5 m^3$) that have been designed and constructed, mostly for LNG storage, have been installed in surface locations, even if they are partially or wholly set into the ground.

The design and installation of the LAr20 Detector will be of significant interest to multi-national engineering contractors, who are experienced in the management of large-scale, technologically challenging construction work and in the enumeration and mitigation of the associated hazards. These firms will draw on knowledge from a range of specialist advisors, including people experienced with large cryogenic-storage tanks, people with underground hazardous-material experience and people who understand the integration and management of complex environmental and safety systems.

Specific construction issues to be addressed will include:

- Underground working environment.
- Confined working conditions.
- Provision of multiple, independent exit paths from any working area.
- Working at height using scaffolding or custom-designed access systems.
- Personnel movement underground during normal access and egress, including access-control systems. A typical access system for membrane storage tank construction is detailed in the proposal received from GTT.
- Emergency systems (lighting, drainage, HVAC).
- Emergency procedures.

- Materials handling with limited access and restricted height clearances.
- Large numbers of vehicle movements associated with the delivery of personnel and materials and the execution of the work.
- Multi-trade working **FIXME:** *means: people in different trades working in close proximity?*
- Segregation of controlled activities (weld inspection, hydrotest, etc.)
- Hazardous operations that may affect ventilation systems, including containment of hydrogen sulfide emissions during glass-foam cutting.

Maximizing safety during construction requires planning, development of procedures, training and supervision. Both senior and on-site management must repeatedly emphasize safety and accident prevention. Supervision and follow-up is essential. For example, for the NOvA Far Detector Laboratory construction project, the contractor is required to provide a full-time, trained Safety Supervisor, onsite for every shift. The LAr20 project may employ a similar strategy.

10.2 Cryogenic Systems

World-wide there is considerable experience with the design, installation and operation of large-scale cryogenic systems. Generally, these systems are of custom, proprietary design and they prove reliable over long periods of operation. Cryogenic systems (as contrasted with storage cryostats) are designed to minimize inventories of cryogens (and pressurized gases) and to include multiple layers of containment, as well as fault-tolerant and redundant control systems. Particular fault-tolerant features will include isolation valves–both between the cryogenic system and the cryostat–and between various components of the cryogenic system, redundant components and piping, so that sections can be isolated for maintenace and repair, while maintaining system operation, albeit with reduced capacity. We will consider the use of remotely actuated isolation valves to avoid the need for personnel intervention within the LAr20 Detector cavern following an unplanned cryogen release.

10.3 Commissioning, Operation and Maintenance

The principal operational concern is the risk of asphyxiation due to a release of argon. Argon in gas form is colorless, odorless and heavier than air. LAr discharged inadvertently within the cavern will evaporate and displace the oxygen, resulting in a significant Oxygen Deficiency Hazard (ODH). Argon is an inert gas and therefore does not present a flammability or explosion risk.

Liquid argon and liquid nitrogen are also extremely cold and can cause frostbite if they come in contact with skin. Personnel making connections between the delivery trucks and the system and personnel working with the plumbing must wear protective equipment including gloves, aprons and face shields. Training will be provided and personnel will have to be qualified for tasks involving either ODH or cryogenic hazards as provided in the FESHM. The design and implementation of the cryogenic system will follow Fermilab and DUSEL environmental safety and health standards.

The cryostat and associated cryogenic plant form a single closed-process plant. The containment of argon and the exclusion of contaminants from the argon inventory are two determining tenets of the design. As stated earlier in this chapter, no *normal* operations, processes or circumstances should ever result in an underground release of argon.

The operation of the LAr20 Detector Facility will be controlled by formalized procedures covering normal operations, upset conditions and emergencies. Plant-control operation will be the responsibility of a dedicated team of trained and experienced operators, who are fully conversant with the plant operating instructions and procedures.

Strict management-control systems will be implemented to audit the operation of the facility.

Operating procedures will preclude free access to the underground caverns or to cryogenic components in the shafts or on the surface. Access will be controlled by a strict permit-to-work system that recognizes the hazards associated with entering the caverns and that controls all activities that are to be undertaken.

The design of the cavern will include the following facilities to ensure the safety of personnel entering the caverns:

- Ventilation
- Oxygen-level monitoring
- Lighting
- Remote monitoring of personnel and activities
- Access control

Emergency escape and rescue procedures and the necessary facilities will be provided. These may include but should not be restricted to:

- Breathing Apparatus
- Air-tight safe refuges with independent air supplies

- Trained rescue and recovery personnel
- Alternative means of escape.

A program of scheduled maintenance will be developed for the cryostat and all of the associated cryogenic systems. Avoiding exposure of personnel to ODH during routine maintenance tasks is an import design criterion. This goal will be achieved by (a) locating most components requiring periodic maintenance in a surface location and (b) minimizing required maintenance through the selection of underground components. Equipment that must be underground is either located within the cryostat (e.g., circulation pumps) or is benign plant **FIXME:** *don't understand* (e.g., re-condenser vessel) with minimal long-term maintenance requirements.

10.4 Analysis

A preliminary *Failure Modes and Effects Review* has been carried out. The review covered the cryostat tank and mechanical plant, under operating conditions. The review did *not* include the following aspects:

1. Purifiers
2. Electrical systems and security of supply
3. The cryostat fill-and-empty sequence
4. Commissioning activities

As the potential release of argon was deemed to be the most significant hazard, the review focused on those failures mechanisms that would result in the release of either gaseous or liquid argon.

The review noted that, for all options **FIXME:** *like modular vs membrane? which options?*, the fundamental containment was provided by the cryostat, that all penetrations were above the maximum liquid level and that every penetration of the containment would be valved so that whatever the state of the plant and the need for repair work, it would be possible to isolate the main inventory of LAr.

All mechanical plant **FIXME:** *I don't understand the phrase "all mech. plant". Does it mean "all mechanical plant components"?* required during normal operations has been provided on a duty-and-standby (a minimum of 100% redundancy) basis.

For certain predictable maintenance and repair operations, the detailed design will need to include provisions to isolate and purge elements of the plant, bring them to room temperature,

and open them up for work without either contaminating the LAr stream or endangering the maintenance personnel.

The review concluded that, at this concept stage of the design, appropriate arrangements had been made to contain the cryogenic liquids and protect the operational and maintenance personnel. A summary of the review is shown in the following table:

References (again, from microboone doc) [1] One example of such a company is General Plastics Manufacturing Co LAST-A-FOAM at www.generalplastics.com [2] http://lartpc-docdb.fnal.gov/cgi-bin/ShowDocument?docid=410 [3] G. Carugno at al., “Electron lifetime detector for liquid Argon" NIM A292 (1990), 580. and D. Finley et al., “Work at FNAL to achieve long electron drift lifetime in liquid argon." FERMILAB-TM-2385-E, Oct 2006. 9pp

DUSEL Cryo Tank and Plant		Failure Mode and Effects Review			April 12 201
System	Component	Failure Scenario	Consequence	Protection	Action/ Note
Membrane Structure	Membrane	Leakage through defect in construction	Loss of liquid Ar to insulation. Insulation effectiveness reduced. Ar leak to purge / vent system	Conventional detailing for cryogenic conditions from LNG experience. Construction of membrane includes leak tightness test as standard.	
Membrane Structure	Membrane	Leakage through contact with TPC – abrasion, corrosion	Loss of liquid Ar to insulation. Insulation effectiveness reduced. Ar leak to purge vent system	Designed interface between membrane & TPC to control contact forces and return of purified Ar to cryostat at low level to reduce turbulence and vibration	
Membrane Structure	Membrane	Leakage at pipe penetration of membrane	Loss of vapor Ar to cavern above cryostat; Possible entry of air to cryostat if internal pressure is below ambient	Conventional detailing for cryogenic conditions from LNG experience. Construction of membrane includes leak tightness test as standard.	

Fig. 10.1. Preliminary Failure Modes and Effects Analysis

Bibliography

[1] "Title", Month, year.

11 Quality Assurance

All activities relating to the LAr20 will be performed at a level of quality appropriate to achieving the technical, cost and schedule objectives of the project and, at the same time, ensuring that all related environmental safety and health (ES&H) considerations are properly addressed. All work on the project **FIXME:** *Do we want to call it a project in and of itself?* will be performed in compliance with the Quality Assurance (QA) program established by both Fermilab (Fermilab Director's Policy Manual, Chapter 10) and DUSEL.

The LAr20 Project will develop a detailed QA Plan that describes how QA is implemented on the project. All detector subsystems will undergo reviews, which include as major topics ES&H and QA aspects of the system. Internal reviews, Director's reviews and DOE reviews are an integral part of the QA process.

The design life of LAr20 is 20 years **FIXME:** *make sure this is consistent*, during which time the detector must maintain high operating efficiency. The consequences of a component failure inside the detector cryostat are particularly significant, especially if the component requires access or replacement. Such a scenario would likely interrupt data taking for one year, and may require replacement of the argon inventory, unless the liquid can be stored. High operating efficiency will be achieved by multiple quality-assurance measures summarized below for each of the major subsystems–Conventional Design and Construction, Cryogenic **FIXME:** *cryostat, maybe?* & Cryogenics, Time Projection Chamber (TPC), Active Shield and Software.

11.1 Conventional Design and Construction

Conventional design and construction include the design and construction of the cavities and ancillary systems required for the LAr20 Detector. These systems include Heating, Ventilating and Air Conditioning (HVAC), electrical power distribution, fire protection, telecommunications and environmental monitoring. Fermilab has extensive experience in these areas with its various accelerator and detector projects. Based on international best practice and experience with these projects, Fermilab has developed time-tested methods for achieving high-quality designs and implementations. **FIXME:** *ref a few?*

Quality assurance in design requires extensive and disciplined review of plans and planning documents, including use of available software to check for spatial, schedule and other conflicts among various subsystems. The LAr20 cavity and system designs will be addressed by ongoing evaluations and reviews, both during the design process and at the end of design, before final construction packages are approved for bidding.

Quality assurance in construction requires ongoing monitoring and third-party testing by experienced testing-engineering firms. **FIXME:** *Funny phrase. Are these eng firms that specialize in testing?* For example, the construction project for the NOνA Far Detector Laboratory employs a resident engineer, who, independently of the contractor, provides oversight and daily and weekly reporting of construction activities. NOνA also employs third-party testing firms to evaluate the contractor's compliance with the project specifications. Other third-party firms will commission and test NOνA's mechanical systems. LAr20 will use similar methods to assure quality in conventional construction and systems installation.

11.2 Cryostat & Cryogenics

The LAr20 Detector project has developed an effective working relationship with Arup, an engineering firm with many years of experience in the design of Liquified Natural Gas (LNG) storage systems around the globe. LAr20 expects to rely heavily on the experience and technical expertise of Arup and possibly other qualified engineering firms in the implementation of the project's QA program. Overall QA control and responsibility will remain with the project management, which will implement Fermilab and DUSEL QA procedures, in addition to the QA programs of its experienced engineering consultants.

The following excerpt from the Arup proposal for the Cryogenics & Cryostat design study describes Arup's QA program, which is likely to comprise a significant portion of the LAr20 QA protocol.

The management of Arup is totally committed to the following policies and objectives:

- *To achieve a quality service by meeting client's requirements.*
- *To define and document the Quality System for all functions of the organization to comply with the requirement of ISO 9001.*
- *To perform in accordance with the documented Quality System with the aim of developing all designs and project management services correctly the first time.*
- *To continually evaluate the Quality System's suitability, monitor and update its operation to improve its effectiveness.*

4.3.1 Quality and Verification Procedures within the Firm

Arup uses a task-force approach in the execution of its projects and staff is assigned to suit particular project scope-of-work requirements. A project director/coordinator is always appointed for every project and it is mandatory that the director have adequate experience, appropriate to the particular project. Prior to preliminary design, the project engineers must review and agree their proposed schemes with the project director and Quality Assurance engineer. The basis of our approach to Quality Control and Quality Assurance is to place the project in the hands of the Project Director (a Partner) who, with a team of skilled staff, is totally responsible for achieving agreed objectives and for mobilizing the necessary firm's resources and external resources to do so.

Committees are set up within the firm in the various skill and business groups and these committees meet regularly to ensure that quality is maintained in our work. They are also responsible for selection of the Quality Assurance engineer for each particular project. The senior partners are responsible for approving the Corporate Quality Standards and committing the firm to the objectives defined in the Corporate Quality objectives. They represent the firm on all quality matters.

The Quality Assurance engineer is responsible for the day-to-day quality assurance matters on a particular project. He provides the firm with the assurance that work on the project is being conducted in accordance with established procedures and ensures that corrective actions are implemented and recorded for compliance with policy requirements.

All the firm's personnel are responsible for performing their work with the necessary care and attention to detail by understanding and implementing the Firm's Procedures and where relevant, project specific procedures and requirements applicable to their scope of work. The firm achieves this by ensuring that the right caliber project managers and staff are engaged on any given project.

Interactions between Arup and the LAr20 team are already well defined. Arup has specified a single point of contact with the LAr20 team. The LAr20 team has defined two points of contact; the project manager and the project engineer. Arup submits weekly status reports that summarize the work completed the previous week, the work planned for the following week, a list of meetings held, information required from Fermilab, man-hours expended, progress percent complete, areas of concern, change-order requests, and an interface register **FIXME:** *list of interfaces? Not sure what this is*. Coordination meetings were initially held on a weekly basis. Information is now regularly exchanged between the points of contact on an ad-hoc basis. Teleconferences are arranged at mutually agreed upon milestone dates, e.g., at the expected design half-way point, at the 90% design completion point, and for reviews. Each design cycle has at least two meetings, where participants are physically present: a kick-off meeting and a close-out meeting.

The first deliverable in the Arup scope of work was the Design Basis document, which listed the functional requirements, regulations, codes and standards, the input data for the design study

(e.g., site elevation and access, cavern configuration, ground-water conditions, ambient conditions), construction and operating requirements for the facility, expected response to abnormal conditions and ES&H requirements.

The preferred design recommended by Arup is based on the use of the membrane cryostat. This technology has been used for 40 years for the transport and storage of LNG. The cryostat design is based on the GazTransport & Technigaz (GTT) Mark III system (http://www.gtt.fr/). GTT-licensed technology has been employed in LNG transport ships in volumes between 18,900 m^3 and 266,000 m^3, as well as in off-shore structures such as regasification vessels, floating production and regasification platforms, and on-shore storage tanks between 8,000 m^3 and 200,000 m^3. To date, more than 200 vessels and 30 storage tanks have been equipped with GTT-licensed technology. GTT qualifies materials used in construction by testing and qualifies component suppliers of these materials. GTT also provides in-depth training for the installation crew.

11.3 Time Projection Chamber (TPC) and Electronics

FIXME: *This section should be in Risks, not here*

The use of large-scale integrated cryogenic electronics has been identified as a significant risk. **FIXME:** *let's make sure it's in Risks chap* Failure of a large fraction of electronics channels would require emptying the detector cryostat for repairs. As described in Chapter 3 **FIXME:** *use ref – and shouldn't it ref the Risks chap, not chap 3?*, this risk can be factored into two categories, each addressed by a different quality assurance strategy.

The first category is the well understood physical process of "hot electron" damage to CMOS devices. This risk is mitigated by careful design and a robust testing process. These quality assurance measures are described in Chapter 3. **FIXME:** *ditto*

The second category includes electronics failures due to mechanical stress induced at low temperature in composite materials or assemblies containing components with different thermal expansion coefficients. Such failures can occur at the board level (e.g., cable and solder connections) and within integrated circut chips that use bump-bonded sub-structures. LAr20 will operate in a unique mode compared to most cryogenic applications. Unless the LAr20 cryostat or TPC requires an unplanned repair, LAr20 will only undergo one thermal cycle **FIXME:** *define 'thermal cycle'* over the lifetime of the facility. Chapter 3 **FIXME:** *use ref* describes the electronics-testing program that will ensure high electronics reliability.

The APA and CPA mechanical structures will also have mechanical stresses induced on them due to low temperature operation potentially creating significant failures. Chapter 3 describes the cryogenics testing program for these components.

FIXME: *Finally, some QA*

Quality assurance in the selection of construction materials is highly important for successful operation. All materials that will be exposed to liquid argon have been qualified for use in the Fermilab Materials Test Stand, described in Chapter 2. **FIXME:** *use ref* The LAr20 QA program will also include regular testing of detector sub-assemblies and vendor-procured items in the Fermilab Materials Test Stand to ensure that construction processes and materials are of consistent quality.

11.4 Active Shield

FIXME: *this is the Veto Counter? Let's call it the same thing everywhere.*

The LAr20 Active Shield includes two major components–the drilling of holes **FIXME:** *clarify where* and the active detectors that will be inserted in the holes. Hole-drilling will likely be contracted together with cavity excavation. The resident engineer and third-party testing firms will monitor the accuracy of hole-drilling and specify corrective action, as needed.

Active Shield detectors will likely be a physics-detector construction project, undertaken by one or more LAr20 collaborating universities. Quality Assurance in this area will require design reviews, accelerated stress testing of prototypes and procedures for testing each detector both at the point of manufacture and after arrival at the DUSEL site. Both the specification and execution of these QA procedures for Active Shield Detectors will be assessed by LAr20 reviews.

11.5 Software

LAr20 Detector software consists of detector-control software, data-acquisition software and physics-analysis software. To the extent possible, the LAr20 detector will adopt standard particle-physics software frameworks, such as ROOT, and re-use software from existing experiments, such as miniBooNE, MINOS and NOνA. Some existing software has already been adapted and implemented for use in simulation studies for the LAr20 Detector.

The use of well-tested frameworks and adaptation of existing software will minimize software quality-assurance issues. In addition, LAr20 will utilize existing Fermilab software quality-assurance procedures, including reviews, mock data challenges and rigorous testing of individual software components.

Bibliography

[1] "Title", Month, year.

12 Risks

This chapter focuses on risks specific to the LAr20 Detector and on those overall LBNE Experiment risks that may be different for the LAr20 Detector than for other elements of the LBNE Experiment. As discussed in the introductory chapter to this volume, the risks associated with the LAr20 Detector can be categorized as technology risks or project risks.

12.1 Risk assessment for Large, Underground LAr TPC Detectors

There has been strong interest in kiloton-scale liquid-argon detectors for a number of years. An Integrated Plan **FIXME:** *ref* has been developed to guide work on improving liquid-argon technology for use in tracking calorimeters for a range of elementary particle physics experiments.

The plan, developed by a group with extensive experience in U.S. and European LAr R&D activities, is intended to ensure that the risks associated with the construction of a large underground LAr TPC are well understood and that the R&D currently underway is adequate to identify and mitigate these risks.

FIXME: *This chapter doesn't need methodology, I don't think. The Integrated plan was mentioned in chap 1. We could add a bit to VE, maybe. I vote to drop this pgraph.* To develop the Integrated Plan, the group discussed each risk individually and reached a consensus determination of the likelihood of each adverse outcome occurring, as well as the consequences of each of these possible outcomes. As a risk analysis methodology, they employed an adaptation of a standard technique used for project management **FIXME:** *Does the technique have a name?*. The NSLS-II project managed risks using these same methods. The primary deliverables of this approach to risk analysis include risk identification, risk classification and the definition of risk mitigation action items (e.g., R&D activities). A section of the risk matrix is shown in Figure 12.1.

FIXME: *Resume here:* The primary deliverables of the group's risk analysis methodology (**FIXME:** *called what?*) include risk identification, risk classification and the definition of risk mitigation action items (e.g., R&D activities). A section of the risk matrix is shown in Figure

12.1.

The Integrated Plan lays out a number of **FIXME:** *risk mitigation?* steps to be completed in preparation for a LAr Detector the size of LAr20. These steps include: **FIXME:** *the following aren't steps, they're things. What does the plan say we must DO with these things?*

- **FIXME:** *E.g., Completion and use of ???* Materials Test Stand at FNAL
- Existing electronics test stands at BNL and FNAL
- The Liquid Argon Purity Demonstrator (LAPD)
- The ArgoNeuT LAr TPC
- The MicroBooNE experiment
- The integrated software development effort (LArSoft)

FIXME: *Let's cover big risks first.*

The group identified as "residual risks" those that will remain after the activities in the currently envisioned R&D plan are completed successfully. These include:

FIXME: *The statements in the items below are hypotheticals, right? In other words, "X has completed Y" means that "success is defined by X completing Y", right? If something has in fact already happened, let's distinguish that by "Completed" or some such. I'm going to wait to edit this list till I know.*

- ArgoNeut has completed taking data in the NuMI neutrino beam. Current indications are that ArgoNEUT will achieve both its R&D and its physics goals. **FIXME:** *what time scale?*
- The LArSoft group has completed work on a detailed Monte Carlo simulation and is actively developing reconstruction software. At the current pace of development, full 3-D track and electromagnetic-shower reconstruction will allow detailed physics studies to begin in late 2010.
- First results from LAPD are expected in the summer of 2010. **FIXME:** *Are we on target?* The Integrated Plan group assumed that LAPD will successfully demonstrate the ability to achieve long electron lifetime without first evacuating the cryostat. Recent information suggests that evacuation may be possible for both membrane and modular cryostat designs, which will facilitate achieving the required LAr purity level.

- MicroBooNE is scheduled to begin operation in 2013. For the risk analysis, the Integrated Plan group assumed that MicroBooNE will provide a second demonstration of the ability to achieve long electron lifetime in a fully functioning TPC without first evacuating the cryostat. The group assumed that by the time MicroBooNE starts acquiring data, sufficient analysis tools will exist to reconstruct neutrino events. Thus,MicroBooNE will be able to acquire useful physics data.

The Integrated Plan study group proposed the following new R&D activities **FIXME:** *to mitigate some other possible risks?*:

- Construction of a membrane-cryostat mechanical prototype to evaluate and gain expertise with this technology.
- Construction of an installation and integration prototype, to investigate issues pertaining to detector assembly, particularly in an underground environment.
- Conducting a ∼5% scale electronics systems test to understand system-wide issues as well as individual-component reliability.
- Construction of a test stand that would consist of a small TPC exposed to a test beam for calibration studies, relevant to the study and evaluation of physics sensitivities.

All of these activities fall naturally within the scope of LAr20 project R&D with the possible exception of the calibration test stand.

To ensure accuracy and completeness, the group presented a description of the residual risks to the LBNE Collaboration in October 2009 and to the LAr detector working group in November 2009. At a Director's Review of the R&D plan in November to assess the risk identification and the mitigation plan, the review committee identified new project risks but did not identify any new technology risks. **FIXME:** *Do we care who added what risk?*

FIXME: *Marvin: I have finished editing up to here. At this point, there should be a discussion of risks. Use the text from Ch. 1???*

12.2 Cryogen Storage Considerations for LAr and LN2

FIXME: *New section 6/16/10 from Russ, added but not yet edited by Anne*

FIXME: *Maybe this is supposed to go into vol 6? See email of this date from Russ.*

FIXME: *7/23 AH: no risks identified in following pgraph* There is the possibility of using large quantities of liquid argon (on the order of 20,000 tons) in lieu of water to capture neutrinos. At this time it is most likely that the liquid argon detector will be located in a new excavation at 800 feet with an egress connection to the DUSEL facility. During filling of the detector, liquid argon will be supplied via pipelines running in a dedicated shaft from the surface. Refrigeration for the argon detector comes from a 50 kW refrigeration system that uses nitrogen (liquid and high pressure gas) as a working fluid. A modest amount (3 days refrigeration), 100 cubic meters, of liquid nitrogen will be stored at the surface as reserve cooling.

While the probability of a cryogenic fluid release is extremely small, the consequences, should one occur, are not. The expansion ratio of liquid to gas for argon is on the order of 840 to 1. A release of cryogenic fluids within a confined volume will displace oxygen and cause an oxygen deficiency hazard (ODH). The maximum possible release rate of cryogens will need to be minimized **FIXME:** *kept to what level?* and the ventilation system designed to keep the oxygen concentration at acceptable levels **FIXME:** *specify acceptable level*.

The large liquid-argon inventory for the detector and any intermediate storage tank will be contained in a double-walled insulated pit. All transfer lines and ports are located at the top of the tank(s) above the liquid level. With no side-wall exposure, a secondary containment membrane within the insulation, and tertiary containment provided by the concrete-lined pit, cryogenic-liquid release can be limited to the inventory and flow rates of cryogens (liquid argon or liquid nitrogen) within piping sections. While the flow rates of cryogens within those piping lines are significant (of order 600 gpm = 70,000 scfm), the cryogenic transfer lines will be vacuum-jacketed (double-walled) welded stainless-steel piping with negligible probability of failure.

Risks associated with cryogenic piping of this sort are comparable to other underground accelerator facilities. A release of gaseous argon from the top of the vessel is limited to (about 300 scfm) the boil-off rate of the fluid inventory. Main pressure-relief safety valves on the tank(s) or components will be piped to the surface in large-diameter, dedicated exhaust piping. The area around the vent stack will need to be analyzed and designed for safe mixing and release of inert gas to the atmosphere.

Oxygen-depletion sensors will be installed in-area to provide local and remote alarm annunciation in the event of low oxygen levels, see Facility Automation **FIXME:** *ref*. This is motivated by safety (Oxygen Deficiency Hazard - ODH) and best engineering practices. The ventilation design will incorporate an emergency exhaust system in case of failure. The design is based upon a maximum of one release event yielding a maximum venting of 5,886 CFM [10,000 mÃĆÂș/h] based on LNGS, Grand Sasso.

12.3 Risk Identification & Mitigation

This section presumably will list the risks identified by the LBNE risk identification process (which has yet to be defined) and will describe the mitigation plan.

ID	Risk	Category	Consequence	Likelihood	Likelihood comments	Consequence comments	Risk	Mitigation	Mitigated Likelihood
1	Achievement of adequate lifetime requires evacuation. (MicroBooNE and/or LAPD were not successful)	Argon Purity	3	1	Consensus likelihood is consistent		Med	Keep modular cryostat as an option	0
2	Cannot achieve required drift length	Argon Purity	3	1	e.g. feedthrough leaks, cable outgassing, microscopic cryostat		Med	Develop QA procedures for leak checking (warm & cold) and materials qualification	0
3	Argon purity immediately following filling is poor requiring several volume recirulations before operations can begin	Argon Purity	1	3	We deferred to Flavio's experience on this issue (high likelihood) but the		Med		3
4	Increasing the drift distance is a low impact method of reducing the cost of LAr20, however drift distances >2.5m may not have been demonstrated	Argon Purity	2	1	Long lifetime has been demonstrated, but not long drift distance		Low		1
5	"Hot electrons" at 87K damage the cryogenic ASIC's over the lifetime of the detector with a loss of >50% of the detector channels	Electronics	3	1	There is already in place an R&D plan to address this risk	Revised the risk description	Med	Perform stress test on ~5% of the LAr20 channel count	0
6	Single point failure in electronics requires emptying cryostat to repair	Electronics				Integrated Plan Review comment			
7	The membrane cryostat develops a major leak during operation.	Membrane cryostat	3	0	Ref GEOSTOCK risk assessment < 110k years		Low		0
8	Extrapolation from LNG experience/design to LAr is invalid or not understood adequately	Membrane cryostat	3	1	Consensus likelihood is consistent		Med	Engineering analysis will mitigate this	0
9	Vessel ruptures due to ground water pressure	Cavern	3			Integrated Plan Review comment			
10	Rock freezing causes fracture of supporting rock	Cavern	3			Integrated Plan Review comment			
11	Rock bolt failure cases rupture of cryostat	Cavern	3			Integrated Plan Review comment			
12	Cryostat ruptures due to falling rock	Cavern	3			Integrated Plan Review comment			
13	Suppliers are unable to deliver the needed quantities of cryogens on the schedule needed for filling	Management	2	1	Argon availability is more of an issue in Europe than in the U.S. Stephen: 50kton		Low		1
14	Critical components have a single supplier - procurement & operations	Management	2	0	The CMOS ASIC's are the only critical component that may	Membrane cryostat is the only candidate for single supplier	Low	There is already an R&D plan in place	1
15	There are insufficient technical resources to conduct the planned and proposed R&D	Management	2	3			High	Increase FNAL resources	2

Fig. 12.1. A section of the LAr20 risk matrix.

Bibliography

[1] "Title", Month, year.